

POLITECNICO DI TORINO

Collegio di Ingegneria Energetica

Corso di Laurea Magistrale

in Ingegneria Energetica e Nucleare

Tesi di Laurea Magistrale

Energy saving strategies in diesel railcars



Relatore:

Prof. N. Bosso

Co-relatore:

Ing. N. Zampieri

Tutor aziendale:

Ing. A. Tosetto

Ing. D. Gerardi

Candidato

Giuseppe Boccardo

Matricola: 221059

Aprile 2018

ABSTRACT

This thesis aims to analyze different energy recovery strategies available on an existing Diesel Multiple Units (DMU) railway vehicle, developed by *Blue-Group*, in order to improve its efficiency and environmental impact. Since the vehicle makes available three different energy recovery opportunities that include exhaust gas or cooling water heat recovery as well as regenerative braking, firstly a pre-feasibility study has been conducted in order to identify the most feasible and effective energy recovery opportunity among those available.

Exhaust gas heat recovery for power production has been briefly analyzed but it resulted in low efficiency (11%) of the process and high complexity of integration in the existing vehicle and, thus, no further investigated.

Exhaust gas heat recovery for hot water production has been analyzed also, resulting in high efficiency of the process but still too complex to be integrated into the existing vehicle since it requires a substantial modification of the vehicle layout and electrical system.

Cooling water heat recovery combined with Organic Ranking Cycle (ORC) for power production highlights low cycle efficiency (13%) and very low energy production (5% of the total energy demand) and, therefore, it has been not further investigated.

Once regenerative braking has been individuated as the most promising energy recovery strategy, the second part of the thesis is focused on sizing, design and modeling the onboard battery pack capable of harvesting braking energy of the vehicle, making it electrically propelled when it is necessary.

The simulation developed in Matlab® environment shows encouraging results because the vehicle is able to recover almost 20% of the total energy demand and about 85% of electro-dynamic braking energy involved in the selected urban track and completely wasted in the baseline vehicle. Additionally, by means of substitution of the battery pack in place of one of the four diesel-generators, the vehicle can operate in a wider range of tracks such as underground sections and non-electrified urban stations, obtaining a strong reduction of particulate and pollutant emissions in that critical areas.

In conclusion, installation of the onboard energy storage system in the existing vehicle makes possible to reduce vehicle energy consumption through harvesting braking energy and allows the vehicle to operate in a wider range of tracks.

ACKNOWLEDGMENTS

First and foremost, I would like to express my sincere gratitude to my thesis supervisors, Professor Nicola Bosso and Eng. Nicolò Zampieri in the department of Mechanical and Aerospace Engineering, for their patience and guidance throughout the completion of my degree.

Additionally, I would like to express my deepest appreciation to my supervisors at Blue-Group Engineering & Design, Eng. Andrea Tosetto and Eng. Daniele Gerardi for their advice and willingness to share with me their invaluable knowledge and great intuitions. Without their help, it would be impossible for me to complete the simulations developed in this thesis.

I am also very grateful to the Blue-Group ICT team for being so kind, courteous and cooperative and, in particular, my thanks go to Mr. Pierangelo Farina for his interest in my work and unambiguous management skills.

Last but not least, I would like to thank my family for their unconditional support and for trusting in me over the years of pursuing this degree. In particular, I am grateful to my family for teaching me value of perseverance and loyalty. Additionally, I would like to sincerely thank my sister Serena and my girlfriend Rositsa for their affection and strong belief in my abilities.

RINGRAZIAMENTI

Ringrazio sinceramente il Prof. Nicola Bosso e l'Ing. Nicolò Zampieri del dipartimento di Ingegneria Meccanica e Aerospaziale (DIMEAS) per la pazienza, la disponibilità e la professionalità con le quali mi hanno assistito e guidato durante lo svolgimento di questa tesi. Senza il loro impegno questo lavoro non sarebbe potuto essere realizzato.

Un profondo e sincero ringraziamento va all'ing. Andrea Tosetto che mi ha supportato dall'inizio del tirocinio in Blue-Group fino alla conclusione di questa tesi. Lo ringrazio sia per aver condiviso con me la sua indiscutibile conoscenza e le sue brillanti intuizioni, sia per l'infinita pazienza e disponibilità dimostratami.

Ringrazio inoltre l'ing. Daniele Gerardi per il grande aiuto fornitomi durante lo sviluppo della simulazione e per essersi dimostrato sempre disponibile nel fornirmi chiarimenti e spiegazioni. Sono molte le persone che ho incontrato in Blue-Group e che ringrazio per avermi accolto nel migliore dei modi, ma un particolare ringraziamento va al project manager Pierangelo Farina per aver agevolato lo svolgimento della mia tesi presso l'azienda Blue-Group.

Infine, ma non per minore importanza, ringrazio la mia famiglia per aver sempre creduto in me, per avermi dato l'opportunità di studiare e di raggiungere gli obiettivi che mi sono posto nella vita. Ringrazio mio padre per avermi dimostrato infinito affetto e sostegno, e per avermi insegnato i valori dell'onestà e della perseveranza; ringrazio mia madre perché il suo sorriso, affetto e determinazione mi hanno sempre accompagnato e motivato. Ringrazio mia sorella per avermi dimostrato affetto incondizionato e per avermi sempre stimolato a migliorare. Un grazie di cuore va a tutti gli amici che ho incontrato durante questi anni e in particolare Rositsa con cui ho condiviso intense giornate di studio, ma anche tanti viaggi, serate, momenti felici e risate. Se sono arrivato alla fine di questo percorso è anche grazie a lei.

Table of contents

1. Introduction	7
1.1 Electrification and fuel-mix sources	8
1.2 Efficiency Improvements	10
2. Reference railway vehicle description	12
2.1 Vehicle layout and operating principle.....	12
2.2 Powertrain system.....	14
2.3 Braking systems typologies	17
2.3.1 Electro-pneumatic braking.....	18
2.3.2 Dynamic braking.....	19
3. Energy saving strategies and analysis	21
3.1 Exhaust gas combined with a steam cycle.....	22
3.1.1 Methodology	23
3.2 Exhaust gas combined with Organic Rankine Cycle.....	25
3.3 Exhaust gas heat recovery for hot water production	26
3.4 Regenerative braking	27
3.4.1 Regenerative braking and power grid issues.....	28
3.5 Considerations on energy recovery strategies	29
4. Energy Storage Systems (ESS)	30
4.1 Batteries	31
4.1.1 Nickel-Cadmium (Ni-Cd)	32
4.1.2 Nickel-Metal Hydride (Ni-MH).....	33
4.1.3 Lithium-Ion	35
4.1.4 Applications of Lithium-Ion battery	37
4.2 Super-capacitors	40
4.3 Flywheel	42
4.4 Selection of the Energy Storage System.....	44
5. Case Study.....	45
5.1 Input data	46
5.2 Vehicle longitudinal dynamic modeling.....	47
5.3 Battery pack sizing and design	50
5.4 Algorithm and assumptions	51
5.5 Simulation results and discussion.....	57
6. Conclusions and future developments	64
7. References	67

8. APPENDIX: Matlab TM program for dynamic simulation.....	72
List of figures.....	84
List of tables	85

1. Introduction

Nowadays, the global warming and environmental pollution concerns are involving a large part of research efforts and government policies in order to reduce climate change and its tragic consequences. To achieve that, an important measure is the “Horizon 2020” project that puts focus on climate change by financing innovations, researchers and industrial leadership, in order to reduce pollutant emissions and primary energy demand of different industrial sectors.

Since today goods and people move around the world more frequently and travel over longer distances than in the past, the transport sector has become largely responsible in terms of CO₂ emissions and energy consumption. This could be attributable to the low environmental awareness and low efficient technologies adopted in the past, meanwhile freight and passenger transport was growing rapidly because of globalization driven by the IT revolution.

Still today, rail transport is one of the most eco-friendly modes of transportation, especially for covering long distances and carrying heavy and bulky goods. However, rail transport has a great potential in terms of energy reduction, indeed, as has been demonstrated in [1], specific energy consumption in rail transport has decreased by 37% between 1990 and 2013, but a lot of work has still to be done for making it really sustainable and respectful of the environment.

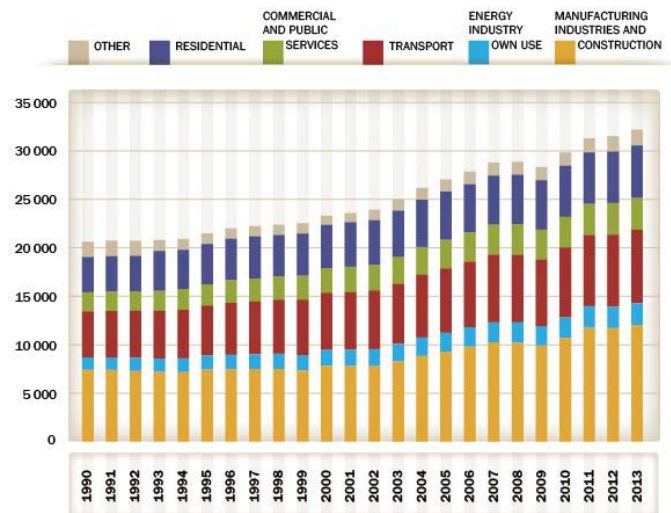


Figure 1 Million tCO₂ by fuel combustion by sector from 1990 to 2013. Source: reference

According to [1, 2], the transport sector is the main source of CO₂ emissions in the European Union and in the USA. The rail sector is responsible for 1.5% of the global transport-related CO₂ emissions, but in countries like China or India around 10% of the total transport-related emissions are due to rail-transport, having a high impact on environmental pollution and air quality. In the USA, the transport sector is considered the most CO₂ source and rail transport produces 2.2% of the total transport-related CO₂ emissions [1].

On the one hand, trends of transport energy consumption are positive: the contribution of rail-transport emissions in Europe has decreased by more than half since 1990 to 2013 [1]. On the other hand, rail-transport is continuously increasing in countries such as China and India that contribute to this quick growth with an eight-fold increase of their railway activity [1]. In addition, China is going to improve its rail freight transport by building the “New Silk Road”, an impressive roll-out infrastructure that will

connect China to Europe countries, confirming the strategic role and the continuous development of railway transport in today's economy [3].

1.1 Electrification and fuel-mix sources

In 2013, European electrified railway networks was about 60% of the total, while US railway network had a very low electrification rate, mainly because railway networks and rolling stock fleet are owned by private companies that have not incentive for investing in electrification of railway networks, a process considered very expensive and justifiable only for heavily-used lines [4]. On the other hand, from 2000 to 2013, China has tripled use of electricity in rail transport and 13.1% of that is produced by renewable energy sources [1], whereas in India the percentage of electrified tracks is stable around 55% since 2004.

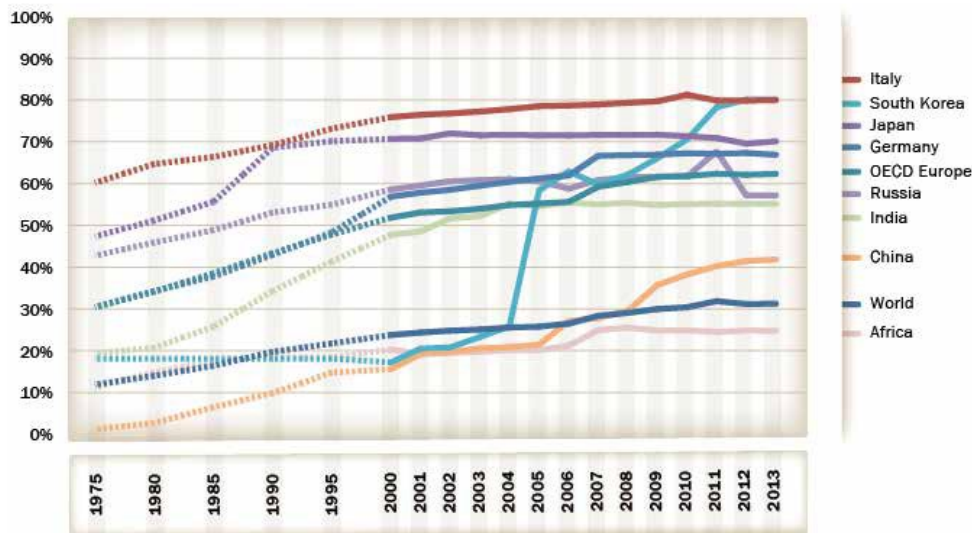


Figure 2 Share of electrified railway tracks in selected countries and geographic areas. Source: [1]

Looking at figure 2, clearly railway vehicles still operate in non-electrified sections more or less frequently according to electrification rate of each country. Moreover, it is remarkable that intensifying electrification rate is not a real improvement if that electricity is produced by fossil sources. Thus, a quick analysis on the fuel-mix used in rail transport is useful to understand reasons of this dissertation.






ENERGY MIX BY SOURCE		1990	2013
OIL PRODUCTS		96.7%	92.8%
BIOFUELS		0.0%	2.7%
ELECTRICITY		3.3%	4.5%
of which Fossil		2.3%	3.0%
of which Nuclear		0.6%	0.9%
of which Renewable		0.4%	0.6%

Table 1 USA railway energy fuel mix evolution. Source: [1]






ENERGY MIX BY SOURCE		1995	2013
OIL PRODUCTS		44.6%	29.0%
ELECTRICITY		55.4%	71.0%
of which Fossil		37.6%	47.0%
of which Nuclear		6.4%	11.6%
of which Renewable		11.4%	12.4%

Table 2 Russia railway energy fuel mix. Source: [1]







ENERGY MIX BY SOURCE		1990	2013
OIL PRODUCTS		36.6%	67.3%
COAL PRODUCTS		54.9%	0.0%
ELECTRICITY		8.5%	32.7%
of which Fossil		6.2%	26.3%
of which Nuclear		0.2%	0.9%
of which Renewable		2.1%	5.5%

Table 3 India railway energy fuel mix evolution. Source: [1]

ENERGY MIX BY SOURCE		2000	2013
OIL PRODUCTS		77.1%	36.4%
ELECTRICITY		22.9%	63.6%
of which Fossil		18.8%	49.3%
of which Nuclear		0.3%	1.3%
of which Renewable		3.8%	13.1%

Table 4 China railway energy fuel mix evolution. Source: [1]

Looking at the type of primary energy sources used in railway systems, clearly oil products still play a relevant role in propelling railway vehicles. For instance, in India and China, more than 50% of electricity is generated using fossil fuels and this could be attributed to the low electrification ratio [1].

Additionally, tables 1,2,3,4 show that generally increase of electricity use is accompanied by an increase of fossil fuel consumption, while renewable-electricity production is almost constant, except for China that increased its renewable power production from 3.8% to 13.1% in 3 years. On the contrary, India has almost doubled oil consumption, whereas in the US fossil products propel essentially the majority of railway vehicles and no significant changes have been done from 1990 to 2013.

After this brief analysis on electrification and primary energy sources used in rail transport, it is possible to conclude that:

- 1) Due to low electrification of railway networks, some countries widely adopt diesel-electric railway vehicles, since they are the most diffused technical solution to run along non-electrified sections.
- 2) Although electric railway vehicles increasingly been used, it is important to improve their efficiency and to reduce losses of power supply grids because a large part of that electricity is still produced using conventional fossil sources.

1.2 Efficiency Improvements

Based on afore-mentioned issues, it is necessary to undertake measures for ensuring a sustainable transportation for passengers and goods. According with [1, 2], rail transport is one the most effective way of moving goods and passenger, however The European Rail Industry (UNIFE) confirms that a huge amount of energy can be saved in railway sector, especially in light rail vehicles and in Diesel Multiple Units (DMU) trains [2].

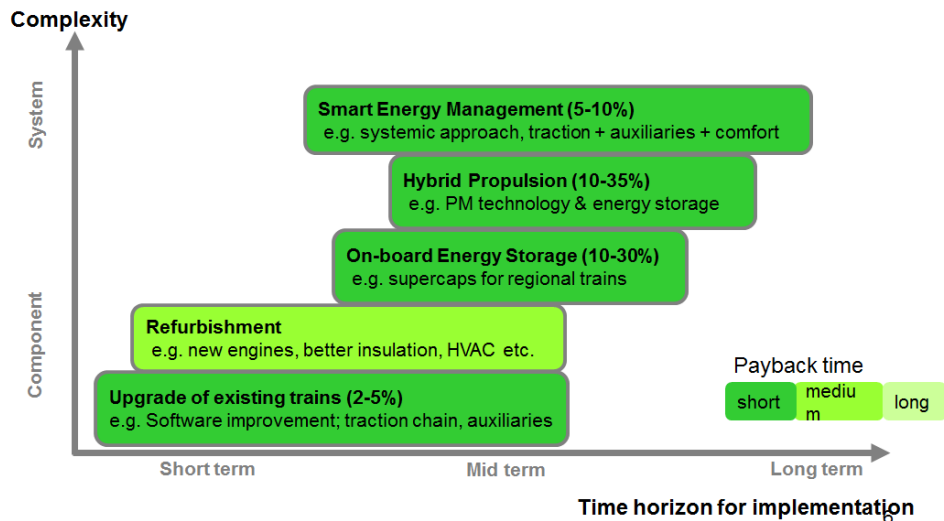


Figure 3 Recommendations for Diesel Rolling Stock (DMU). Source: [5]

In addition, The International Union of Railways (UIC) has committed to reducing (-60% by 2050) the specific energy consumption per traffic unit respect to the baseline of 1990. To achieve this target, UIC has launched the “Modal Shift Challenge”, a call for investors that want to encourage a change towards rail transport, looking away from carbon-intensive transport [1].

Because of complexity and wide variety of the railway transport systems, it is almost impossible to provide a general guideline for improving the efficiency of the overall system. Nevertheless, spanning from power supply operators to railway vehicles manufactures, everyone should put efforts in order to obtain a more efficient and environmental-friendly way of transportation. More in detail, effective methods for improving the energy efficiency of the railway system can regard both “grid-side” and “vehicles-side”.

From the *vehicle-side* perspective, different options are available to improve railway vehicle’s efficiency however, *regenerative braking* seems the most promising and effective since it can provides up to 30% of the overall traction-energy demand [2, 6, 7], resulting in higher efficiency of rail-vehicles and lower GHG emissions.

A short list of remarkable energy efficiency improvements applicable on DMU trains follows [5]:

- Energy efficiency train operation (EETROP): it comprises in a better planning and handling train operations through real-time monitoring and a more effective timetabling, in order to optimise global energy demand and smooth out the power demand;
- Trackside energy storage: an energy storage system such as flywheel, super-capacitor or battery pack, is connected in parallel to the power supply system (i.e. catenary or third rail); when the vehicle is braking, the energy storage system (ESS) absorbs the energy generated during braking until the vehicle again requires energy to re-accelerate. This process can be useful in energy saving application as well as voltage stabilisation;
- On-board energy storage: it works on the same basic principle of the previous option, but it differs in some technical aspects. In a DMU train, the diesel engine and a generator provide

power through the DC-Link that feeds traction motors. During braking, the generated energy is sent to the onboard energy storage system (OESS) for later use, typically to re-accelerate the vehicle. This method results in energy and time savings since it allows grid losses reduction and faster acceleration of vehicles;

- Waste heat recovery: typically, in a diesel engine the cooling system and the exhaust air contain around the 60% of the input energy of the engine. This technology allows recover part of the wasted heat for heating or cooling the coaches or reducing auxiliary energy demand. Waste heat recovery is possible through an absorption refrigerator (*cooling*) or using an air-water heat exchanger (*heating*).
- Hybrid propulsion with permanent magnet synchronous machine: it comprises a diesel engine and a generator with permanent magnet which is lighter and more efficient than other electrical machines; moreover it is easily integrated with existing technologies and with energy storage system for regenerative braking;

The list above contains the main and more effective technics to reduce energy demand, improving energy efficiency and carbon footprint of conventional railway vehicles [5].

In conclusion, to achieve goals regarding primary energy savings and *GHG* emission reduction, it is essential a development of a more efficient way of using fossil fuels, avoiding energy losses and reducing wasted energy in the existent technologies. This dissertation aims to analyze different options for energy recovery available on a diesel-powered railway vehicle such that the chosen retrofit process results as effective and easy-to-integrate as possible.

2. Reference railway vehicle description

The first part of this work is focused on identification of different energy saving strategies available on an existent DMU train model developed by *Blue-Group Engineering and design* (from now on *Blue-Group*), firm who supported me on the development of this master thesis. For a better understanding of the following energy recovery analysis, this chapter provides a comprehensive description of the vehicle layout and its operating principle.

Generally, as the name well describes, DMU vehicles are equipped with a variable number of diesel engines and, according to transmission design criteria, with an additional power supply system such as pantograph or third rail. Usually, this kind of railway vehicle uses diesel power system in the non-electrified area, whereas in urban or underground sections vehicle adopts an electrical power supply system.

It should be noted that no additional power supply systems are fitted on the selected vehicle, indeed diesel engines represent the only power source available. Since vehicle exploits electrical transmission system, each diesel engine works coupled with alternator, providing power to auxiliary equipment and to electric motors responsible for providing tractive effort. In order to identify available energy recovery strategies, it is fundamental to analyze architecture and operating principle of the power supply system fitted on the selected vehicle.

2.1 Vehicle layout and operating principle

The *Blue-Group* firm developed a DMU railway vehicle that comprises four wagons distinguished into two types called *car 2* and *car 4*, head and body of the trainset respectively. Table 5 and Figure 4 synthesize technical details of both car types and the overall vehicle arrangement.

	Car 2	Car 4	
Length/Height/Width	27.18 / 4.28 / 2.82	25.72 / 4.28 / 2.82	[m]
Wheel diameter	915		[mm]
Track gauge	1435		[mm]
Boogie wheelbase	2500		[mm]
Nominal Boogie centre spacing	19		[m]
Axle load [tons/axle]	18		[tons/axle]
Number of axles	4	4	[-]
Primary power source: diesel engine	560	560	[kW]
Transmission system: electric motor	180 x 2 units	180 x 2 units	[kW]
Maximum speed	120		[km/h]
Wheel arrangement	(2B)(22) (22)(B2)		[-]
Layout	Driver's Cabin and passenger compartment	Passenger compartment	
Capacity	228	201	[persons]

Table 5 Car 2 and Car 4 technical details



Figure 4 Layout of the train arrangement

Both car types have frame based on H-shape where the trailer and motor bogies are fitted, on the front and rear part of the frame respectively, as it is shown in Figure 5. The diesel generator, HVAC units and brake resistor bank are roof-mounted. Essentially, the heating/cooling system of *car 2* differs from *car 4* because of the HVAC unit of the driver's cabin.

Both car types are equipped with electro-dynamic (ED) and pneumatic braking systems: the former operates in normal braking operation, whereas pneumatic braking is activated at very low speed, in emergency operations or in case of failure of ED braking system. Indeed, when the vehicle has to decelerate, the control unit sends a braking signal to the traction converter that enables the motor to act as a generator, applying a resistant torque to the wheel-axle of the motor bogie. The existing vehicle has been developed such that, during the braking phase, part of the ED braking power feeds auxiliary equipment, while the exceeding part is wasted through the brake resistor bank. Once vehicle reached very low speed (i.e. in the proximity of the station), the control unit activates pneumatic braking system ensuring short braking distance despite its high operational costs.

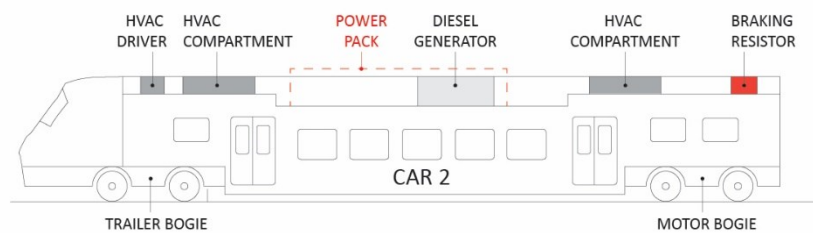


Figure 5 Roof-mounted equipment in car 2

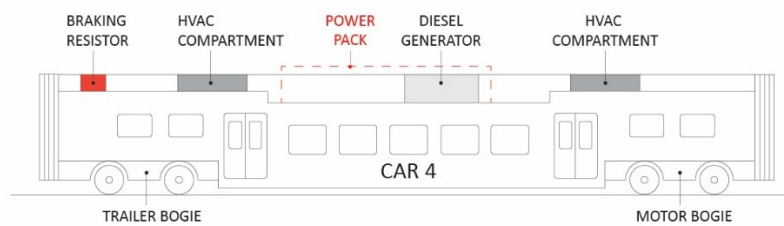


Figure 6 Roof-mounted equipment in car 4

	Car 2	Car 4
Electric motors	2 x 180 kW	2 x 180 kW
Compressors	7.5 kW	7.5 kW
Compartment HVAC units	24 kW x 2 units	24 kW x 2 units
Driver HVAC unit	5.8 kW	None
220V sockets	2 kW	2 kW
Power pack cooling system	18 kW	18 kW
Total	435.5 kW	441.3 kW

Table 6 Vehicle's loads

2.2 Powertrain system

Actually, the majority of railcars are fully or partially electric because these systems are highly efficient and more suitable for high tractive effort. Indeed, diesel-electric powertrain provides almost constant torque at low speed and have high efficiency and fewer concerns about motion transmission between engine and wheels [8]. On the analyzed DMU model, each car is equipped with its own diesel-generator and there are not any other external power supply systems, thus diesel engine plays an essential role for the proper functioning of the whole system. However, because of safety issues, the vehicle has been developed such that it is capable to complete its mission even in case of failure of two of the four diesel engines.

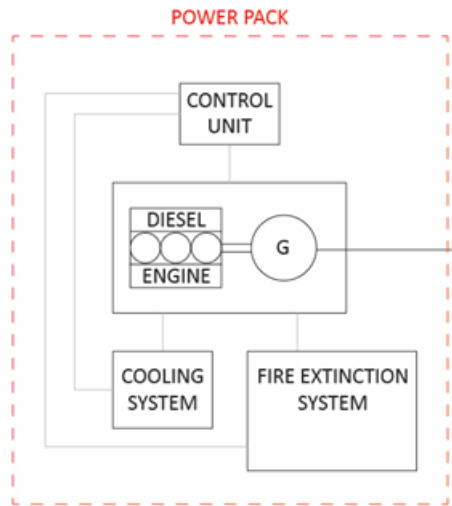


Figure 7 Power pack scheme

Moreover, each coach has its own roof-mounted power system, the so-called *power pack*, which includes:

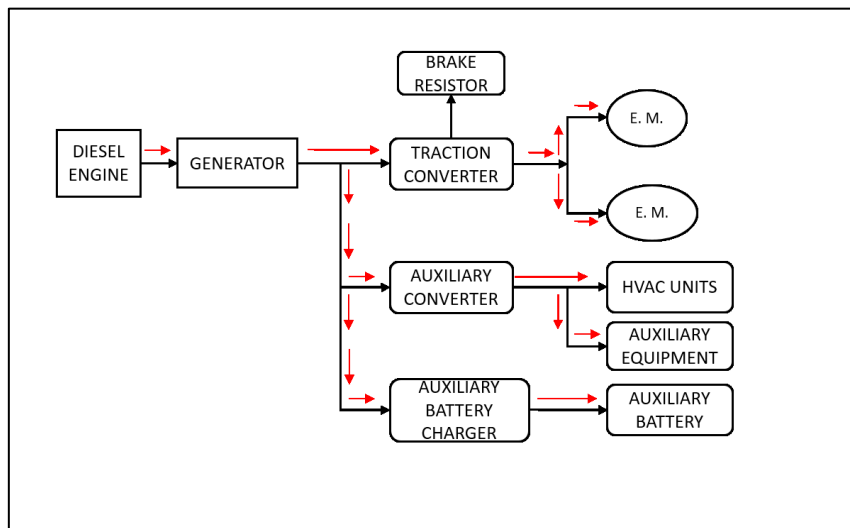
- Diesel engine coupled to the electric generator (*diesel generator*);
- Control and monitoring system;
- Fire Fighting system;
- Cooling system;

The power pack weighs about 8 tons and provides power to traction converter, auxiliary converter (medium voltage *MV* loads) and to a battery charger (low voltage *LV* loads). More in detail, diesel generator supplies power to the rectifier that converts alternating current (AC) to direct current (DC); then power flows DC to traction and auxiliary converters and the battery charger. The traction converter again converts DC to AC, supplying power to two traction motors connected to two different shafts of the same motor bogie.

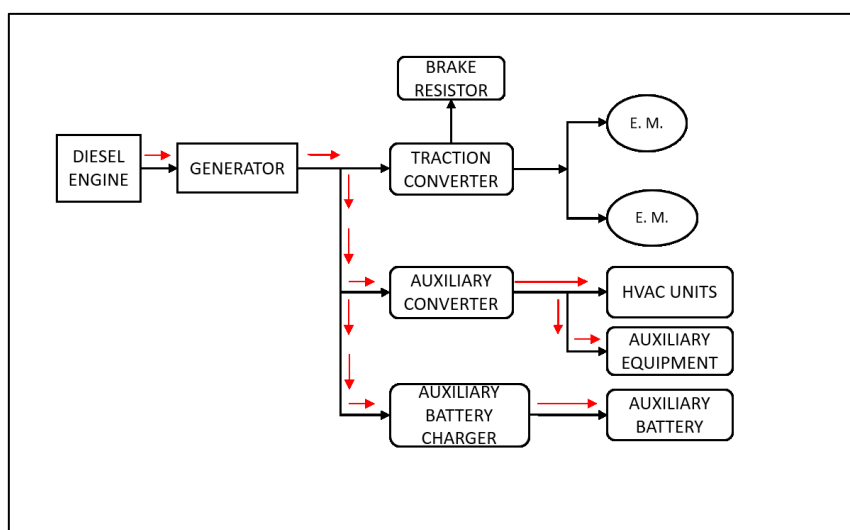
The control unit is based on *PID* controller and sends a signal to traction converter that regulates ED braking and traction efforts by means of VVVF inverter. As mentioned before, ED braking is activated in normal operations and ED braking power is wasted through brake resistor bank, if the auxiliary equipment does not require power. The brake resistor bank has rated power of 340 kW each and mass of about 360 kg each. The auxiliary converter feeds and regulates the power of the *MV* loads such as HVAC units, compressors and other auxiliary systems, whereas battery charger supplies power to the existing battery pack used in start-up and emergency operational mode.

Errore. L'origine riferimento non è stata trovata., 9, 10 below show vehicle power flow in different operational modes synthetized as follows:

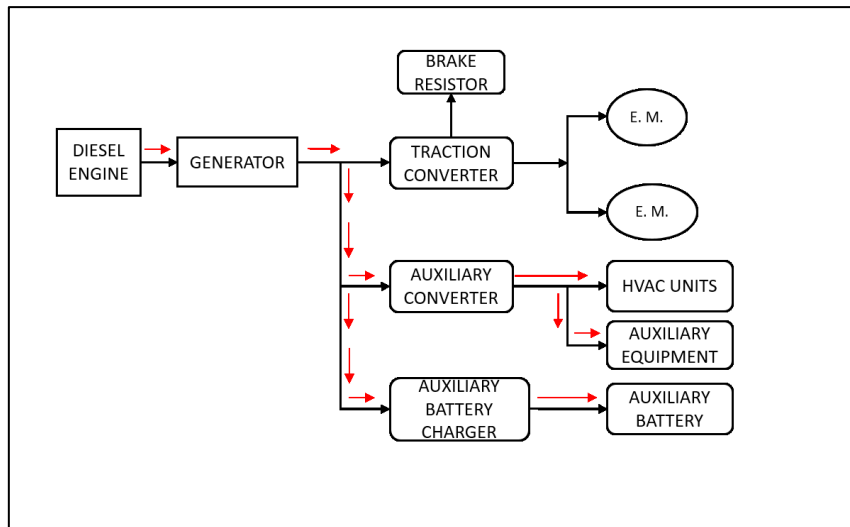
- *Departure*: the vehicle has to accelerate until reaching cruise speed. During this phase, electric motors have to provide the maximum torque and thus they require the maximum power demand because of the inrush current.
- *Constant speed*: once vehicle reached cruise speed, electric motors have to overcome drag force only and their power demand decreases. In this phase, diesel generator has to provide power to auxiliary equipment and electric motors.
- *Coasting*: vehicle runs by inertia and slowly decreases its velocity. The diesel generator provides power to auxiliary equipment only.
- *Braking*: when the vehicle has to decelerate, initially ED braking energy is applied by means of VVVF inverter that enables electric motors to act as a generator. Once the speed is very low, vehicle activates pneumatic braking.



8 Power flow of the single car in acceleration phase



9 Power flow of the single car in coasting operation



10 Power flow of the single car in ED braking operation

The described powertrain system suggests different energy recovery strategies involving both diesel engine waste heat recovery and ED braking energy recovery. The former shall be exploited for thermal or electrical power production, although it is well known that energy transformations strongly reduce the overall system efficiency. While, in contrast, the second strategy involves a more efficient energy transformation and could lead to a more effectiveness of the energy recovery strategy.

2.3 Braking systems typologies

When a conventional vehicle applies brakes, usually braking energy is wasted into heat, dissipating it to the surrounding environment. Braking, from a physical point of view, is intended as a variation of vehicle's kinetic energy expressed as follows:

$$\text{Eq. (2.1)} \quad E_{kinetic} = \frac{1}{2} * mass * speed^2$$

Since railway vehicle has a mass of the order of magnitude of tons and speed can reach some hundreds of kilometers per hour, a huge amount of energy is involved in braking phase. As an example, a TGV train runs up to 310 km/h and when it stops, each brake disc dissipates up to 25 MJ [9]. For this reason, braking systems must provide huge braking effort in a very short time and distance, according to track slope, intermediate station distance and initial velocity.

Because of that, usually railway vehicles are equipped with different types of braking systems that generally are distinguished in:

- 1) Mechanical braking systems: the braking effort is applied through pads pushed on the brake-discs mounted on the wheels. Since friction forces have opposite direction with respect to the motion, a resistant torque is applied on the wheels, resulting in vehicle deceleration. In these systems, the braking energy is wasted into heat due to friction between pads and brake-discs, enhancing wheels' temperature and mechanical stress. In addition, although friction-braking systems have a great braking effort, this type of system requires very high maintenance and high costs, thus are preferred in emergency or low-speed operational mode [10].
- 2) Dynamic braking systems: they exploit the fact that electric motor can act as a generator. In these systems, traction converter regulates voltage and frequency of the power supply system according to with the tractive/braking effort required. These systems allow a very precise braking effort control, but they required complex electrical circuits and electronic devices. Moreover, *dynamic braking* cannot totally replace mechanical braking, thus the so-called *brake blending* is still required, especially in high-speed trains [11].
- 3) Eddy current braking systems: these systems take advantage of the electromagnetic force between a magnet and a conductive object in relative motion. Essentially, a conductive surface experiences circular currents (*eddy currents*) when exposed to a magnetic field. Eddy currents again generate their own magnetic field opposes to the first one. Through this process, the conductive object is subjected to a drag force in opposite direction of the motion, resulting in vehicle deceleration [12]. Although these systems do not use friction forces, the vehicle's kinetic energy is not recovered anyway.

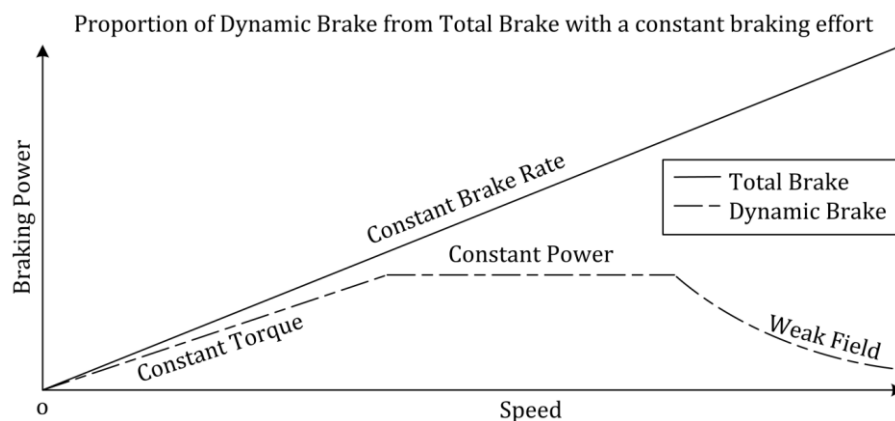


Figure 11 Amount of ED brake power and total brake power desired. Source:[13]

2.3.1 Electro-pneumatic braking

In the pneumatic braking system, the principle of operation is the conversion of the driver's electrical braking command into a pneumatic signal through energization of electro-valves that enable compressed air to flow into brake cylinders, pushing pads against brake-discs through the pressure of compressed air. The pneumatic signal is possible using compressed air available onboard, thanks to dedicated pipelines, valves, and compressors. When the brake electrical signal is sent to the application valve, compressed air flows into brake cylinders and air pressure presses brake pads on the axle-mounted brake-discs. This creates friction between them and, consequently, a braking effort is applied to wheels and train decelerates [14, 15]. In this system, the vehicle kinetic energy is dissipated into heat because of friction forces.

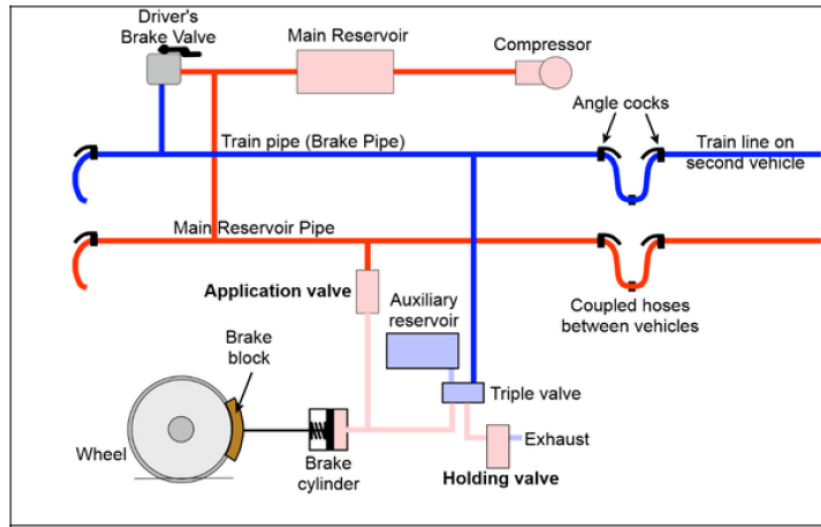


Figure 12 Simplified scheme of the electric-pneumatic braking system. Source: [15]

On the one hand, the braking effort is applied simultaneously to each wheel since the electrical signal has almost no delay when it is sent along the train. On the other hand, this system required pipelines, compressors and auxiliary equipment, resulting in an increase of weight and complexity of the train equipment. In addition, pneumatic cylinders for storing compressed air and other equipment require an expensive amount of power (up to 10 MW per locomotive) [11].

In addition, braking system components such as pads or brake-discs need to be constantly checked and replaced, increasing maintenance cost and reducing the availability of each coach. In other words, this system is more suitable in emergency or low-speed applications than in conventional operations. To reduce maintenance costs and to improve braking efficiency, ED braking systems are widely utilized on railway vehicles.

2.3.2 Dynamic braking

Commonly used in railway vehicles, dynamic braking system converts the electric motor into a braking generator through a traction converter capable of controlling electrical parameters such as voltage and frequency. By switching the motor armature connections across the load, the electric motor works in generator mode and through armatures current reverses itself, generating a torque in the opposite direction of the rolling velocity. Essentially, the electric motor is able to convert kinetic energy into electricity determining electric braking.

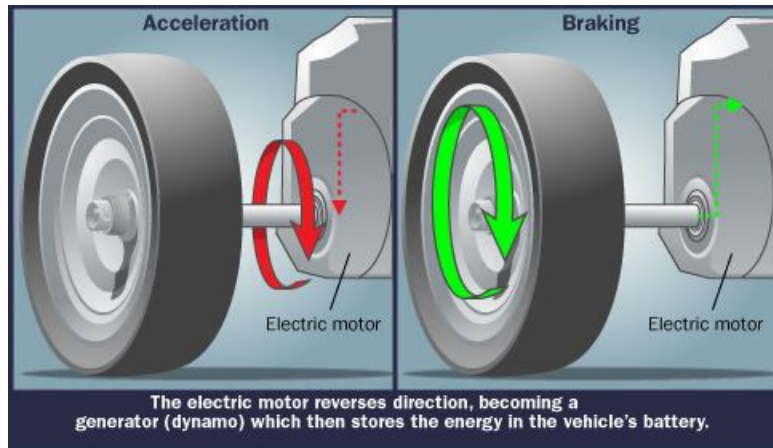


Figure 13 Dual operation of electric motor/generator. Source: [16]

This braking system is economic because it uses electromagnetic force instead of friction elements. In addition, ED braking allows precise regulation of braking forces, as well as the stability of the system operation [17]. On the other hand, dynamic braking cannot totally replace mechanical braking, thus the so-called brake blending is still required, especially in high-speed trains [11]. However, dynamic braking reduces maintenance and usage of friction braking.

Depending on the usage of the electricity generated during dynamic braking, it can be classified in rheostatic and regenerative braking. The former sends power generated by the motor-generator into a relatively simple resistor bank that dissipates energy into heat to the surrounding environment through a cooling system. On the contrary, regenerative braking can store braking energy into an energy storage system (ESS) or sends braking power back to the electrical grid. Generally, by using dynamic braking system, air quality improvement and noise reduction are achieved.

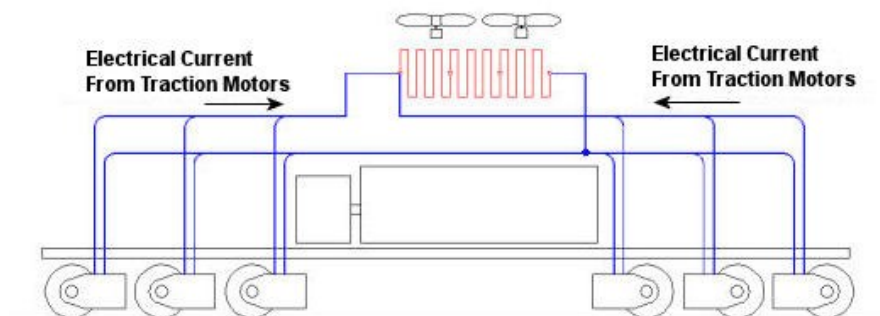


Figure 14 Principle of rheostatic braking. Source: [10]

Although rheostatic braking allows a more precise regulation of braking effort compared to the mechanical braking, braking energy is wasted into heat, thus this system only improves braking control with no regards to efficiency. By the way, rheostatic braking is widely diffused because of its low cost and its very low maintenance [18].

It is well known that electricity is a valuable form of energy, therefore a remarkable amount of high-quality energy is lost when there is no chance to feed back energy to the grid or to an EES. Thanks to researcher efforts, recently energy storage technologies have reached capacity large enough to harvest large amount of energy in very short time (high power energy storage device), which is very suitable in railway vehicle applications.

3. Energy saving strategies and analysis

Since diesel engine efficiency is generally not higher than 40%, about 60% of the primary energy is wasted through the cooling system and exhaust gas. Therefore, it is reasonable to consider strategies capable of harvesting part of that energy through heat recovery process that obviously needs a thermal load such as heat exchanger/evaporator could be.

From an energetic point of view, exhaust gas has great energy potential because of its high temperature (about 500°C), but it also has a large range of operative temperature due to regulation at partial loads of the diesel engine. This feature can significantly affect power production and further complicate logic governing the heat recovery system. On the contrary, cooling water has a lower energy potential than exhaust gas (temperature about 90°C), but it shows a more stable operating temperature that implies easier control logic and almost constant power source. Regenerative braking seems to be the most promising option in terms of efficiency since it directly provides electrical power and no transformation from thermal to electrical power is involved.

In order to identify the most feasible, easy to integrate and effective energy recovery strategy, both diesel engine heat recovery and regenerative braking have been briefly analyzed in the pre-feasibility phase of this work. However, after an initial analysis, regenerative braking has resulted as the most promising strategy in terms of project complexity and potential amount of saved energy.

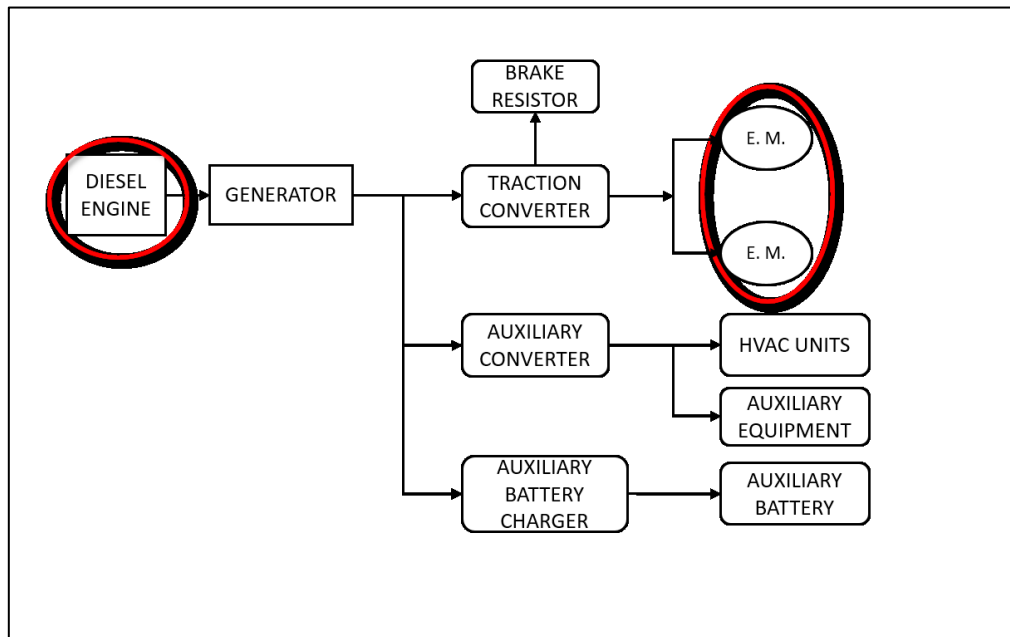


Figure 15 Identification of potential energy recovery sources

3.1 Exhaust gas combined with a steam cycle

As previously mentioned, a possible heat recovery process consists in deviating exhaust gas flow to a heat exchanger that acts as a steam generator for the subsequent steam cycle. Figure 16 below schematically describes a possible configuration of the heat recovery system. Since the amount of recovered energy strictly depends on exhaust gas temperature and mass flow, it is fundamental to know those technical parameters at different diesel engine loads.

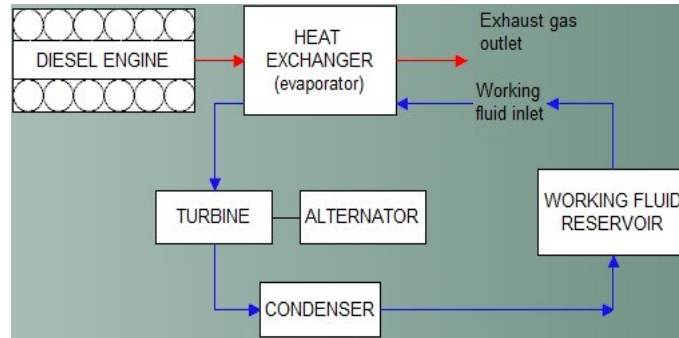
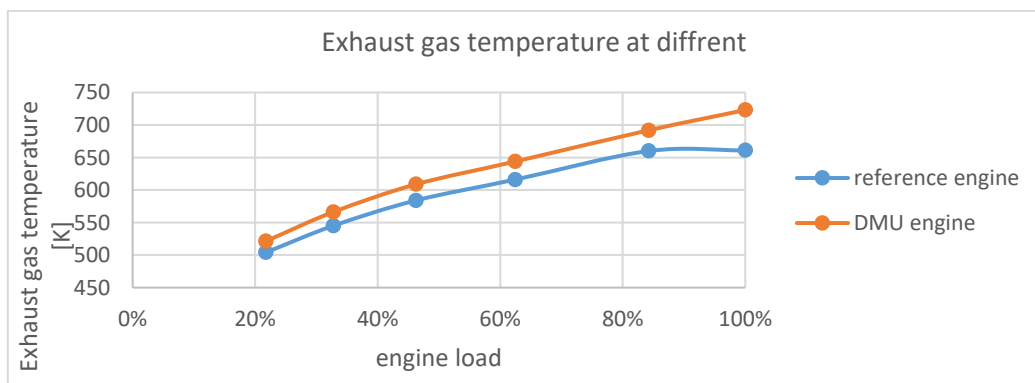


Figure 16 Heat recovery scheme for power production

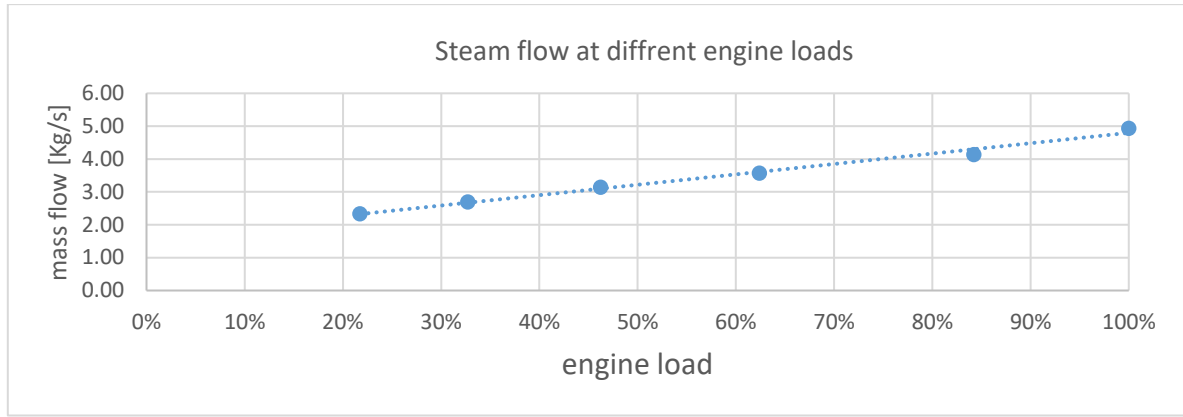
As Table 7 shows, the supplier provides specifications only on two operating points very close to each other and, as a consequence, it is difficult to extrapolate exhaust gas mass flow and temperature at partial loads. In the view of lack of data, engine parameters have been extrapolated through a similar engine those data were largely available at different loads.

Diesel engine D 2862 LE633			
	Peak torque	Rated power	
Power	588	570	[kW]
Speed	1800	2100	[rpm]
Torque	3120	2592	[Nm]
Exhaust Gas Power	440	470	[kW]
Exhaust Gas Temperature	450	440	[°C]
Exhaust Gas Mass Flow	59.67	65.25	[Kg/min]
Available Heat From Exhaust	299.3	315.6	[kW]

Table 7 Diesel engine specifications. Source: Engine Datasheet



Graph 1 Exhaust gas temperature at different engine loads



Graph 2 Exhaust gas mass flow at different engine loads

3.1.1 Methodology

The calculation of energy production is based on the previous assumptions and has been done for two tracks very different in energy demand. Parameters adopted in the calculation of the power production of the ideal steam cycle are summarized below.

- Turbine total efficiency = 80%;
- Isentropic turbine efficiency = 85%;
- Generator efficiency = 95%;
- Outdoor temperature = 35 °C.

	Pressure	Temperature	Enthalpy
	[bar]	[°C]	[kJ/Kg]
Pump Inlet	0.75	80	335
Heat Exchanger Inlet	20	80.23	337.5
Turbine Inlet	20	251	2905.8
Condenser Inlet	0.75	91.8	2418.7

Table 8 Steam thermodynamic properties adopted in the calculus

Additionally, in order to simplify the calculation, steam conditions at turbine inlet are assumed to be constant and consequently working fluid mass flow has to change according to exhaust gas power available. Since vehicle power demand and engine load are known beforehand, calculation of theoretical power production is based on the following steps:

1. Power of exhaust gas has been calculated as follows:

$$\text{Eq. (3.1)} \quad \dot{Q} = \dot{m} * c_p * (T_{in} - T_{out})$$

2. Supposing an efficiency of 75% of the heat exchanger, water receives a heat flow of:

$$\text{Eq. (3.2)} \quad Q_w = 0,75 * \dot{Q} \quad [W]$$

3. Since working fluid conditions are assumed to be constant at the turbine and heat exchanger inlet, steam flow changes as a function of available exhaust gas power:

$$\text{Eq. (3.3)} \quad \dot{m} = \frac{Q_w}{h_3 - h_2}$$

4. Once the mass flow is known, the turbine power and the electrical power output are calculated as follows:

$$\text{Eq. (3.4)} \quad P_{turbine} = \dot{m} * (h_3 - h_4)$$

$$\text{Eq. (3.5)} \quad P_{el} = \eta_{alt} * P_{turbine}$$

STEAM CYCLE RESULTS	Track 1	Track 2	
Average Engine Load	86%	80%	Kwh
Trainset Energy Produced	4.4	17.53	Kwh
Trainset Energy Required	85.9	350	Kwh
Energy Recovered Percentage	5%	5%	[-]
Steam Cycle Average Efficiency	11%	11%	[-]

Table 9 Results of the steam cycle calculation

Certainly, obtained results do not exactly reflect real production because of assumptions adopted in the calculation that, anyway, results useful for having an idea of the order of magnitude of the potential energy saved. Looking at Table 9 clearly this solution is not feasible because of the very low amount of theoretical recovered energy, despite the complexity of the whole system.

3.2 Exhaust gas combined with Organic Rankine Cycle

ORC for waste heat recovery works on the same basis of the previous steam cycle, but ORC takes advantage of lower evaporating temperature that should lead to a higher power production, even at low engine loads. Among the wide variety of organic fluids, the R245fa resulted suitable for heat recovery purpose because of its low boiling point, the low latent heat of evaporation and high density.

ORC works as described in the scheme of Figure 16, indeed exhaust gas flows into a heat exchanger where organic fluid evaporates, thereafter it expands in the turbine connected to the generator. R245fa allows a greater expansion rate of the cycle with respect to the steam cycle and, consequently, it leads to higher energy production.

	Pressure	Temperature	Enthalpy	State
	[Bar]	[°C]	[kJ/Kg]	
Pump inlet	2.5	40	251.0	Subcooled liquid
Heat exchanger inlet	20	40	253.7	Subcooled liquid
Turbine inlet	20	140	512.5	Superheated steam
Condenser inlet	2.5	57	450.9	Superheated steam

Table 10 Thermodynamic properties of R245fa

Taking into account same engine data adopted in steam cycle calculation and thermodynamic properties of the R245fa resumed in Table 10, the outcomes of ORC are listed in Table 11 below.

ORC RESULTS	Track 1	Track 2	
Single Car Energy Produced	1.35	4.91	Kwh
Trainset Energy Produced	5.41	19.63	Kwh
Trainset Energy Required	86	350	Kwh
Energy Recovered Percentage	5.1%	5.6%	[-]
ORC Cycle Average Efficiency	13%	13%	[-]

Table 11 Exhaust gas combined with ORC results

Because of the very low energy production and complexity of system integration, heat recovery based on ORC for power production seems inappropriate. In addition, this heat recovery strategy adds safety concerns to the existing project because of toxicity of R245fa (as the majority of organic fluids) in case of leakage.

3.3 Exhaust gas heat recovery for hot water production

Both previously analyzed energy recovery strategies involve the transformation of thermal to electrical power: this process introduces transformation that strongly affects the efficiency of the overall heat recovery system, producing discouraging results. Thereby, it is preferable to avoid energy transformations for enhancing the effectiveness of the energy saving strategy. From this point of view, a reasonable heat recovery strategy shall be the utilization of exhaust gas for hot water production, exploiting it for feeding thermal loads such as HVAC units or a radiant floor system. Despite its simplicity, this energy recovery strategy is hard to integrate since the existing vehicle is not equipped with a radiant floor system but with air-based heating/cooling system and additional electric heaters used for fast warming of the coach environment.

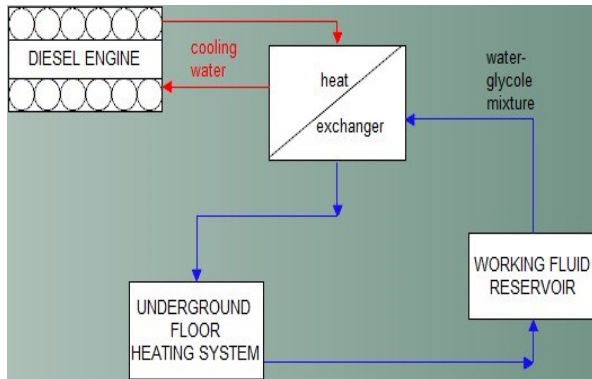


Figure 17 Ideal scheme of the heat recovery strategy

	Car 2	Car 4	
Available Surface	65.48	73.93	m ²
Floor heaters driver	0.5	[-]	kW
Compartment floor heaters (HVAC2)	7	7	kW
Compartment floor heaters (HVAC2)	7	7	kW
Total	14.5	14	kW
Required heat flow	221	189	W/m²

Table 12 Technical requirements of the underfloor heating system

From an energetic point of view, electrical heating is inappropriate and thus, it is interesting to evaluate the suitability of different heating systems such as feeding radiant floor system through hot water produced by recovering the heat of the exhaust gas.

Radiant floor is a quite straightforward technology based on hot water flowing in pipes under the floor: the most commercial solutions and sizing guide regard heating floor applications in residential buildings, where commonly floor is made of concrete or wood, both characterized by low thermal conductivity. DMU car floor materials, instead, completely differs from those adopted in residential buildings. Therefore, in the calculation of the thermal conductivity, the radiant floor structure has been considered as the pre-existing one, just adding necessary layers of the radiant floor.

Before proceeding to size process, it should be evaluated the capacity of the floor heating system to provide required thermal load, according to spatial constraints. Indeed, usually, the maximum floor heat flux should not exceed 100 W/m² because of thermal comfort issues.

Firstly, it is necessary to know the thermal load each car requires as well as available floor surface for installing the radiant floor. Thermal loads are different for each car and were already known thanks to existing DMU project.

Looking at the results of Table 12, clearly, the required heat flow is very high and exceeds 100 W/m² that is the maximum allowable value on this type of system. Indeed, higher values of heat flux decrease thermal comfort of the environment because of the large temperature gradient from bottom to top. In addition, this application involves a significant change of the existing DMU model, thus this heat recovery strategy has been abandoned.

3.4 Regenerative braking

Regenerative braking (RB) is a process able to harvest part of the vehicle kinetic energy, using it for later use such as to re-accelerate the vehicle or to feed auxiliary equipment [19]. RB takes advantage of electric motor behavior to act as a generator.

The regenerative braking is very effective since it can supply up to 30% of the overall traction energy demand [6, 20]. Moreover, regenerative braking returns “additional” energy for a given energy input, thus efficiency of the vehicle increases and GHG emissions decrease since the vehicle can cover a given distance using a smaller amount of fuel [19]. According with [21], CO₂ emissions can be reduced by 15% and 30% when regenerative braking is applied to intercity trains and suburban commuter trains, respectively. On the other hand, RB is not very effective at low speed and mechanical braking is still required, especially in emergency operations when RB is not able to stop the vehicle in the required time and distance [22].

The amount of available braking energy depends on intensity, frequency, and duration of the braking phase [19], thus RB is very suitable for commuter trains or intercity subways which stop frequently. The portion of recovered energy depends on motor efficiency and power capacity of the power control system, as well as by the grid receptivity if power is sent back to the grid. However, when regenerative energy is stored, the most limiting issue regards energy storage system, in particular, the most critical points are capacity acceptance in heavy braking events [6] and the optimization of the problem during braking operations [23].

Essentially, the regenerative energy can be expressed as following balance equation:

Eq. (3.6)
$$\text{Initial kinetic energy} = \Delta \text{Stored Energy} + \text{Energy Lost}$$

Eq. (3.7)
$$\text{Initial kinetic energy} = \frac{1}{2} * \text{vehicle mass} * (\text{velocity})^2$$



Figure 18 Different power supply systems for urban rail vehicles. Source: [7]

Typically, road-vehicles are lighter than railway vehicles and (on average) velocity is much lower in city driving than that of the railway vehicles, thereby road-vehicles involve a smaller amount of kinetic energy in braking events. This disproportion affects the choice and availability of ESSs that must have much higher energy and power capacity when train-mounted. As an example, a 4 wagons train weights around 200 tons and requires more than 1MW of braking power [23]. This huge amount of energy and power have been a very strong limit for onboard ESS diffusion in rail sector until the recent development of high-capacity batteries and super-capacitors.

3.4.1 Regenerative braking and power grid issues

In electrified railway networks, power is provided by overhead wire or third rail systems connected to the public grid, thus in these situations, braking power can be fed back to the power supply grid. This is possible if:

- 1) A vehicle decelerates meanwhile another vehicle requires power to accelerate nearby.
- 2) The electrified line is powered in AC mode, otherwise, reversible substations or inverters are required to overcome the unidirectional rectifiers between the public grid and DC catenary [24].
- 3) The line receptivity is high enough to absorb the regenerative energy, otherwise, the line voltage increases and damages can occur.

More in detail, considering a third-rail power supply system, when the train decelerates closely to the arrival station, the third-rail voltage raises very quickly and the regenerative energy can feed another train that is departing: in this case, the braking time must be short and the third rail voltage quickly returns to the rated value. Otherwise, when braking is long lasting the regenerative energy could be used to feed other loads of the arrival station, slowly decreasing the third rail voltage [21]. This last operational mode is shown in Figure 19 where braking energy feeds low-voltage grid through the connection between third rail and low voltage grid, obviously this process is not always possible if any loads require power.

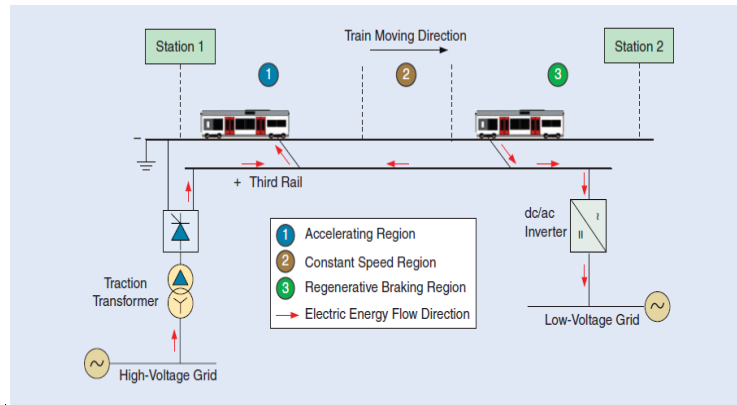


Figure 19 Scheme of regenerative braking energy sent back to the grid. Source: [21]

Actually, ESS represents one of the most effective methods to overcome grid concerns such as line-voltage fluctuations or peak power reduction in stationary applications, while in onboard applications, among other purposes, ESS can allow trains to travel in non-electrified sections thanks to the stored *regenerative* energy used to feed electric motors and auxiliary equipment. In addition, when a vehicle is equipped with onboard ESS, the vehicle rheostat can be downsized because a smaller amount of braking energy has to be dissipated.

In stationary applications, ESS can stabilize grid voltage or cover peak power demands as well as ensure continuity of service (UPS applications). Whereas onboard stored energy can be used for different purposes such as:

- 1) Energy demand and GHG emissions reduction because of the braking energy recovery;
- 2) Feeding auxiliary equipment such as HVAC systems;
- 3) Allowing catenary-free operations;
- 4) Propelling DMU trains in tunnels and galleries where diesel engine cannot work because of safety issues;

3.5 Considerations on energy recovery strategies

This paragraph aims to summarize pro and cons of the previously analyzed heat recovery strategies as well as to highlight motivations that led me to focus this dissertation on regenerative braking such as most effective and feasible energy-saving strategy.

Exhaust gas heat recovery combined with the steam cycle for power production is mature and developed technology. In addition, exhaust gas has great energy recovery potential due to its high temperature (about 500°C) that dramatically decreases at partial engine loads, affecting power production. Furthermore, it should be noted that steam system start-up period could last almost one hour and this is unacceptable compared with the operative time of the selected application. Moreover, taking into account dimensional constraints and a small amount of power production, exhaust gas heat recovery strategy has not been further investigated.

Issues regarding steam cycle are still valid for the exhaust gas combined with the ORC application. Additionally, organic fluid toxicity adds safety concerns that cannot be ignored and unjustifiable because of low efficiency of the system and the small amount of power production. For these reasons, even this energy recovery strategy has not been object of further developments.

Heat recovery for hot water production is the most efficient heat recovery strategy since it exploits direct thermal energy usage, avoiding energy transformations that significantly affect the efficiency of the whole system.

On the one hand, radiant floor application enhances the thermal comfort of the coach environment and strongly reduces the use of electrical heaters and consequently its energy consumption. On the other hand, the retrofitting process has been considered unfeasible by Blue Engineering's team because underfloor heating system leads to re-designing large part of the electrical system and introduces further changes of the existing DMU project.

Based on the aforementioned considerations and thorough research activity focused on the state of the art of hybrid railway vehicles, harvesting braking energy through an onboard energy storage system (OESS) seems the most promising, effective, feasible and valuable energy recovery strategy for the DMU train subject of this dissertation.

Regenerative braking takes advantage of a direct electrical energy recovery generated by electrical motors during braking phase. As it is well known, electrical energy is a valuable type of energy, but in the existing DMU model, electro-dynamic braking energy is wasted through the brake resistor bank.

According to Blue Engineering's team, the feasibility of installing an OESS has been in-depth analyzed, as next chapters describe. Firstly, I researched the most suitable energy storage technology for the on-board application.

4. Energy Storage Systems (ESS)

This chapter describes ESS technologies and provides some today's remarkable applications of them, with a special focus on train-mounted ESS. Actually, in the railway sector, the most diffused ES technologies for braking energy recovering are batteries, ultra-capacitors, and flywheel [23], although interest in fuel cells (FC) and superconducting magnetic energy storage (SMES) is growing, these last two technologies are still not widely adopted. Essentially, each technology can be used in onboard (OESS) and in stationary applications (SESS), however, the choice strictly depends on the specific application.

SESS have more freedom in sizing process than OESS, indeed OESS should be compact in size and should have long charge/discharge lifecycle and fast charge/discharge time because of operational issues in railway transport sector [23]. In general terms, ESSs should be easily fixed and should require low maintenance costs [21]. Moreover, important parameters in the choice of ESS are specific energy and power density since weight, volume and capacity requirements are more critical points in onboard than in stationary applications.

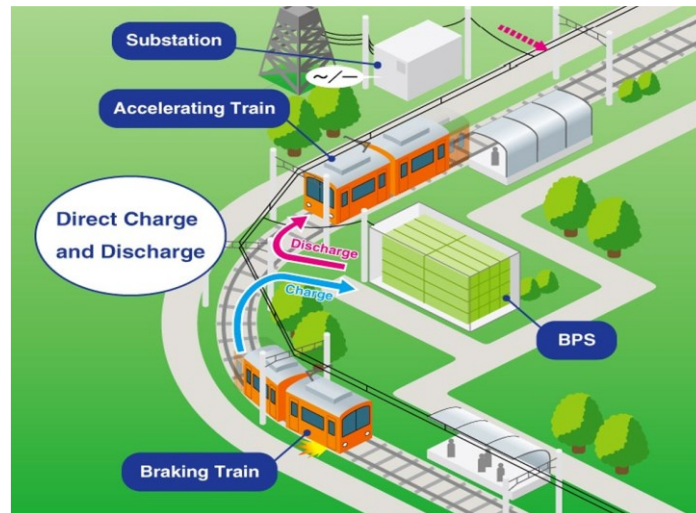


Figure 20 Example of stationary energy storage system. Source: [25]

All these technical constraints lead to a complex design process that shall be optimized taking into account technical-economic targets such as minimizing energy consumption or investment payback time, without affecting vehicle performance. Indeed, according to [26], OESSs are not always a feasible option in technical-economic terms, especially in heavy haul trains.

Based on these issues, this dissertation wants to analyze feasibility, effects and technical-economic limits of an OESS fitted on a DMU train-set in order to harvest regenerative braking energy and to propel DMU train-set through the energy stored in the OESS.

Because of the aforementioned issues, an overview of ESS technologies is provided in the chapters in order to get a better understanding of their working principle and their different individual characteristics that have been considered in the choice of ESS in each specific application.

First of all, ESSs can store energy in different ways and forms such as mechanical for flywheel-based ESS or chemical and electrostatic in batteries and ultra-capacitors respectively. Each technology has different characteristics that should match with operational requirements such the afore-mentioned charge/discharge time. Figure 21 gives an idea on different features of ES technologies. The next chapter provides a more detailed description of most diffused ES technologies in the railway sector.

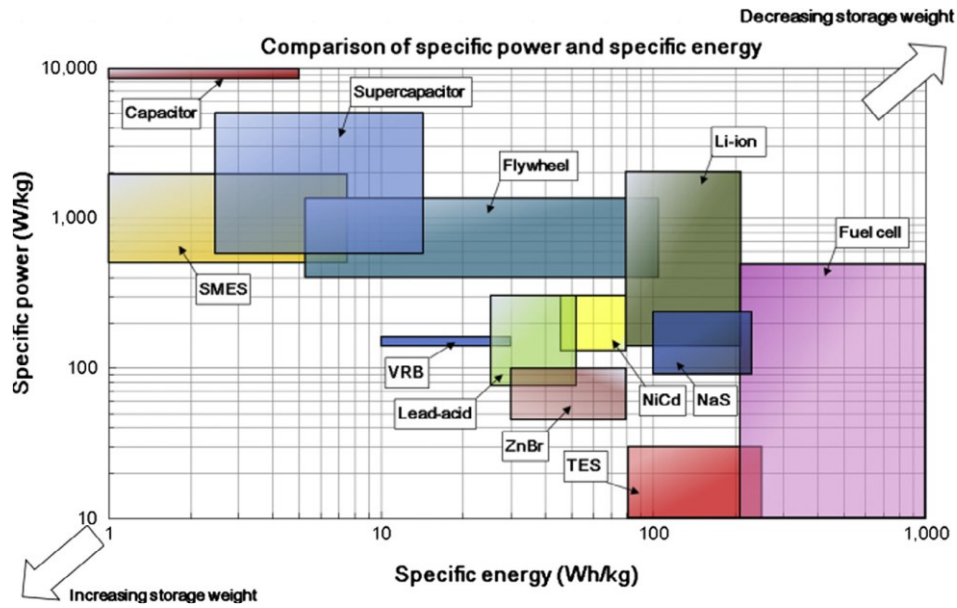


Figure 21 Comparison of specific energy and specific power for different ES technologies. Source:[27]

4.1 Batteries

A battery is an electrochemical device able to store energy based on the chemical reaction that makes electrons free to move from anode to cathode and backward through a solid or liquid electrolyte. As shown in Figure 22, actually, batteries are available in a wide range of sizes and power ratings on the market, but the choice of chemistry will depend on response time, energy and power ratings and operating temperature required from the specific application[28]. In addition, generally, batteries can provide higher energy capacity and lower voltage fluctuation with respect of ultra-capacitors [23].

The battery was used for energy storage purpose since mid-1800, when the most common battery was the Lead-Acid type that still has low energy and power density for onboard applications, despite several improvements have been done up today [29]. Nowadays, according with [7, 23] the most common batteries in railway transportation are Nickel-Cadmium (*Ni-Cd*), Nickel-Metal Hydride (*Ni-MH*) and Lithium-Ion (*Li-Ion*) chemistries. Figure 22 shows individual characteristics in terms of specific energy and specific power of different battery chemistries. However, all batteries present a strong limitation in power intensity (i.e. rate at which battery can be charged/discharged), thus usually they cannot accept all the energy produced during regenerative braking and portion of it is still dissipated into resistors [30].

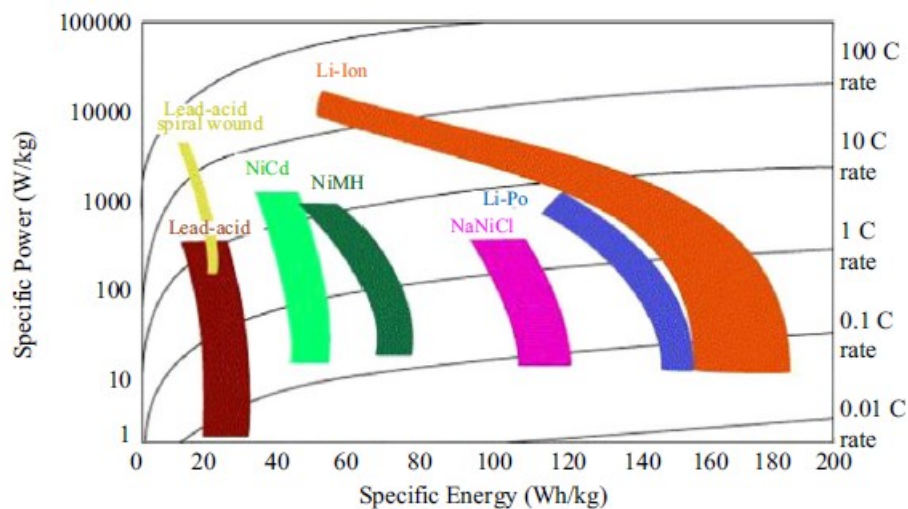


Figure 22 Specific Energy, Specific power and C-rate for different battery technologies. Source: [31]

A battery energy storage consists of a number of cells connected in series or parallel providing different configurations of rated voltages, energy capacity, and maximum allowable current, depending on manufacturer technical choices and chemistries used. Generally, batteries are able to bi-directionally convert energy between electrical and chemical energy [27]: during discharging, reactions occur at both electrodes simultaneously and electrons flow from anode to cathode where they are collected. During charging, the process is inverted by applying an external voltage to the electrodes.

Generally, main barriers of batteries are low cycling time, power limitation and high maintenance costs. In addition, the fact that lifetime strongly depends on Depth-of-Discharge (DOD) [23] [27] leads to the impossibility of using the overall cell/module capacity since generally a battery cannot be fully charged/discharged. To conclude, battery key-parameter list follows and in the next paragraphs a more detailed description of most diffused battery technology is provided.

Parameters:

- Energy and power density;
- Specific energy and power: (Wh/kg) and (W/kg) respectively;
- Calendar life: is the elapsed time before a battery becomes unusable whether it is in active use or inactive [32];
- Cycle life: is the number of complete charge - discharge cycles a battery can perform before its nominal capacity falls below 80% of its initial rated capacity [32];
- Cost per kWh, efficiency, and self-discharge level.

4.1.1 Nickel-Cadmium (Ni-Cd)

Since 1915, Ni-Cd battery was largely used technology for energy storage purpose and from 1970 to 1990 it was the choice for high-performance applications until the completed development of Nickel Metal Hydride battery in 1995 [33]. Ni-Cd battery uses cadmium hydroxide and nickel hydroxide as negative and positive electrodes immersed in a soluble electrolyte. Equations below shows chemical reactions at anode and cathode respectively: during discharge, reactions are from left to right and backward in charging operation [27].

- *Anode:* $Cd + OH^- \leftrightarrow Cd(OH)_2 + 2 e^-$
- *Cathode:*
 $2NiO(OH) + 2H_2O + 2e^- \leftrightarrow 2Ni(OH)_2 + 2 OH^-$
- *Overall reaction potential:*
 $E^0 = 1.0V \text{ to } 1.3V$

Ni-Cd batteries experience well operations even at low temperature (from $-20\text{ }^{\circ}C$ to $-40\text{ }^{\circ}C$), great resistance to deep discharge and low self-discharge. On the other hand, pronounced memory-effect and environmental concerns of cadmium usage are the main limits of this technology [29]. Other disadvantages of Ni-Cd batteries are the short lifecycle and the negative temperature coefficient that can cause thermal run-away [28].

Nevertheless, because of their high reliability and low maintenance, Ni-Cd batteries are very suitable for uninterruptible power supply (UPS) applications [34] as well as in spinning reserve services such in the application in Golden Valley, Alaska (US), where Ni-Cd battery facilities are able to provide 27 MW of rated power for 15 minutes or 40MW for 7 minutes [35]. However, the driving force behind choice in this application was due to very low operational temperatures (233K - 323K) [36]. Actually, Ni-Cd technology is mature and seems that it not will be heavily used for large-scale projects [27].

4.1.2 Nickel-Metal Hydride (Ni-MH)

Ni-MH batteries have been developed to overcome memory-effect of the previous Ni-Cd batteries as well as the fact that cadmium is an environmentally hazardous material. MH stands for Metal Hydride that consists into a hydrogen-absorbing alloy used as electrode material instead of cadmium. Reactions at anode and cathode are written below [27]:

- *Anode:*

$$MH + OH^- \leftrightarrow M + H_2O + e^-$$
- *Cathode:*

$$NiOOH + H_2O + e^- \leftrightarrow Ni(OH)_2 + OH^-$$
- *Overall reaction potential:*

$$E^0 = 1.0 \text{ V to } 1.3 \text{ V}$$

On the one hand, Ni-MH batteries have higher energy density than Ni-Cd (170 Wh/L to 420 Wh/L [37]) and longer lifecycle than Lithium-Ion batteries [37], thereby they are suitable for portable products and UPS applications [33, 37, 38]. From the 1990s to 2000s, Ni-MH batteries have been also the choice in hybrid and fully electric vehicles (HEV and EV) because of the relatively high power density, very long life at partial SOC and proven safety because water is split and recombined when the battery is overcharged [28, 39] reducing thermal run-away hazardous. On the other hand, Ni-MH batteries have high self-discharge (up to 20% of its capacity in the first 24h) and moreover, they are also very sensitive to deep cycling that strongly reduces lifecycle to some hundreds of cycles [40]. Looking at applications of Ni-MH batteries, Figure 23 displays that they are utilized in different HEV and EV directly competing with Li-ion batteries described next. However, according with [7, 41], Ni-MH battery applications on Light Rail Vehicle (LRV) and Trams have been done also.

Company	Country	Vehicle model	Battery technology
GM	USA	Chevy-Volt	Li-ion
		Saturn Vue Hybrid	NiMH
Ford	USA	Escape, Fusion, MKZ HEV	NiMH
		Escape PHEV	Li-ion
Toyota	Japan	Prius, Lexus	NiMH
Honda	Japan	Civic, Insight	NiMH
Hyundai	South Korea	Sonata	Lithium polymer
Chrysler	USA	Chrysler 200C EV	Li-ion
BMW	Germany	X6	NiMH
		Mini E (2012)	Li-ion
BYD	China	E6	Li-ion
Daimler Benz	Germany	ML450, S400	NiMH
		Smart EV (2010)	Li-ion
Mitsubishi	Japan	iMiEV (2010)	Li-ion
Nissan	Japan	Altima	NiMH
		Leaf EV (2010)	Li-ion
Tesla	USA	Roadster (2009)	Li-ion
Think	Norway	Think EV	Li-ion, Sodium/Metal Chloride

Figure 23 List of EV and HEV using different battery technologies. Source:[42]

More in detail, since 2007 in Nice, twenty *Citadis-302* LRV vehicles operate in a catenary-less mode, thanks to Ni-MH battery pack produced by SAFT. LRV is battery powered when they cross Place Garibaldi and Place Massèna for a distance of 500m each. In this case, battery pack shall provide an operational life of at least 5 years and shall ensure tram velocity up to 30km/h with air-conditioning operation [41]. The battery pack consists of 408 battery cells achieving rated values of weight, maximum power and installed energy of 1450 kg, 200kW and 27.7 kWh respectively [43].

However, this application highlighted Ni-MH batteries have a relatively limited range of operation (such as low-speed operation only) and long recharge time with respect to super-capacitors [41]. On the other

hand, Ni-MH batteries were the choice because they offer a good compromise between performance, weight and lifecycle cost [44].



Figure 24 SWIMO by Kawasaki Heavy Industry Ltd (left) and ALSTOM Citadis (right) in catenary-free operation in Nice (France) and Sapporo respectively. Source:[7, 25]

Another relatively recent improvement of Ni-MH technology has been done by Kawasaki Heavy Industries that developed GIGACELL®, a large-sized high-power battery module that has been tested in different application such as Battery Power System (BPS) and OESS on the SWIMO-X® LRV. Indeed, since December 2007 to March 2008, the battery-driven SWIMO-X® was tested on the experimental track in Sapporo (Japan). SWIMO-X® requires a peak power of 250kW, the maximum speed of 40 km/h [45] and is able to cover up to 10 km of non-electrified line by using 16 on-board GIGACELL® modules (115 kWh) without recharging them [25].



Figure 25 SITRAS-HES by Siemens Mobility



Figure 26 GIGACELL module by Kawasaki Heavy Industry Ltd.

As a side note, other two applications of GIGACELL® Ni-MH batteries have to be mentioned. The first has been done in New York City where 400kWh SESS has been installed to stabilize the voltage of a third-rail power supply system. As result, stabilization of 55V (from 673V-555V to 671V-608V), smoother voltage waveform and peak power demand reduction were obtained [46]. The second application has been done by SIEMENS, the SITRAS-HES® essentially consists into a hybrid OESS combining Ni-MH batteries (18 kWh) and super-capacitors (0.85 kWh) for a total weight of 1646 kg [47]. The SITRAS-HES® has found its application on 19 AVENIO vehicles that operate in completely catenary-free operations along an 11.5 km line in Doha Education City (Qatar) [48]; furthermore, in Lisbon (Portugal), redesigned COMBINO vehicles run between Almada and Seixal and can cover up to 2.5 km without being supplied from other power sources [49].



Figure 27 AVENIO vehicle in catenary-free operation, Doha (Qatar). Source: [48]



Figure 28 COMBINO operating in Portugal. Source: [49]

4.1.3 Lithium-Ion

Although this technology puts its origins in the late 60s, the first Lithium-ion battery (LIB) was commercialized by Sony Corp. in 1991 [50]. After decades of research, actually, LIBs are widely used in portable electronic devices such as laptops, smartphones as well as in HEV and full EV as shown in Figure 23. According with [23, 24, 27, 31] LIBs are very promising technology for traction power supply systems.

Despite to other batteries, LIBs have a distinctive characteristic because of its internal structure and operation of lithium-particles. Indeed, at the electrodes, reactions consist of insertion and extraction of lithium ions from/to electrodes, therefore no side reactions and no morphological changes happen [51]. As consequence of no presence of side reaction, longer life is expected [52] and confirmed from several researches[23, 27, 31, 53].

During charging operation, the negative electrode acts as a “lithium sink” and the positive as a “lithium source”, this process is inverted during discharge. It is to be noted that the accepting/releasing ions is a crucial point to ensure longer battery life which actually is one of the most crucial points of this technology [54]. Reactions at anode and cathode for a generic LIB follows [27]:

- *Anode:*

$$C + nLi^+ + ne^- \leftrightarrow Li_nC$$
- *Cathode:*

$$LiXXO_2 \leftrightarrow Li_{1-n}XXO_2 + nLi^+ + ne^-$$
- *Overall reaction potential:*

$$E^0 = 3.7 V$$

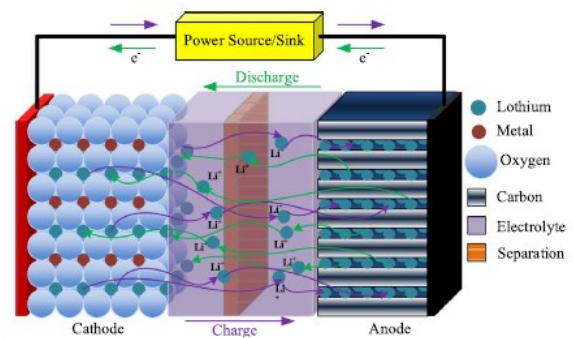


Figure 29 Schematic operating principle of a Li-ion battery. Source:

In LIBs, the electrolyte is typically a lithium salt (i.e. $LiClO_4$) dissolved into a non-aqueous organic liquid, nevertheless, polymer-based electrolytes have been developed to increase power acceptance of LIBs and actually they are relatively mature for the market [54]. The cathode is made of lithium metal-oxide while the anode is commonly composed of a carbon-matrix [55] which recently is going to be replaced with nanostructured materials such $Li_4Ti_5O_{12}$. An example of the application of these novel

materials can be seen in [55] where faster charging/discharging time was obtained. However, since several materials have been more and more tested in order to increase performances of LIBs, nowadays a variety of anode and cathode materials are available on the market. Figure 30 shows a list of materials commonly used as electrodes and their characteristics.

	Lithium Iron Phosphate	Lithium Manganese Oxide	Lithium Titanate	Lithium Cobalt Oxide	Lithium Nickel Cobalt Aluminum	Lithium Nickel Manganese Cobalt
Cathode chemistry descriptor	LFP	LMO	LTO	LCO	NCA	NMC
Specific energy (Wh/kg)	80-130	105-120	70	120-150	80-220	140-180
Energy density (Wh/L)	220-250	250-265	130	250-450	210-600	325
Specific power (W/kg)	1400-2400	1000	750	600	1500-1900	500-3000
Power density (W/L)	4500	2000	1400	1200-3000	4000-5000	6500
Volts (per cell) (V)	3.2-3.3	3.8	2.2-2.3	3.6-3.8	3.6	3.6-3.7
Cycle life	1000-2000	>500	>4000	>700	>1000	1000-4000
Self-discharge (% per month)	<1%	5%	2-10%	1-5%	2-10%	1%
Cost (per kWh)	\$400-\$1200	\$400-\$900	\$600-\$2000	\$250-\$450	\$600-\$1000	\$500-\$900
Operating temperature range (°C)	-20 to +60	-20 to +60	-40 to +55	-20 to +60	-20 to +60	-20 to +55

Figure 30 Specification of different Lithium-ion battery chemistries. Source: [56]

Essentially, LIBs have the following advantageous features: high cell voltage (depending on cathode materials can reach up to 4.0 V, thus the number of cells in a battery pack can be lower), high specific energy up to $200 \frac{Wh}{kg}$ [31], operation temperature range can vary from $-40^{\circ}C$ to over $150^{\circ}C$ [57]. Moreover, LIBs have flat discharge characteristic, relatively long lifecycle, low memory effect, low self-discharge and cycle efficiency in the range of 95%-98% [58]. In addition, LIBs are more environmental friendly than Ni-Cd and Ni-MH [23], although safety issues regards electrolyte because of its combustibility [59].

On the other hand, LIBs are still very expensive and lifecycle strongly depends on temperature and dramatically decreases when a deep discharge is applied [60]. Moreover, another disadvantage of LIBs is the mandatory battery management system (BMS) that shall at least provide overvoltage, under-voltage and overcurrent protection as well as temperature control [28]. It should be noted that BMS increase weight and volume of the whole battery system, reducing the specific energy of the overall battery system in real life applications.

4.1.4 Applications of Lithium-Ion battery

This paragraph provides some recent and remarkable applications of LIB technology with special focus on railway vehicles equipped with OESS based on LIBs. As aforementioned, batteries cannot accept a great amount of power with respect to super-capacitors, this is a strong limit in applications that require high power such as train acceleration. For this reason, battery manufacturers are concentrating their efforts to produce batteries capable to be charged/discharged at high current (hundreds of Ampere). Some of these products are described as follows.

GS Yuasa and Mitsubishi Heavy Industries Ltd (MHI) have recently developed two LMO-based battery characterized by high C-rate (C-rate express the discharge capacity of the battery). GS Yuasa has launched on the market the *LIM series*, in particular, the LIM-25H module can be charged up to 90% of State-of-Charge (SOC) within 10 minutes and discharged up to 24C [61]. in 2012, MHI developed the P140 and P060 LMO-based module that can be discharged at 8C and 15C (300 A) respectively [62].

Rated capacity (Ah)	25
Nominal voltage (V)	43.2
Maximum charging / discharging current (A)	Charge:600 (24C) Discharge: 600 (24C)
Operating temperature limits (°C)	Charge: -10~45 Discharge: -20~45
Weight (kg)	27

Table 13 Specifications of the GS Yuasa LIM25H-12.

Source: [63]



Figure 31 Twilight Express Mizukaze. Courtesy of West JR Company

The *LIM series* of GS Yuasa was the choice for the OESS in the retrofitted 87-series train adopted by West Japan Railway Company in the remote area of Japan. More in detail, the 87-series vehicle has been recalled “Twilight Express Mizukaze” and it is luxury hybrid DMU equipped with LMO-battery that allows the train to travel in the non-electrified section of Sanin Main Line [63]. Table 13 summarize characteristics of the LIM25H-12 adopted in the “Twilight Express Mizukaze” that started service in June 2017.

Another important application of LIBs in railway vehicles has been done thank to the cooperation of Hitachi Ltd. and the East Japan Railway Company (JR East) that developed a battery drive system for the JR Kyushu Series BEC819 and a hybrid drive system for JR East Series HB-E210 and HB-E300.

BEC819 can travel on electrified sections thank to the overhead wire contact system that supplies power to the whole train including the power to charge the battery pack. When the train is going on non-electrified sections, the required power is provided by a battery bank that consists into three modules of 72 high-energy batteries (*model CH75-6*) developed by Hitachi Chemical Company Ltd., for a total capacity of 360 kWh. The battery pack enables the train to cover a distance of 30 km without charging. The BEC819 began service in October 2016 [64].

For HB-E210 and the HB-E300 vehicles instead, the hybrid system consists into an internal combustion engine (ICE) and a battery pack that uses high-output density modules produced by Hitachi Automotive

Systems Ltd. (*model MA2a*). Both types of vehicle operate between Sendai and Ishinomaki, connecting Tohoku and Senseki lines that have different types of electrification.


Item	High output density
	
Model	MA2a (Hitachi Automotive Systems, Ltd.)
Configuration	48-cell series connection
Voltage/capacity	173 [V]/5.5 [Ah]
Energy density	46 [Wh/L] (100%)
Power density	865 [W/kg] (346%)
Features	<ul style="list-style-type: none"> • Compatibility between battery output and capacity that provides rapid high-charge performance for regenerative power charging • Thin module designed for onboard automotive use

Figure 32 Specifications of high output density modules.
Source: [64]



Figure 33 Series HB-E300 train. Source: [65]

In addition, in March 2014, JR East has placed in service the series EV-301 based on the previous encouraging results. This application has highlighted the following issues [66]:

- Battery pack changes its SOC from 69% to 89% within 10 minutes, matching requirements of the application;
- The optimal volume of battery pack depends on track characteristics.

Another more recent application of hybrid system on railway vehicle results in the new Electrostar class 379 in the UK. The collaboration between Bombardier Transportation and UK Network Rail (Department for transport) results in the first UK battery-powered train that entered trial service in 2015 in the Essex line. This project is part of the Future Railway Programme which includes the operator Greater Anglia and the Rail Executive Research Group [67].



Figure 34 IPEMU class 379. Source: [67].



Figure 35 On-board battery pack for the Series EV-E301.
Source: [66]

Electrostar class 379 has been called “Independently Powered Electric Multiple Unit” (IPEMU) since it can be powered from catenary in electrified sections, while in non-electrified sections a large capacity battery pack provides power for traction and auxiliary loads. Valence Technology Inc. supplied technical knowledge and provided battery pack composed of lithium iron magnesium phosphate (LiFeMgPO₄) or LMP cells. Valence Technology Inc. affirms that their own batteries are safer than LCO battery, in particular for thermal runaway [68]. Outcomes of the IPEMU trial test are still under evaluation,

although the expectation is a reduction about 20% of the running costs. However, it is important to highlight that IPEMU is the first UK's battery-powered train-set, thus it is expected that more railcars will be converted to become hybrid trains if outcomes of that test will be positive [69].

Looking at new materials adopted for achieving high-power modules in battery technology, Toshiba and Altairnano developed noteworthy products because of the use of lithium titanate electrode. More in detail, the former has developed the SCiB® module, the 20Ah module has high specific power (2200 W/kg) and can be quickly recharged up to 80% of SOC within 6 minutes [70]. Altairnano developed a nanostructured material and its application is found in the nano lithium-titanate battery module described in the table below. It is remarkable that the module can handle up to 36.3 kW and 22.6 kW, in charge and discharge respectively. In addition to the aforementioned applications, Table 15 provides additional applications LIBs in hybrid railway vehicles.

Altairnano 24V-70Ah module	
Voltage range	17.0 V – 27.5 V
Energy discharge capacity @ 1C	1450 Wh
Specific power (discharge-charge)	806-1,296 W/kg
Specific energy	51.8 Wh/kg
Weight	28 kg

Table 14 Specifications of Altairnano LTO module



Figure 36 24V-70Ah Altairnano module

Model (abbreviated name)	HD300	HB-E300	LFX-300 ameri TRAM	DGBC2 Smart BEST	223 series	817 series DENCHA	EV-E301 ACCUM	HB-E210
Owner	Japan Freight Railway Company (JR Freight)	JR East	Kinki Sharyo	Kinki Sharyo	JR West	Kyushu Railway Company (JR Kyushu)	JR East	JR East
Month and year of production	Mar. 2010	Jun. 2010	Jul. 2010	Oct. 2012	Feb. 2013	Mar. 2013	Jan. 2014	Jan. 2015
Power supply system	Diesel engine and lithium-ion battery (67.2 kWh)	Diesel engine and lithium-ion battery (15.2 kWh)	Switching between overhead contact line and lithium-ion battery (40 kWh)	Diesel engine and lithium-ion battery (72 kWh)	Switching between overhead contact line and lithium-ion battery (102 kWh)	Overhead contact line (AC) or lithium-ion battery (83 kWh)	Overhead contact line or lithium-ion battery (190 kWh)	Diesel engine and lithium-ion battery (15.2 kWh)
Remarks	To replace DE10	tourist version of Kiha E200				Commercial vehicles to be produced.		
Commercial operation	Started	Started					Started	Started

Table 15 List of hybrid battery-driven railway vehicles. Source: [71]

4.2 Super-capacitors

A capacitor consists of two metal foils (electrodes) separated by a dielectric material that usually is made of ceramic, glass or plastic film. Capacitors store energy because of the electric field generated by opposite charges that occur on the electrodes' surface when a voltage is applied [27]. Capacitors are well-known technology, but they have limited capacity, low energy density, and high self-discharge. To overcome these limits, electrochemical double-layer capacitors (EDLC) have been developed rising energy density and capacity.

Since the energy stored also depends on the surface area of electrodes, nanostructured materials such carbon-based material or ultra-small silicon nanoparticles are used, in order to increase the area to host electrons [72]. In addition, EDLC does not use the conventional dielectric material because electrodes are separated electrochemically, thus for a given volume surface area of electrodes is larger than that capacitor [30]. In capacitors and EDLC, the stored energy can be calculated using the following equation:

$$Q = C * V = \frac{A * \epsilon}{d} \quad \text{Eq. (4.1)}$$

where C is the capacitance, V is the applied voltage, A is the surface area of electrodes, d is the distance between them and ϵ is the permittivity of the dielectric material [28].

The main feature of EDLC is the very high lifecycle (more than 10^5 cycles) and high efficiency 84% to 97% [34]. In addition, EDLC can be charged/discharged faster than batteries, are almost maintenance-free and can work in a wide range of temperature. Moreover EDLC has power capability around 3-6 times higher than lithium battery [73], on the contrary, specific energy is ten times lower of conventional batteries [58]. On the other hand, due to the thin layer of the separator and the very short distance between plates, EDLC have low rated voltage, typically about 2-3 V [28].

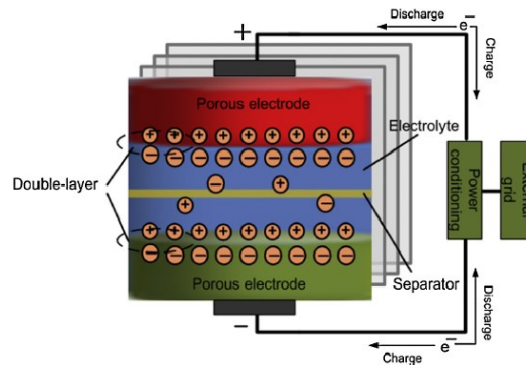


Figure 37 Schematic diagram of a super-capacitor. Source:[27]

Recently, EDLC has been adopted in power applications and hybrid system such as the aforementioned SITRAS-SES® that combines battery and EDLC, taking advantage of different characteristics of both: high power density for EDLC and high specific energy of batteries. Furthermore, because of their characteristics, EDLC are suitable in applications that require large number of fast charge/discharge cycles, such the case of voltage stabilization application or in some EV & HEV applications where EDLC are used to store braking energy and to extend battery life which will be less stressed by fast charge/discharge cycles [60] [74]. However, EDLC because of its high power density and short time of charge/discharge is typically used in urban LRVs to cover short distance (less than 10 km) with frequent and fast acceleration/deceleration events [48].

As batteries, EDLC can operate as SESS in two different operation modes: in energy saving applications, EDLC absorbs and store braking energy until the vehicle reaccelerate. Whereas, in voltage stabilization applications energy level is kept high and energy is released when the voltage falls down [75].

Looking at onboard applications, EDLC has principally used for power assist during acceleration and for regenerative braking. Recently, EDLC also takes place in hybrid systems combining their high power capability with the high energy density of batteries [23].



Figure 38 Roof-mounted MITRAC Energy Saver on LRV in Mannheim. Source:[76]

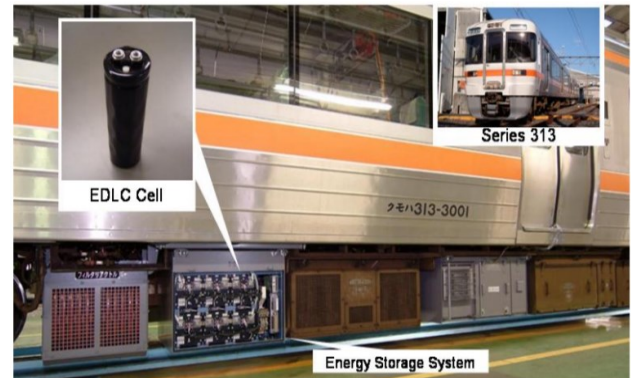


Figure 39 Series-313 equipped with EDLC. Source: [77]

From 2003 to 2007, a remarkable application of EDLC for recovery braking energy involved Bombardier Transportation that developed MITRAC® Energy Saver: an OESS that enabled a prototype LRV, operative in Mannheim (Germany), to save up to 30% of traction energy. Ultra-capacitors used in the MITRAC® have a specific energy of 6 Wh/kg and very high power density (6 kW/kg); basically, in this application, EDLC was preferred to NiMH batteries because of their poor power cycle capability [76]. However, the amount of saved energy could vary according to speed limits and track parameters such as slope and number and distance of stops. Indeed, according with simulations of [78], EDLC can save from 10.4% up to 16.2% when applied on Suburban and Regional DMU vehicles. In addition, that simulation shows that up to 26% of fuel saving can be achieved by using a hybrid system of EDLC and lithium batteries.

Another important facility of EDLC has been done on the existing *Series 313* vehicles that operate in the Chuo Line in Japan. The retrofitted vehicles achieved 1.6% of energy saving compared with the existing not-retrofitted vehicles; each vehicle is equipped with 570 EDLC cells with rated values of maximum power, installed energy and weight of 200 kW, 0.28 kWh and 430 kg respectively [43].

Moreover, Alstom and RATP (a public transport operator) have collaborated in the STEEM project that aims to improve the energy efficiency of railway vehicles. As result of the project, an EDLC-equipped *Citadis* vehicle was launched on the tramway T3 of Paris, in late 2009. The STEEM vehicle is normally powered by overhead contact line and uses EDLC bank for a distance of 300 m, achieving daily energy reduction of 13% [79].

To conclude, in [48] a list (updated until October 2015) of EDLC-equipped railway vehicles is provided and it is clear the most on-board EDLC applications have done on vehicles that run in urban tracks no longer than some hundreds of meters. Thus, EDLC is not very suitable for long distance because of the relatively low energy density and the mandatory presence of intermediate recharge stations.

4.3 Flywheel

The flywheel is the earlier mechanical energy storage system and it is based on rotational object able to maintain its rotational kinetic energy for a long time through its own inertia. After 1784, the flywheel has been used as energy accumulator on steam engines boats, trains and factories [80], however over the time flywheel's shapes and materials have been developed to increase rotational speed, efficiency, and capacitance. Indeed, in the 1960s and 1970s, flywheels took place in space missions, early EV, and stationary power back-up applications. This enhancement was principally possible because of new fiber composite materials [81]. In addition, recent improvements in high-speed electric machines, magnetic bearings, and power electronics have been crucial to make flywheel a solid option in ESS [82, 83] for traction power system and stationary applications.

In modern flywheels the rotating mass is driven by an electrical motor-generator (MG) that performs the conversion of electrical energy into mechanical energy and vice versa: the flywheel increases its rotational velocity in charging operation, whereas in discharging operation rotational speed decreases because of the resistant torque applied by the generator. It is remarkable that flywheel and MG are coaxially connected, thereby the speed control of the MG enables to control the flywheel's speed also [84].

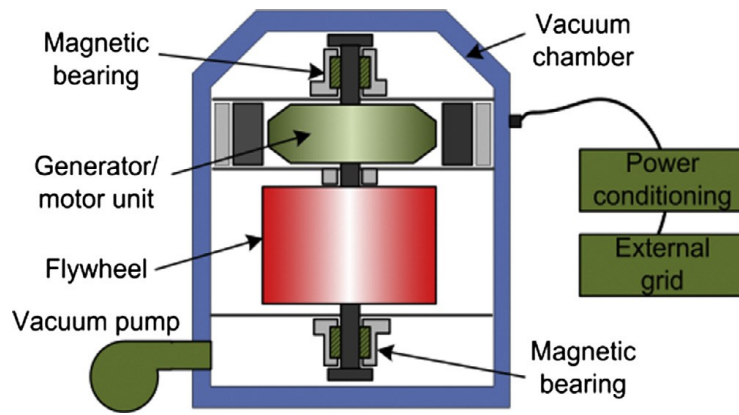


Figure 40 Scheme of a modern flywheel. Source: [27]

The flywheel's stored energy E is described as follows:

$$\text{Eq. (4.2)} \quad E = \frac{1}{2} * I * \omega^2$$

where I is the moment of inertia that depends on the shape and mass of the rotor, ω is the rotational speed or angular velocity. It should be noted that in practical applications, the useful energy stored is comprised within the range of ω_{\max} and ω_{\min} , thus:

$$\text{Eq. (4.3)} \quad E = \frac{1}{2} * I * (\omega_{\max}^2 - \omega_{\min}^2)$$

According to equation Eq. (4.3), the stored energy linearly depends on the moment of inertia while depends on the square of the angular velocity, thus increasing the maximum velocity is more effective than increasing the moment of inertia and thus the mass in order to achieve higher energy density. However, the maximum velocity is limited because of the strength of the rotor material due to centrifugal forces. Nowadays, flywheels are generally classified into low-speed class up to 10,000 rpm and high-speed class up to 100,000 rpm [85].

The high-speed flywheels typically use magnetic bearings and rotate in a vacuum environment to mitigate wear bearings and ventilation losses respectively [27]. Low-speed flywheels are common in short-term and medium/high power applications, whereas high-speed flywheel is expanding its application field mainly in power quality applications such as aerospace industry and wind power system.

Advantages of flywheel technology are long lifecycle (hundreds of thousands), very low maintenance, long calendar life and high capability to transfer high power within few seconds [80, 86]. In addition, since power and energy ratings of the flywheel are independent, each of them can be optimized taking into account specific application requirements [87]. On the other hand, flywheel have high self-discharge up to 20% of the stored energy can be lost within one hour [58, 88], furthermore, flywheel rotors can be hazardous if not well designed.

Flywheels are commonly used in UPS, power quality (such as voltage and frequency regulation), HEV & EV applications or wherever high power and short energy-release time is required [87]. Moreover, the rail traction industry expressed interests to flywheel technology for trackside voltage support and onboard applications for energy storage purpose [89]: a remarkable flywheel trackside application has been studied in [90] showing improvements of energy efficiency up to 21.6% and 22.6% for single and multiple trains respectively. Furthermore, in South Korea flywheels have been installed for peak power reduction purpose on the Panam-Banseok line, achieving peak reduction up to 36.7%, an energy saving of 48 MWh, as well as financial improvement of 24,000 \$/month [91].

Recently, on-board flywheel simulations have been developed in [92] that shows both feasibility of installing flywheel on LRV and that energy saving can be up to 31.2%, although it strictly depends on track characteristics, payload and number of vehicles per train-set. Moreover, encouraging results are shown in [93], the study is based on real measurements of heavy haul locomotives equipped with flywheel OESS, research's outcomes shows fuel and CO reduction can be up to 16.65% and 18% respectively, compared with existing vehicles that operate in the Newcastle-Ulan line in Australia.

Furthermore, Ricardo Company in the last years is concentrating on a high-speed flywheel technology that is still in the testing phase on the high-efficiency Excavator. This technology has the particularity to be axle-mounted on wheels and first tests show a reduction of fuel usage around 50% [94].



Figure 41 Roof-mounted flywheel on the Citadis operating in Rotterdam. Source: [44]



Figure 42 Prototype of the wheel-mounted flywheel system developed by Ricardo. Source:[94]

In conclusion, flywheel offers very high lifecycle and calendar life, instant response and high power capability. These are key parameters in applications such as UPS, power quality, and energy storage in renewable power plants, thus flywheel will have a clear and important role in the future, even if the future Li-ion batteries and other chemistries will be cheaper than today.

4.4 Selection of the Energy Storage System

Based on the previous research on the available energy storage technologies, Li-Ion batteries are quite common in railway field as stationary or as onboard ESS. A moderate number of applications show that batteries are usually combined with super-capacitors since this kind of system puts together high energy density of the battery and high power density of super-capacitors. Since EDLC have low energy density, high self-discharge, and high power density, ESS purely based on super-capacitors seems more suitable for very short tracks and light rail vehicles.

On-board flywheel for braking energy recovery is still a not widespread technology in the railway sector, although flywheel has a modest number of stationary applications that shows high efficiency and several advantages such as peak shaving and voltage stabilizing.

Taking into account the above issues regarding energy storage technologies and powertrain characteristics of the concerned DMU model, a good choice for OESS seems to be lithium batteries. However, as shown in the previous paragraphs, there are many lithium-based battery chemistries available on the market and each of them presents different characteristics that could or not be advantageous, depending on the specific application.

More in detail, railway vehicles are characterized by high and short time power demand because of the very high in-rush current required by electric motors in the acceleration phase. This aspect deserves attention and has been considered as priority criteria in the choice of the Li-Ion chemistries adopted in the ESS.

From this perspective, LTO battery should be considered the most suitable lithium battery type since it releases and accepts current at very high C-rate, despite its lower voltage and specific energy with respect to other battery chemistries. Additionally, LTO batteries have a lifecycle of more than 5000 cycles, fast charging time and a large range of operating temperatures, all these features are essential in railway applications.

To conclude, the next chapter regards sizing and design process of the OESS based on LTO battery module developed by Toshiba Corp. In addition, a dynamic simulation of the battery pack behavior has been developed in Matlab environment, in order to estimate the amount of braking energy recovered effectively.

5. Case Study

This chapter provides a comprehensive description of the retrofit action that essentially consists of the substitution of one of the four existing diesel engines with the OESS. Besides allowing ED braking energy recovery, this choice enables the vehicle to operate in a wider range operation (i.e. underground section) and to reduce pollutant emissions in a critical area such as urban stations. Based on these considerations, the OESS has been designed to satisfy vehicle's power demand during the entire urban track described next.

Figure 43 conceptually shows the hybridization idea which is applied to the existing DMU model. The retrofitted trainset will then have three diesel generators and one battery pack that shall allow the vehicle to recovery ED braking energy as well as to reach non-electrified urban stations and to operate in underground tracks where diesel generator use is forbidden.

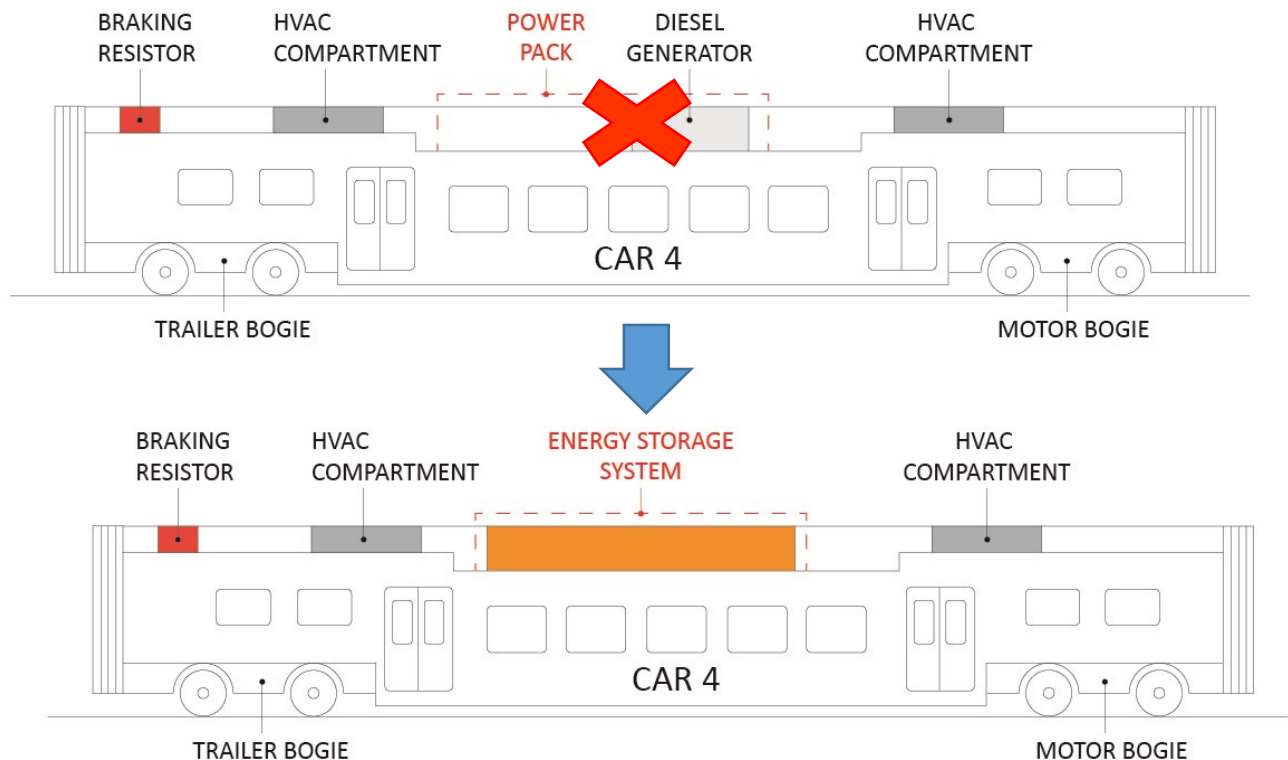


Figure 43 Conceptual Scheme of the Hybridization Process

It should be noted that *dual mode* vehicles are already available on the market and exploit the same operating principle of the retrofitted vehicle. Indeed, dual mode vehicles use diesel generator in non-urban areas, whereas in the proximity of urban stations or underground tracks, they use electrical power supply such as pantograph that rise up powering vehicle through electrical grid. This double power supply system is relatively new and quite diffused in the railway sector, but the vehicle is still dependent on the presence of electrical grid that is not ensured everywhere as explained in the first chapter. On the contrary, the retrofitted vehicle will be capable of travelling independently in non-electrified urban and underground areas thanks to the OESS. In addition, in dual mode vehicles, regenerative braking takes place only when a close vehicle requires power at the same time, this is almost impossible in systems different from funicular railway or similar. Moreover, retrofitted vehicle, through the OESS, could use the engine at optimal efficiency point, reducing its pollutant emissions.

5.1 Input data

Since braking energy recovery becomes possible only through an OESS in this type of vehicle, it is reasonable to take as many advantages as possible of the hybridization process such as allowing vehicle use in underground sections and non-electrified urban stations. To do that and to address the problem of battery pack sizing, it is essential to select a track for which parameters such as track slope, speed limit, and acceleration are known.

In the developed case study, the selected track is about 19.46 km and comprises underground and non-underground sections in the urban area of Turin. Looking at Figure 44, once the vehicle reaches Porta Nuova (PN), acceleration and slope profiles are reversed and this is because of track involves round trip starting from the beginning of the underground section, located at the entrance of Turin, to the central station of Porta Nuova. As a side note, it should be known that speed profile is imposed and controlled by railway operator, thereby vehicle power demand can be easily calculated as explained in the next chapter.

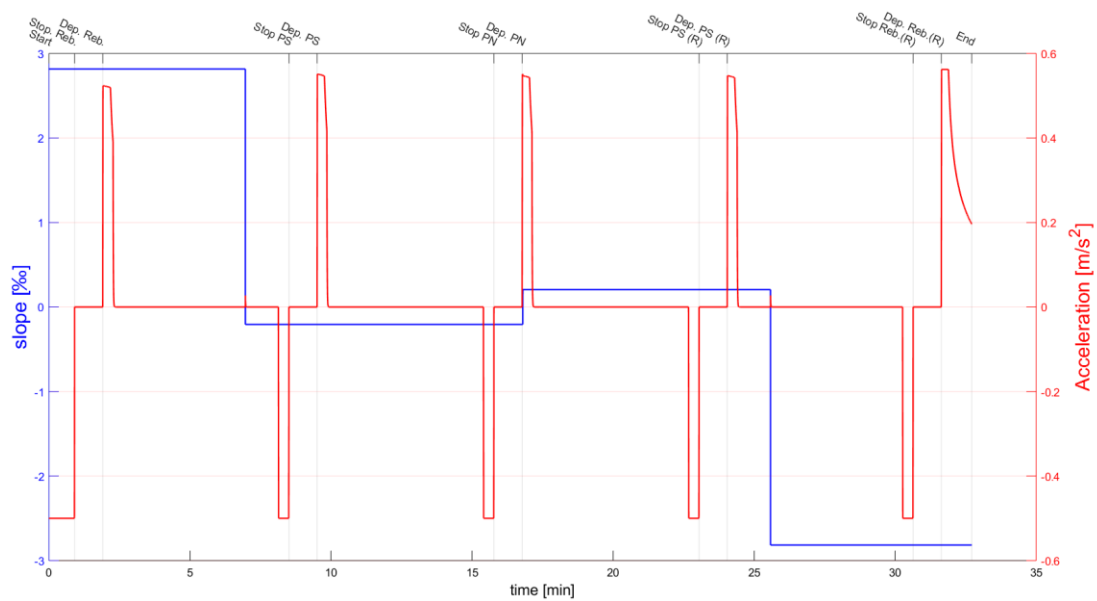


Figure 44 Track slope and acceleration profile

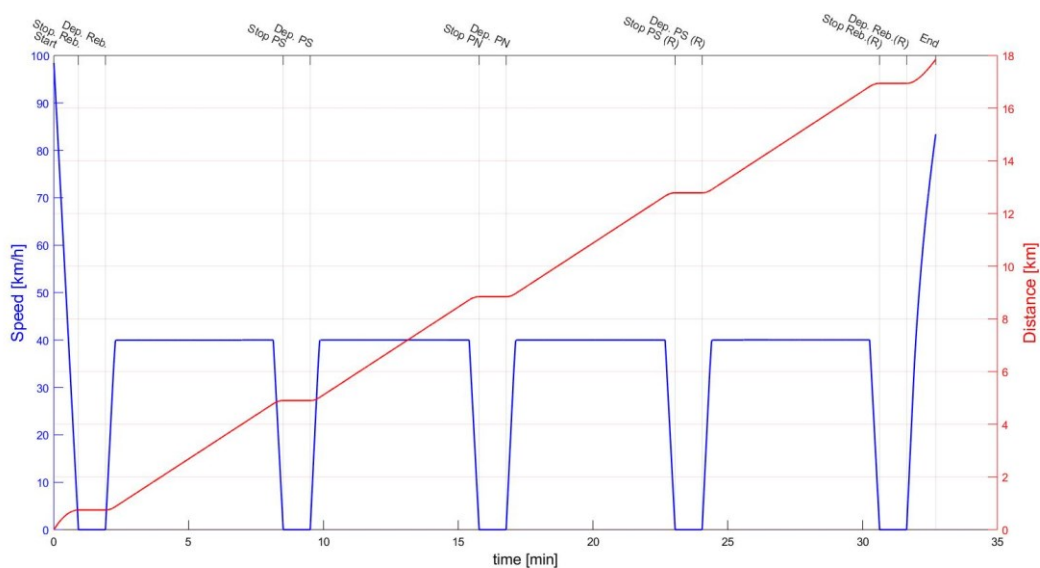


Figure 45 Speed and distance profile

5.2 Vehicle longitudinal dynamic modeling

In order to calculate vehicle power and energy demand, a longitudinal train dynamic model has been developed, taking into account slope, acceleration and speed profile of the given track. Additionally, tractive and braking efforts have been calculated through the *modified* Davis formula obtained by the existing project. Among other considerations, it should be highlighted that regenerative braking power represents part of the total braking effort since ED braking use is limited by the maximum braking power of motors and vehicle speed.

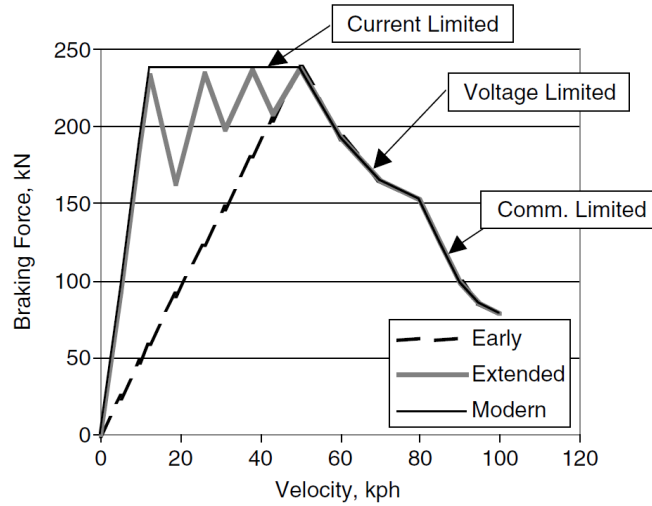


Figure 46 ED braking characteristic. Source: [95]

The longitudinal vehicle dynamic model includes gravitational force and propulsion resistance considered as the sum of rolling resistance and air resistance. Gravitational force is easily calculated by resolving weight vector into perpendicular and parallel components and calculating θ angle thanks to the known track grade.

Eq. (5.1)

$$F_{Slope} = M_{bl\ vehicle} * g * \sin(\theta)$$

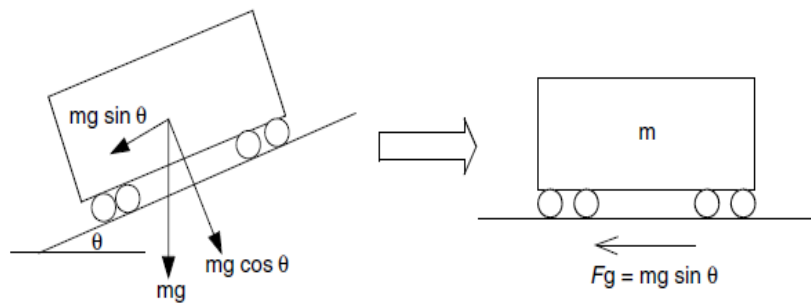


Figure 47 Composition of gravitational force

Propulsion resistance is expressed by a more complicated and empirical formula that usually has a form of $R = A + B * S + C * S^2$, where S is vehicle speed, A is a constant term depending on number of axles and vehicle mass, while B and C represents flanging friction and air resistance respectively.

However, among different versions, the *Davis* formula adopted in the next calculation follows:

$$\text{Eq. (5.2)} \quad F_{Davis} = 6.4 * M_{bl\ vehicle} + 129 * N_{axes} + 0.091 * M_{bl\ vehicle} * S + 0.051 * A_{front} * S^2$$

Since acceleration profile is known in advance, the tractive and braking effort F_{tract} can be calculated as the sum of different forces previously analyzed, as described by *equation (3)*. Consequently, vehicle power demand is calculated by using speed profile of the given track, as shown by *equation (4)* below.

$$\text{Eq. (5.3)} \quad F_{tract} = M_{bl\ vehicle} * a + F_{Slope} + F_{Davis}$$

$$\text{Eq. (5.4)} \quad P_{demand} = F_{tract} * Speed$$

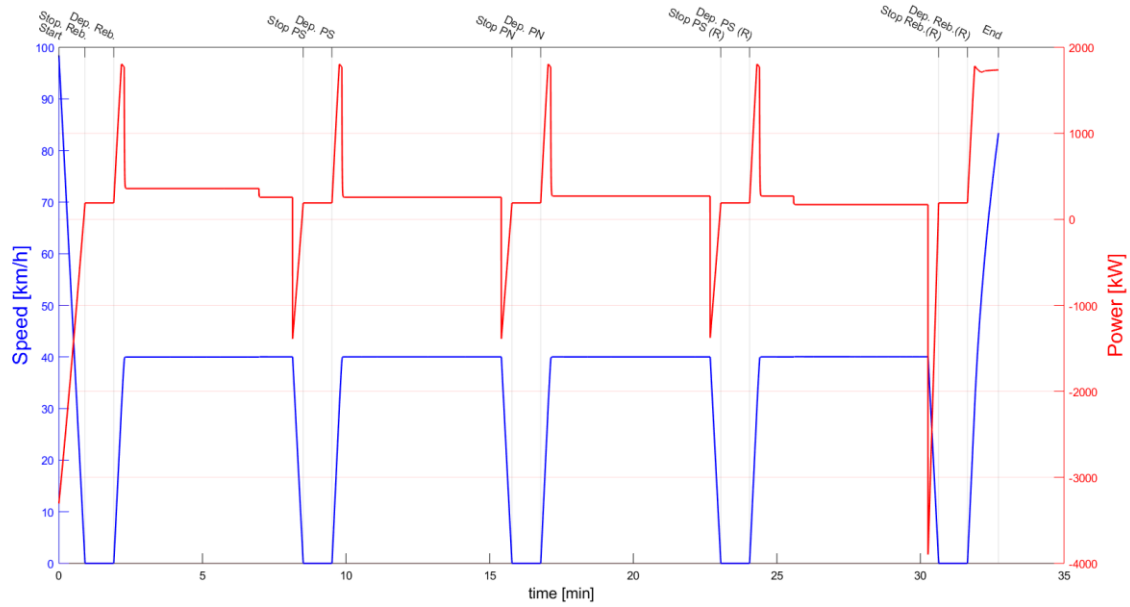


Figure 48 Speed and power demand

Table 16 shows results of the previous calculation:

INPUT DATA		
Total energy demand [kWh]	196	Including auxiliary equipment
Maximum Tractive Power [kW]	1614	Electrical Power
Maximum ED Braking Power [kW]	1584	Electrical Power
Maximum Braking Power [kW]	4088	Pneumatic and Electric braking
Desired Voltage [V]	950	Based on electrical requirements
Minimum Voltage [V]	850	Based on electrical requirements
Power Pack mass [46]	800	
Diesel Generator Power [kW]	560	One diesel-generator each car

Table 16 Input data for battery pack sizing

Once input data are known, the second phase of the sizing process involves selection of the battery module among the wide variety of battery types available on the market. The selection criteria have to take account characteristics of the application such as power and energy demand. For this specific application, the high power demand is a severe parameter that has to be accounted in the module

selection that resulted in an LTO battery module characterized by relatively high C-rate, long lifecycle, short charging time and a wide range of operative temperature. It should be noted that large part of manufacturers' datasheet lacks important information that strongly affects the reliability of computed results, for this reason the next simulation has been conducted by graphical extrapolation of the charging and discharging curves of the module developed by Toshiba Corp.

BATTERY MODULE TECHNICAL DATA (Toshiba SCiB)		
Nominal voltage	27.6	V
Capacity (at C/5)	45	Ah
Minimum/Maximum Voltage	18.0/32.4	V
Maximum charge/discharge current	160 (continuous)	A
	350 (in-rush current)	A
Operative temperature range	-30 to 45	°C
Dimensions	190 x 361 x 125	mm
Mass	15	kg



Table 17 Toshiba battery module type 3-23

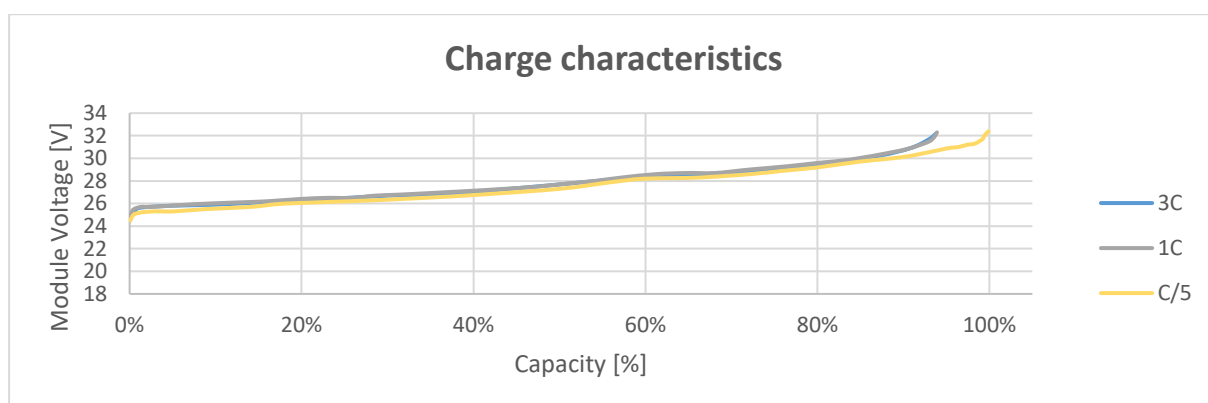


Figure 49 Charge characteristics for different C-rate

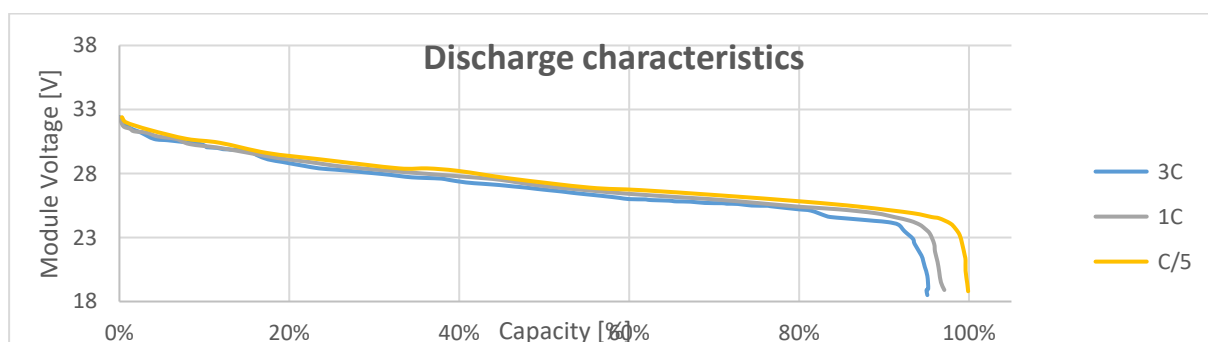


Figure 50 Discharge characteristics for different C-rate

5.3 Battery pack sizing and design

According to [57], the sizing process follows next steps:

1. The calculation of the number of modules to put in series (n_s) is given by:

$$\text{Eq. (5.5)} \quad n_s = \frac{V_{desired}}{V_{module}}$$

2. The second step involves calculation of the required capacity (Ah) of the battery pack, this is possible by dividing the required energy by the battery pack voltage. However, since usually lithium batteries suffer deep-discharge cycle, it is necessary to oversize the installed energy of the battery pack. By acting in this way, Depth-of-Discharge (DOD) of the battery pack will not exceed its maximum allowable value. In this specific application it is considered a maximum DOD of 80%, thus the battery pack energy will be:

$$\text{Eq. (5.6)} \quad \text{Battery pack Energy (Wh)} = \frac{\text{Required Energy [Wh]}}{DOD}$$

$$\text{Eq. (5.7)} \quad \text{Battery pack capacity (Ah)} = \frac{\text{Battery pack Energy [Wh]}}{n_s * V_{module} [V]}$$

3. Once the required capacity of the battery pack is known, it is easy to calculate the number of parallel branches (n_p) needed, just dividing the required capacity by the rated capacity of the single module:

$$\text{Eq. (5.8)} \quad n_p = \frac{\text{Battery pack capacity [Ah]}}{\text{Single module capacity [Ah]}}$$

4. Since the total number of modules is calculated, it is possible to estimate the mass of the battery pack just multiplying the number of modules per mass of single modules. By the way, that weight shall be increased by a factor of 20% because of auxiliary systems such as cooling system. In this case, the total weight is :

$$\text{Eq. (5.9)} \quad \text{Battery pack weight} = 1.2 * n_p * n_s * \text{mass module}$$

The four steps above are useful to obtain an approximate idea of the battery pack configuration but they do not ensure that electrical requirements are satisfied because battery voltage depends on battery state of charge, temperature and internal resistance that dynamically change during operations. However, since the project is still in feasibility phase and because of lack of data, that dependence is not accounted in the following simulation.

The next phase of the battery pack sizing process has to ensure that current never exceeds maximum allowed value during operations, this could occur in the worst condition operation that takes place when battery pack has low SOC level meanwhile vehicle requires high power (i.e. departure phase). This aspect has been taken into account by increasing number of parallel branches of the initial battery pack configuration until discharging/charging current respect battery limits, the algorithm implemented in Matlab is shown in Figure 51.

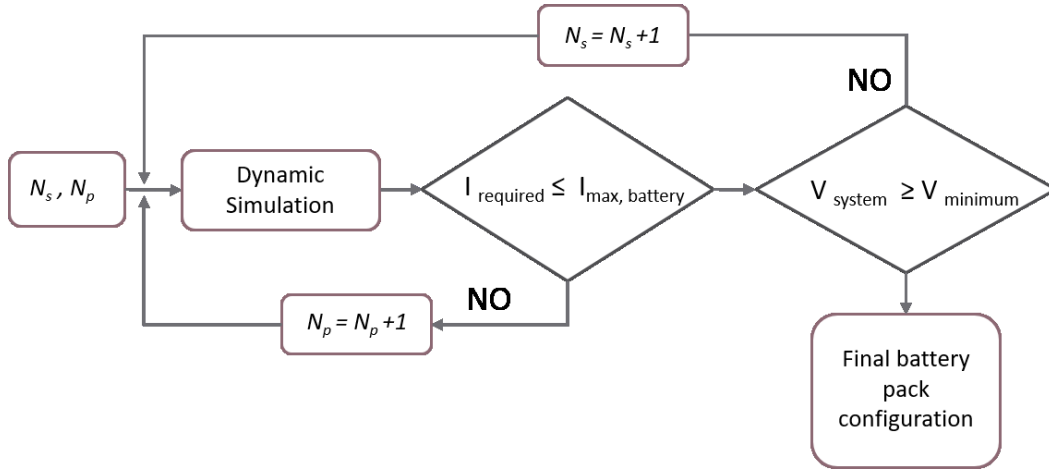


Figure 51 Algorithm adopted in the sizing process

Although battery pack results oversized in terms of energy, the algorithm adopted ensures respect of current and voltage constraints as well as the size and weight limitations that are severe parameters in transport applications. Table 18 shows final battery pack configuration.

Final battery pack configuration	
Number of series modules (N_s)	38
Number of parallel branches (N_p)	12
E_{pack}	566 [kWh]
Maximum Discharge Power (3C-rate and 80% SOC)	1775 [kW]
Mass (including auxiliary equipment)	7660 [kg]
Indicative cost (battery modules only)	113.200 \$- 170.000 \$

Table 18 Final battery pack configuration

5.4 Algorithm and assumptions

The replacement of power pack with the battery pack makes the retrofitted vehicle lighter than baseline vehicle, reducing vehicle power and energy demand. Therefore, for a more precise calculation, tractive and braking efforts have been recalculated through model previously described and taking into account same acceleration and speed profiles being them imposed by railway operator.

It should be highlighted that baseline vehicle dissipates braking power through brake resistor bank while, in contrast, the retrofitted vehicle could theoretically recover totality of ED braking energy, avoiding the use of braking resistor that could be downsized or completely eliminated. For this reason, the mass of the retrofitted vehicle decreases because of both no presence of brake resistor bank and substitution of the power pack with a lighter battery pack. However, mass variation results in about 1.4% and has been calculated as follows:

$$\text{Eq. (5.10)} \quad M_{rf \text{ vehicle}} = M_{bl \text{ vehicle}} - M_{pp} - M_{br} + M_{battery \text{ pack}}$$

Once retrofitted vehicle mass is known, it is possible to calculate tractive efforts and new power demand by using equations (1) and (2) and the mass of the retrofitted vehicle $M_{rf \text{ vehicle}}$. Looking at Figure 52, the power demand of both vehicles is almost the same, this is due to the very small vehicle mass difference that is about 1% and does not affect power required significantly.

$$\text{Eq. (5.11)} \quad F_{tract} = M_{rf \text{ vehicle}} * a + F_{Slope} + F_{Davis}$$

$$\text{Eq. (5.12)} \quad P_{demand} = F_{tract} * Speed$$

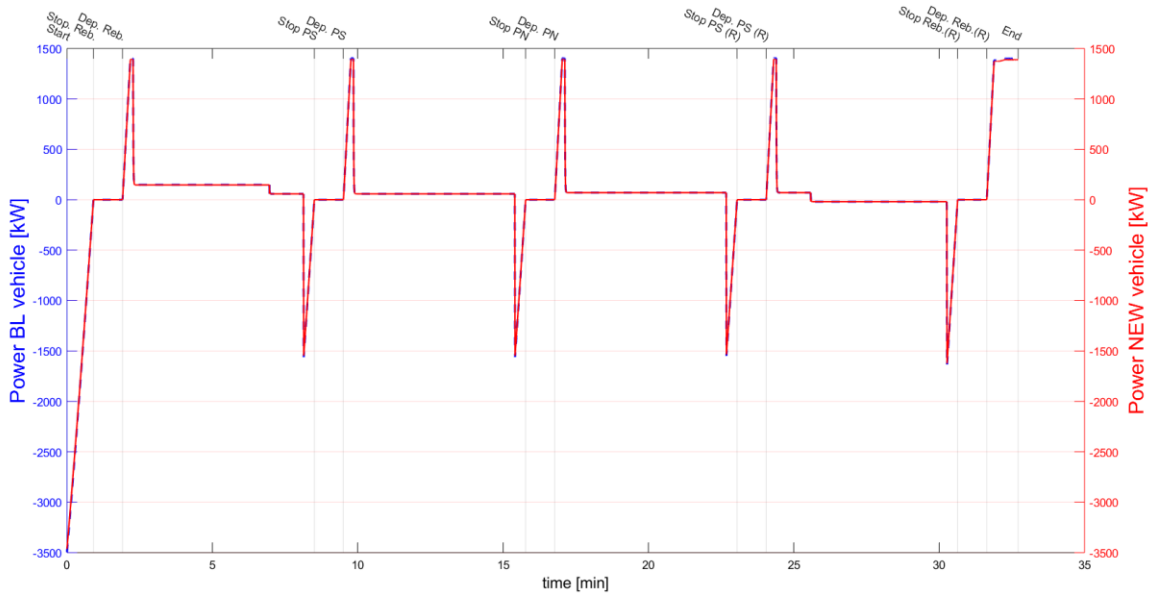


Figure 52 Power demand comparison between baseline and retrofitted vehicle

Being the project in the feasibility phase, parameters such as battery thermal management and internal resistance have not been considered in the following calculation. However, in order to estimate the dynamic behavior of the battery pack and the amount of recovered braking energy, a dynamic measure of battery pack SOC is required during vehicle operations. Scientific literature proposes various SOC measure methods and battery mathematical models [96-98], nonetheless, that methods exploit non-available data in this phase of the study and, consequently, several assumptions have been done and listed below:

- 1) Battery module parameters have been graphically extrapolated from the datasheet.
- 2) It is assumed that braking power firstly feeds auxiliary equipment and secondarily battery pack, according to its State of Charge (SOC).
- 3) If braking power is smaller than auxiliary power demand, the battery pack should supply that power difference.
- 4) Battery manufacturer does not provide internal resistance value, thus it has not been considered in the calculation.
- 5) Battery efficiency is assumed to be 90% for a charge/discharge cycle.
- 6) It is assumed that electric motor efficiency does not change when it acts as a motor or as a generator.
- 7) Auxiliary power demand is assumed to be constant and equal to 191 kW for the whole train set.

Generally, railway vehicles have different operational modes described in the following Table 19:

	<u>Traction</u> <u>(i.e. departure from the station)</u>	<u>Coasting</u>	<u>Station stop</u>	<u>Braking</u> <u>(i.e. arrival to the station)</u>
Operational mode description	Vehicle requires the maximum power demand since electrical motors need very high current in order to provide the maximum tractive efforts necessary in the acceleration phase.	The vehicle has already reached cruise speed and relatively small amount of power is required to the battery pack for powering auxiliary equipment and electric motors.	When the vehicle is stationary, the battery pack is discharging because of auxiliary power demand.	In proximity of the stations, vehicle initially brakes through ED braking system and the battery pack is charged according to its SOC. At very low speed, the pneumatic braking system is activated and vehicle rapidly reaches stationary mode.
Battery pack phase	<ul style="list-style-type: none"> • Discharging. • Positive power in the dynamic simulation. 	<ul style="list-style-type: none"> • Discharging. • Positive power in the dynamic simulation. 	<ul style="list-style-type: none"> • Discharging. • Positive power in the dynamic simulation. 	<ul style="list-style-type: none"> • Charging when braking power is larger auxiliary power. • Negative power in the simulation.

Table 19 Vehicle operational modes

The algorithm exploits Coulomb's counting method as a simple method of evaluating battery SOC through the integration of charging/discharging current over time. This method is not so accurate but very useful, at this stage of the feasibility study, to dynamically evaluate battery voltage.

Eq. (5.13)

$$SOC_i = SOC_{i-1} \pm \int_{t_0}^{t_0+\Delta t} I_i dt$$

In the algorithm adopted, the dynamic evaluation of SOC takes advantage of knowing in advance power demand and initial SOC and voltage of the battery pack. Therefore, it is possible to estimate current released and accepted by the battery in every instant by means of equations Eq. (5.14) and Eq. (5.15) below.

Eq. (5.14)

$$SOC_i = SOC_{i-1} \pm \int_{t_0}^{t_0+\Delta t} I_i dt$$

Eq. (5.15)

$$I_i = \frac{Power_i}{V_{pack_i}(SOC_i)}$$

Eq. (5.16)

$$SOC_{i+1} = SOC_i \pm \int_{t_0}^{t_0+\Delta t} I_i dt$$

More in detail, it has been assumed that traction and auxiliary power demand have positive value, whereas braking power is negative. Same considerations are still valid for current that assumes a positive Figure 53 below shows a flow diagram of the algorithm adopted.

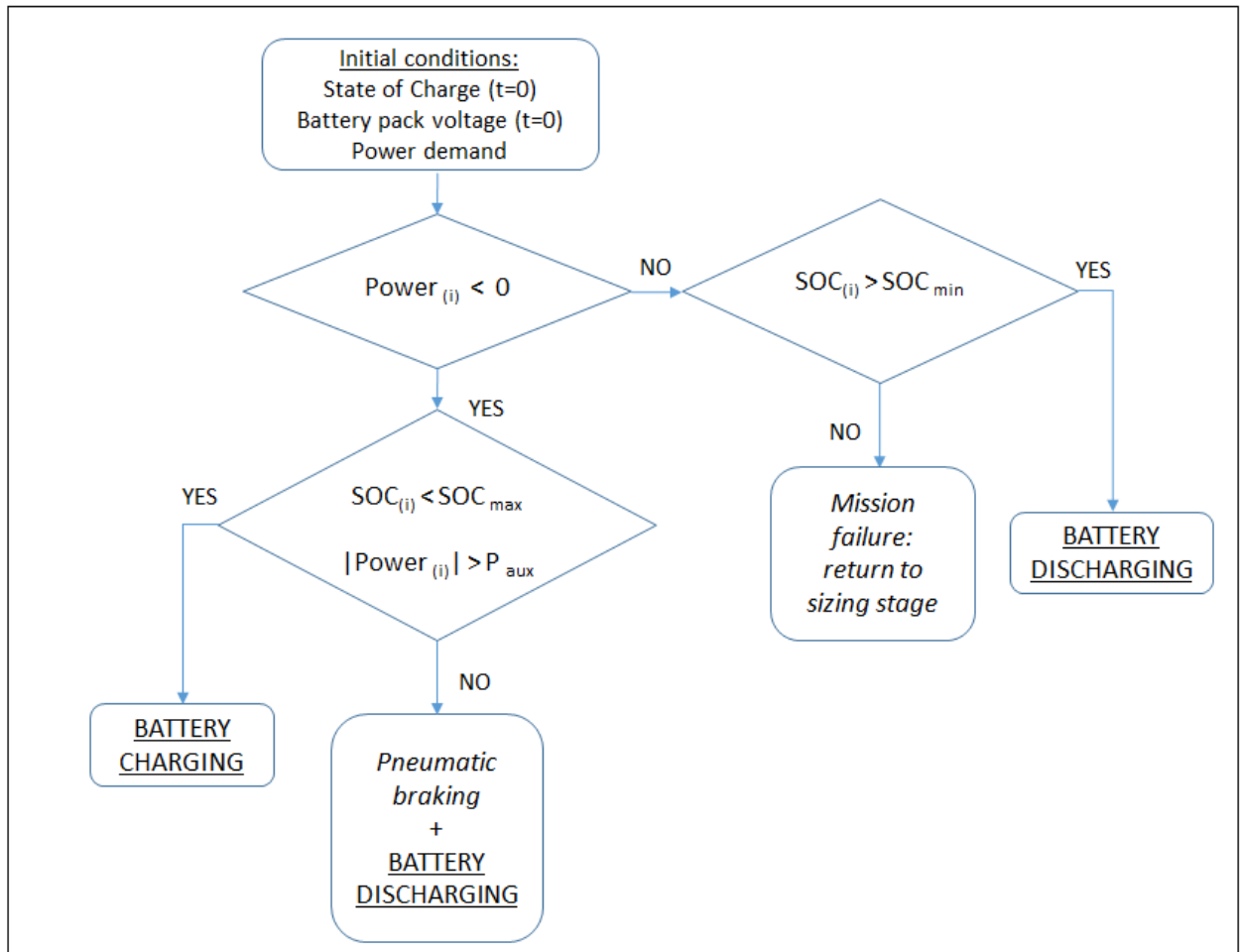


Figure 53 Algorithm adopted for the simulation

As stated previously, battery has different response in charging and discharging modes and thus they requires two different functions called $f_{charge}(SOC)$ and $f_{discharge}(SOC)$ for describing SOC dependence of voltage. Additionally, both functions have been made by means of Matlab function

interp” that linearly fits points extrapolated from manufacturer’s technical datasheet. Algorithms used to describe charging and discharging modes are shown below.

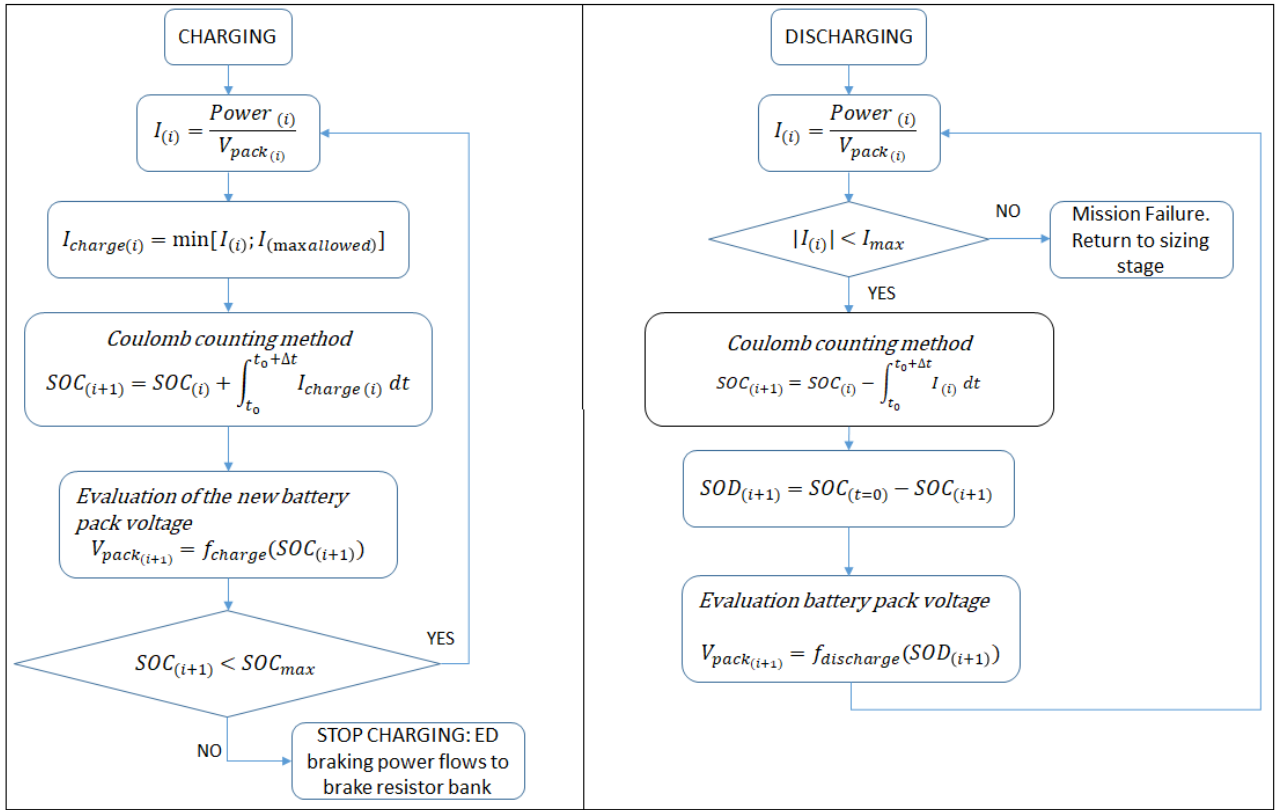


Figure 54 Algorithms adopted in charging and discharging modes

It is important to highlight that when the vehicle starts braking phase, algorithm exploits energy conservation principle such that battery pack has the same value of SOC at the end of instant $i-1$ and at the beginning of instant i . In this way, the battery voltage is calculated using the charge curve as Figure 55 explains. Once the voltage on charging curve has been evaluated, current and SOC at the instant i are calculated using the algorithm of Figure 54. If the vehicle moves from braking (*battery charging*) to traction mode (*battery discharging*) the process shown in Figure 55 is reversed.

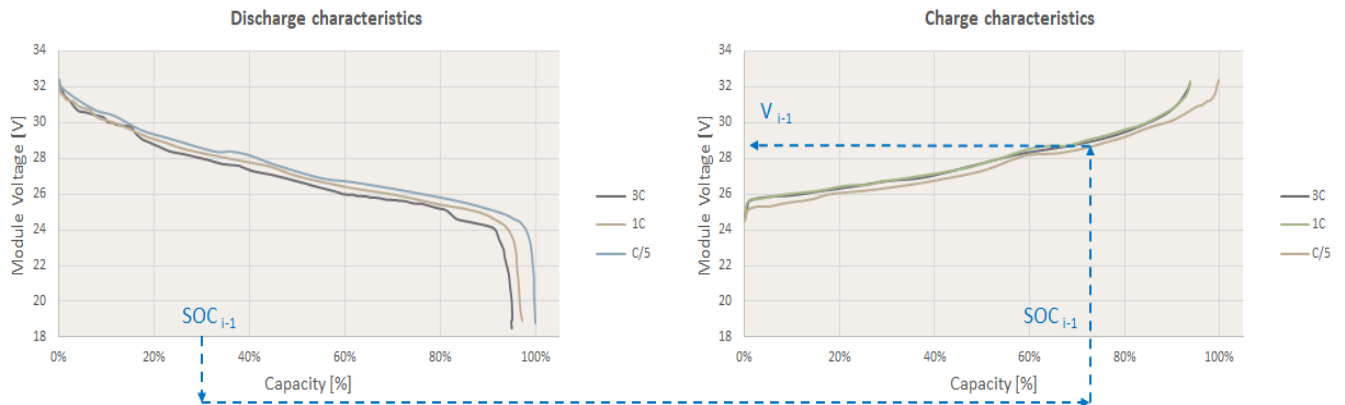


Figure 55 Methodology adopted for evaluating voltage when vehicle moves from tractive to braking phase

Battery Management System (BMS) is responsible for controlling values of currents released and accepted by the battery. The simulation does not account the presence of BMS, therefore limitations on maximum current have been imposed based on actual SOC of the battery pack. As an example, looking at Figure 56, clearly battery module cannot accept currents higher than 0.2 C-rate if SOC level is higher than a certain threshold (92%). This technical constraint has been taken into account in the simulation developed in Matlab environment.

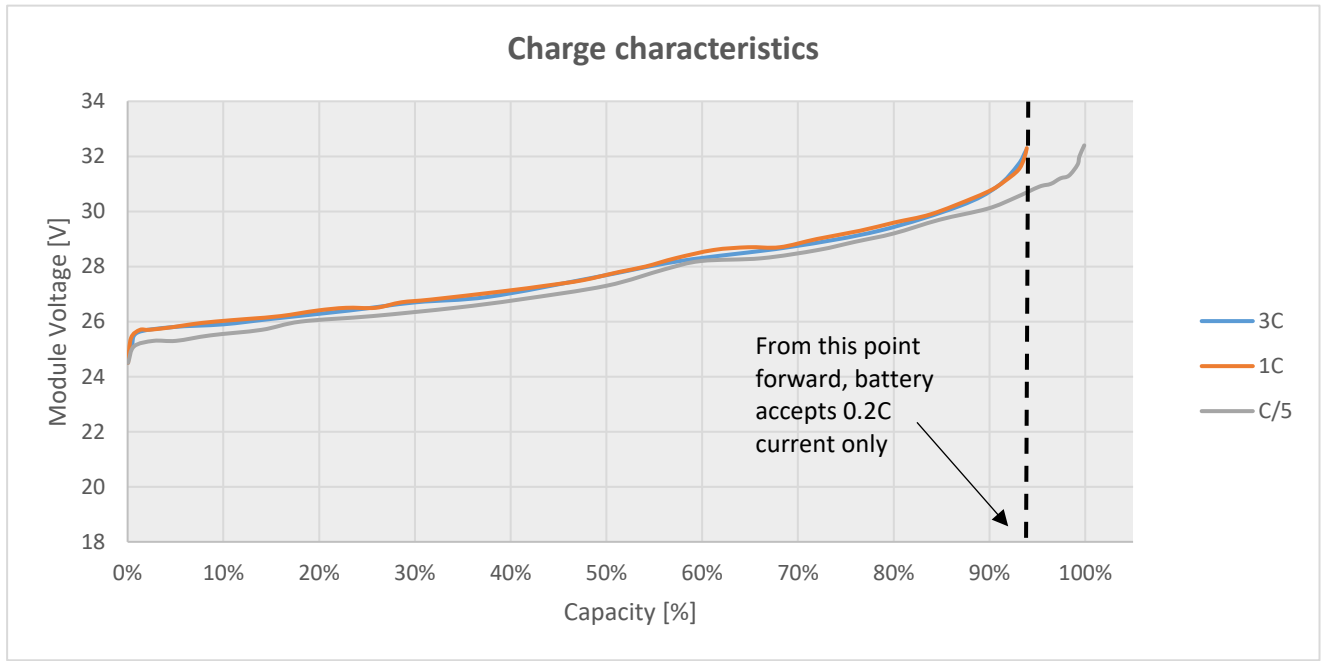


Figure 56 Battery current limitations

5.5 Simulation results and discussion

Dynamic simulation aims to estimate the amount of regenerative energy recovered through battery pack and to evaluate the evolution of electrical parameters for ensuring satisfaction of basic electrical requirements such as maximum current and minimum voltage. Since dynamic simulation neglects factors that, in the real application, will negatively affect battery pack performance, it is essential to satisfy at least electrical, size and weight requirements for considering feasible the hybridization project.

As shown in Figure 57, SOC level slightly increases at every braking event and linearly decreases in the rest of the journey because of linear interpolation of the battery data. Moreover, SOC value dramatically decreases when the vehicle departs from each station, this is as expected and due to the fact that in acceleration mode vehicle requires maximum power from a battery pack that, consequently, has to provide the very high current. The dynamic simulation also demonstrates that SOC level remains in the range of acceptable values since vehicle terminates mission with battery pack SOC about 50%, starting from initial SOC of 75%.

Obviously, the initial value of SOC strongly affects the amount of recovered energy as well as charging time, indeed SOC values higher than 90% should be avoided, otherwise charging time could be too long for this kind of application. On the contrary, if battery reaches very low SOC level, voltage dramatically drops, jeopardizing compliance of electrical requirement and exceeding maximum current permitted by the battery pack. Additionally, the high currents could generate heat so fast that battery thermal management system cannot handle it, leading to battery pack failure.

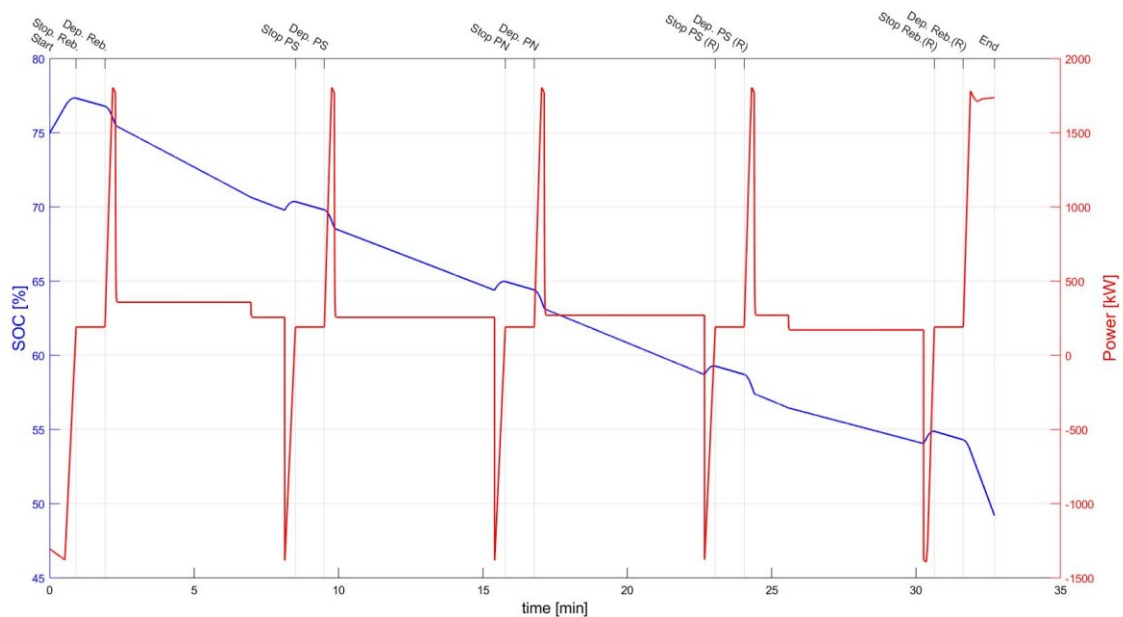


Figure 57 SOC evolution in the given track

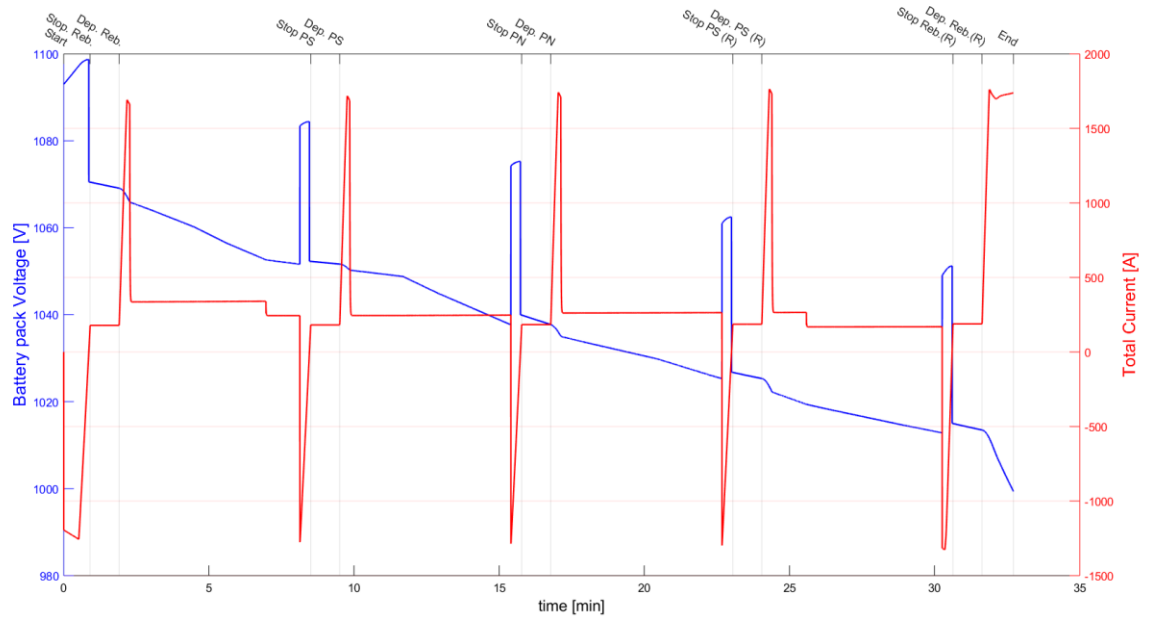


Figure 58 Voltage and current trend in the given track

Figure 57 and Figure 58 above show evolution of battery pack parameters and shows that voltage and current are within the range of desired values. Additionally, in the graph of Figure 58, it is possible to identify regenerative braking events that take place when the current becomes negative and voltage has a very quickly increases, this is due to the activation energy required by battery for reversing lithium-ions flow when battery moves from discharging to charging mode. Once this is done, voltage increases according to its charge characteristics. In addition, it should be noted that current essentially has the same trend of power demand because of the calculation method. Figure 59 shows the evolution of current released/accepted by single battery module and it is ensured that maximum current does not exceed the maximum continuous current value allowed by the battery module (160 A).

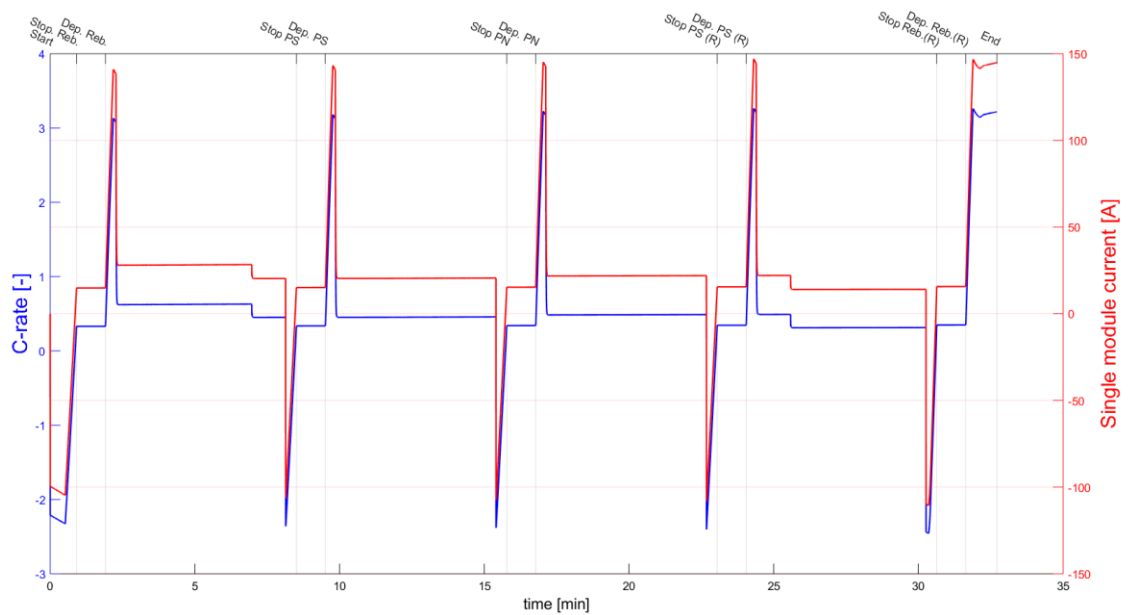


Figure 59 Single module Voltage and C-rate evolution

As stated previously, the satisfaction of basic requirements is the first step for evaluating the feasibility of the project, therefore the relative amount of recovered braking energy, in relation with the total energy demand, plays an important role for evaluating convenience of the hybridization project. Indeed, heat recovery strategies have not been further investigated because of their low energy production while, in contrast, regenerative braking has a great energy recovery potential, especially if braking operations are optimized for braking energy recovery.

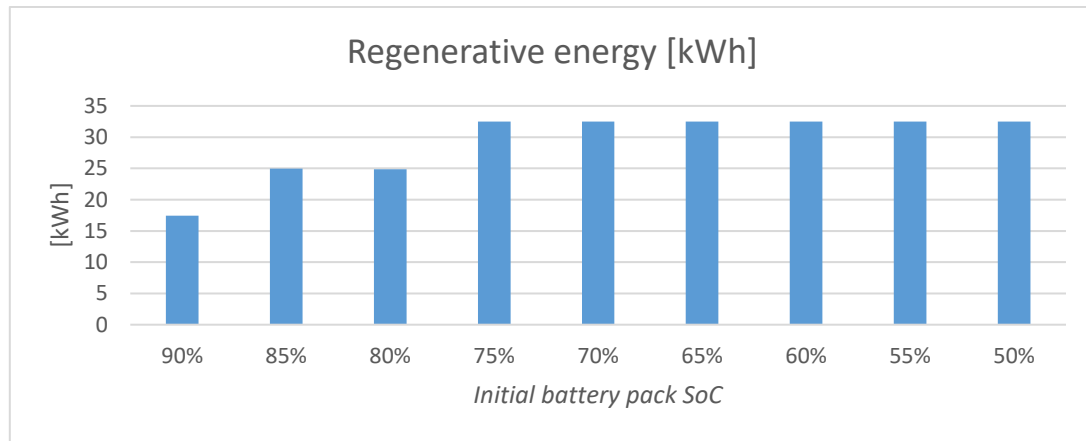


Figure 60 SOC effect on regenerative energy

Looking at Figure 60, clearly amount of regenerative energy has an upper limit due to vehicle's kinetic energy indeed, over a certain value of initial SOC amount of recovered energy does not change. On the contrary, recovered energy decreases as initial SOC level increases, this is due to the battery restriction to accept high current after a certain SOC value, as explained in the previous paragraphs and *Figure 56 Battery current limitations*. Based on these considerations, it is reasonable to find out an acceptable range of initial SOC such that it maximizes braking energy recovery without affecting vehicle performance and battery pack charging time. Essentially, the logic used for charging the battery is imposed by charge characteristics and BMS because battery accepts the high value of current up to a certain value of SOC after that current has to be smaller; this aspect affects charging time, in addition to the amount of energy has to be charged. Moreover, characteristic of the electric motor working as generator was not available during the development of this thesis, thus it has been considered that BMS is able to modify voltage and current handled by traction converter.

Initial SOC	Final SOC	Charging time (up to initial SOC level)	Reg. energy	Reg. energy	Reg. Energy
			Enenergy Demand	Total Braking energy	ED braking energy
[%]	[%]	[minutes]	[%]	[%]	[%]
90%	63%	9.4	10%	31%	42%
85%	59%	7.3	14%	44%	61%
80%	53%	5.3	14%	44%	60%
75%	49%	5.2	18%	58%	79%
70%	44%	5.2	18%	58%	79%
65%	38%	5.3	18%	58%	79%
60%	33%	5.4	18%	58%	79%
55%	28%	5.4	18%	58%	79%
50%	22%	5.5	18%	58%	79%

Table 20 Results of the dynamic simulation for different initial SOC values

Once analyzed effects of regenerative braking, it is reasonable to investigate scenarios involving no use of regenerative braking. This aspect has to be accounted in order to obtain a safe range of SOC level within which vehicle is able to complete its mission.



Through simulation done, it is possible to conclude that vehicle should have an initial battery charge higher than 55% for ensuring mission completion, indeed for initial SOC level below that threshold, battery pack reach an unacceptable value of SOC at the end of the mission.

initial SOC	final SOC	Time to recharge	Maximum voltage	Minimum Voltage	Maximum current	Battery energy discharged	Overall efficiency
[%]	[%]	[min]	[V]	[V]	[A]	[kWh]	[%]
90%	56%	10.28	1089.60	1001.50	146.40	216	85%
85%	51%	8.41	1082.50	996.70	147.10	216	85%
80%	45%	6.65	1062.00	980.90	150.30	209.3	87%
75%	40%	6.69	1054.00	976.50	151.30	206.30	89%
70%	32%	6.78	1039.90	968.40	153.00	203	90%
65%	29%	6.83	1032.20	959.00	153.80	201.2	91%
60%	24%	6.87	1026.80	947.40	154.10	200.00	92%
55%	19%	6.93	1018.00	930.00	155.60	198.70	92%

Table 21 Results of simulation without regenerative braking

Looking at results of Table 21 and Table 20, the initial value of SOC between 55% and 75% ensures completion of vehicle mission as well as achieving maximum braking energy recovery.

At this stage, a further step towards the completion of the feasibility study is represented by evaluation of train capacity to recharge battery pack up to the desired SOC level during the period preceding entrance in the urban section analyzed until now. This has been achieved through estimation of engine power available for charging battery pack during the journey outside of urban section. More in detail, to be a conservative estimate, the following calculation considers that battery pack is charged by the three remaining diesel-generators only when the vehicle runs at constant speeds and without using regenerative braking. In other words, in the period preceding entrance in the urban track, battery charging occurs once vehicle reached cruise speed and without considering the contribution of regenerative braking. Power available for charging the battery pack, named as $P_{charging}$, has been calculated as follows:

$$\text{Eq. (5.17)} \quad P_{charging} = P_{rated\ engine} - P_{traction} - P_{aux}$$

Unfortunately, in the section preceding urban track, speed and acceleration profiles were not available and thus calculation has been developed by basing it on data coming from the railway operator website. More in detail, railway operator provides me speed limit, grade, distance and journey times of the track connecting Aosta to Turin, as shown in Table 22 below.

	Distance [km]	Journey Time [min]	Average speed [km/h]	Stop time [min]	Time to reach average speed [min]
Aosta	0	0	0		0
Nus	12.45	9	83	1	4.3
Chatillon-Saint Vincent	24.57	19	73	1	3.6
Verres	37.84	29	80	1	4.0
Hone-Bard	44.51	34	80	1	4.0
Donnanz	47.42	37	58	1	1.9
Pont Saint Martin	50.01	40	52	1	1.5
Borgofranco	59.94	46	99	1	3.2
Ivrea	66.19	54	47	10	1.3
Strambino	75.24	60	90	5	2.8
Mercenasco	78.52	62	98	1	3.2
Candia Canavese	81.20	65	54	1	1.7
Caluso	84.70	70	42	4	1.0
Rodallo	88.03	73	67	1	2.8
Montanaro	93.39	79	54	5	1.7
Chivasso	98.62	84	63	1	2.4
Brandizzo	103.24	88	69	1	2.9
Settimo	110.38	93	86	1	4.5
Stura	115.21	98	58	1	1.9
Underground track beginning					

Table 22 Characteristics of the track Aosta-Turin

Between each intermediate station, time to reach average speed has been calculated using same vehicle acceleration profile used in the urban section, while braking time has been calculated using deceleration of 0.5 m/s^2 . In addition, charging time has been calculated by subtracting acceleration and braking time out of journey time, whereas average speed has been simply calculated by knowing distance and journey time between two intermediate stations. Based on these assumptions, the following equations allow calculation of power and time available for charging battery pack.

$$\text{Eq. (5.18)} \quad P_{\text{charging}} = P_{\text{rated engine}} - P_{\text{traction}} - P_{\text{aux}}$$

$$\text{Eq. (5.19)} \quad \text{Average speed} = \frac{\text{distance}}{\text{journey time}}$$

$$\text{Eq. (5.20)} \quad t_{\text{accel}} = \frac{\Delta \text{ speed}}{\text{acceleration}}$$

$$\text{Eq. (5.21)} \quad t_{\text{brake}} = \frac{\Delta \text{ speed}}{\text{deceleration}}$$

$$\text{Eq. (5.22)} \quad t_{\text{charge}} = t_{\text{journey}} - t_{\text{acceleration}} - t_{\text{brake}}$$

$$\text{Eq. (5.23)} \quad E_{\text{charged}} = P_{\text{charging}} * t_{\text{charge}}$$

	$P_{traction}$ [kW]	$P_{charging}$ [kW] (for a single engine)	t_{brake} [min]	t_{charge} [min]	$E_{charged}$ [kWh]
Aosta	0	370	0		0
Nus	259	111	0.77	4.0	4.3
Chatillon-Saint Vincent	199	171	0.67	5.7	3.6
Verres	237	133	0.74	5.2	4.0
Hone-Bard	242	128	0.74	0.2	4.0
Donnanz	131	239	0.54	0.5	1.9
Pont Saint Martin	107	263	0.48	1.0	1.5
Borgofranco	378	0	0.92	1.8	3.2
Ivrea	93	277	0.43	6.3	1.3
Strambino	313	57	0.84	2.4	2.8
Mercenasco	377	0	0.91	0	3.2
Candia Canavese	120	250	0.50	0.9	1.7
Caluso	82	288	0.39	3.6	1.0
Rodallo	164	206	0.62	0	2.8
Montanaro	113	257	0.50	3.9	1.7
Chivasso	151	219	0.58	2.1	2.4
Brandizzo	185	185	0.64	0.5	2.9
Settimo	279	91	0.79	0.0	4.5
Stura	133	237	0.54	2.6	1.9
Total			11.6	40.7	130.3

Table 23 Charging timetable

In view of the fact that vehicle has at its disposal the entire round trip to charge the battery pack, the total amount of energy available doubles as well as available time to charge the battery. Therefore, the energy coming from diesel-generators is about 260 kWh that exceeds of about 27% the amount of energy required to charge the battery, giving large room for maneuver in charging operation.

In addition, to be a conservative estimate, this calculation considers that only one diesel-generator is responsible for battery pack charging, while, in the real situation, three diesel-generators are available. In conclusion, according to data available for the non-urban section, the vehicle is able to charge battery pack up to desired SOC level, even using only one diesel-generator and without considering regenerative events.

6. Conclusions and future developments

In the first part of this thesis, different energy recovery strategies have been briefly analyzed in order to identify the most promising, effective and easy-to-integrate retrofit action among those available on a DMU railway vehicle based on diesel-electric power supply system. According to power system architecture, energy recovery strategies involve exhaust gas or cooling water heat recovery and regenerative braking based on OESS. The first two strategies have been briefly studied taking into account that diesel engine typically has an average efficiency of 40% and thus about 60% of the primary energy is wasted through exhaust gas and cooling water. This makes available a great potential of energy may be recovered by means of different systems and for different purposes such as power or hot water production.

On the one hand, exhaust gas heat recovery has great energy potential because of high temperatures (about 500°C) and large flow rate involved. On the other hand, the temperature of exhaust gas strictly depends on engine load and pollutant emission control that, because of urea injection, strongly reduces exhaust gas temperature. The wide range of operating temperature of exhaust gas adds complexity to the system control logic and reduces the amount of saved energy. In addition, exhaust gas heat recovery for power production resulted as low efficient (steam cycle overall efficiency is 11%), unproductive and little suitable process for onboard applications that have severe weight and spatial constraints.

Another possible energy recovery opportunity is represented by engine cooling water since it is a more constant power source than exhaust gas, despite its lower operating temperature and flow rate. Based on these considerations, cooling water heat recovery for power production purpose has been investigated by basing it on an ORC that exploits *R245fa* as working fluid. This strategy takes advantage of low boiling point of organic fluid that is necessary because of the low temperature of cooling water (90°C) that anyway represents the “high” temperature source. Nevertheless, even this strategy has resulted unseemly in terms of efficiency (13%), energy production and integration. Moreover, although efficiency and energy production of ORC are greater than the steam cycle combined with exhaust gas heat recovery, ORC adds safety concerns in case of leakage of organic fluid.

In both previous heat recovery strategies, low efficiency and low energy production are factors that greatly undermines the effectiveness of the retrofit process. A measure to overcome these factors is avoiding energy transformation and, therefore, it is preferable to use available thermal power in a direct way such as hot water production exploited for heating purpose. From this perspective, heat recovery for hot water production has been briefly analyzed and it highlights high process efficiency, although the most difficult and sensitive aspect of this energy recovery strategy is the integration of the heat recovery system with the existing heating system based on floor electrical heaters and HVAC units that use electrical heaters too. Based on this, heat recovery for hot water production has not been further investigated because it requires a heavy and unlikely redesign of large part of the vehicle layout and electrical system. Moreover, thermal power made available by diesel engines is not sufficient to supply the overall vehicle heating power demand, making this energy recovery strategy unfeasible, despite the fact that it could strongly reduce electrical energy use for the heating purpose.

All these considerations have suggested a focus on energy recovery analysis on regenerative braking made possible because of electrical transmission system fitted on the vehicle. However, since the vehicle is not equipped with a secondary power supply system (i.e. third rail or pantograph), the only way to recover ED braking energy is installing an OESS that, moreover, makes vehicle free to handle regenerative energy with no regards to grid capacity of accepting power. As result of the research activity done, lithium battery seems the most appropriate energy storage technology for this type of application characterized by very high power demand and current. Among the wide range of lithium battery chemistries, LTO-based battery resulted as the most suitable because of short charging time, long lifecycle, a wide range of operating temperature and high C-rate.

It should be also noted that regenerative braking involves the transformation of mechanical to electrical energy at the motor/generator level, while the transformation of electrical to chemical energy takes place at battery pack level. Therefore, the efficiency of the overall system is higher than the other energy recovery strategies that are negatively influenced by the transformation from thermal to electrical energy. Installation of a battery pack in place of a conventional diesel-generator not only allows regenerative braking, but it also enables the vehicle to operate in a fully electric mode, if battery-pack is designed properly. That issue is exactly the idea on which hybridization process is based on.

More in detail, the second part of the thesis comprises a first-approach to study the feasibility of substituting one conventional diesel-generator with a battery pack that has to feed vehicle during the entire selected urban path. Although a large number of battery models are available in the scientific literature, the main obstacle to develop an accurate battery model was lack of battery data; indeed, in most cases, manufacturer's datasheet does not provide important parameters such as battery internal resistance and specific heat, parameters that affect the accuracy of results.

Despite these limiting aspects, dynamic simulation has been developed by linearly fitting charge and discharge curves according to battery SOC. Outcomes of the simulation are encouraging because the retrofit process enables the vehicle to recover up to 20% of the total energy demand and almost 85% of the total ED braking energy, at this stage of calculation. Furthermore, based on dynamic simulations done in case of no use of regenerative braking, the vehicle is also able to complete the mission if initial SOC level is at least 55%, while an initial SOC level below 75% maximizes regenerative energy. Based on these considerations, at the entrance of the selected track the optimal SOC range is between 55% and 75% because, in this range of SOC values, mission completion is ensured even without regenerative braking and vehicle harvests the maximum regenerative energy.

Additionally, making vehicle electrically propelled, it can operate in non-electrified urban stations and underground tracks, enlarging vehicle operational field that represents a valuable plus for the retrofitting process. From this perspective, it must be pointed out that retrofitted vehicle also gives an important contribution for reducing local concentration of particulate and CO₂ emissions, a relevant problem in cities as Turin that often experiences pollutant concentration over the threshold level.

In conclusion, at this stage of the feasibility study and among different analyzed energy recovery strategies, regenerative braking with OESS seems the most effective in terms of saved energy and efficiency. In addition, making hybrid DMU railway vehicle generates secondary improvements such as extending applicability field of the vehicle and using the battery pack as acceleration booster. Additionally, by comparing retrofitted vehicle with dual-mode railway vehicle, the first has the advantage of being independent of the electrical grid and this should largely increase positive effects of regenerative braking, reducing vehicle fuel demand. Although results obtained by this work are encouraging, different aspects have been neglected because of lack of data. In order to achieve a more precise estimation of retrofit process feasibility, a model of and the logic used by BMS and battery thermal management system should be further investigated. Moreover, a more precise evaluation of regenerative energy could be achieved through an accurate model of power electronics involved in the power supply architecture.

Since battery pack has been oversized due to power constraints, an important improvement could be achieved by considering different technologies for the OESS. Indeed, the design of hybrid OESS that combines battery pack with a high specific power technology, battery pack shall be less affected by high currents and used in an optimal way. Additionally, a further challenge in the development of the hybridization process is optimization of the hybrid powertrain system such that engine and battery pack are used in the best possible manner. From this perspective, the optimization process should comprise a battery charging strategy such that engine works at its maximum efficiency point as much time as possible. In other words, diesel-generator should partially charge battery pack such that the rest of

energy is provided to battery pack through regenerative energy. Furthermore, safety issues regarding battery use on railway vehicle have to be accounted.

7. References

1. Various, *Railway Handbook* 2016. International Energy Agency & UIC, 2016.
2. UNIFE, *Key Messages for COP21*. 2010.
3. Gracie, C. *Tales from the new Silk Road*. 2016 [cited 2017 25-9]; Available from: http://www.bbc.co.uk/news/resource/s/idx-sh/new_silk_road.
4. Frey, S., *Railway Electrification Systems & Engineering* 1ed. 2012: White Word Publications.
5. Enno Wiebe, J.S., *Innovative Integrated Energy Efficiency Solutions for Railway Rolling Stock, Rail Infrastructure and Train Operation*. 2010, UIC-UNIFE.
6. A. WALKER, M.L., S.WILKINS, *On friction braking demand with regenerative braking*. SAE Technical paper, 2002.
7. François-Olivier Devaux, X.T., *Guidelines for braking energy recovery systems in urban rail networks*. Ticket to Kyoto- final report, 2014.
8. Storer, N.W., *Diesel electric railcars and Locomotives*. Transactions of the American Institute of Electrical Engineers, 1934. **53**(11): p. 1461-1466.
9. Desplanques, Y., et al., *Analysis of tribological behaviour of pad-disc contact in railway braking - Part 1*. Wear, 2007. **262**: p. 582-591.
10. Sharma, R.C. and M. Dhingra, *Braking systems in Railways Vehicles*. International Journal of Engineering Research & Technology, 2015. **4**(1): p. 206-211.
11. Lingaitis, L.P. and L. Liudvinavicius, *Electrodynamic braking in high-speed rail transport*. Transport, 2007. **22**(3): p. 178-186.
12. Ma, D.-M. and J.-K. Shiau, *The design of eddy-current magnet brakes*. Transactions of the Canadian Society for Mechanical Engineering, 2011. **35**(1): p. 19-37.
13. HULL, G.J., *SIMULATION OF ENERGY EFFICIENCY IMPROVEMENTS ON COMMUTER RAILWAYS*, in *Department of Birmingham Centre for Railway Research and Education*. 2009, University of Birmingham: Birmingham.
14. Various. *Railway Technical Handbook*. Technical committee for railway engineering standardization Undeclared 3/10/2017. Available from: <http://www.ctn141.org/mod/folder/view.php?id=1>.
15. Connor, P. [cited 2017 4/10/2017]; Available from: <http://www.railway-technical.com/trains/rolling-stock-index-1/train-equipment/brakes/electro-pneumatic-brakes-d.html>.
16. Gupta, P., et al., *Regenerative braking systems (rbs) (future of braking systems)*. International Journal of Mechanical And Production Engineering, 2014. **2**(5).
17. I. Hasegawa and S. Uchida, *Braking systems*. Japan Railway & Transport Review 1999. **20**.
18. Edward, R., R.J. Collins, and S.G. Whisenant, *Evaluating the Tradeoffs between Regenerative Inverters and Dynamic Braking*. Energy Engineering, 2007. **104**(5): p. 60-80.
19. Clegg, S.J., *A Review of Regenerative Braking Systems*. 1996.
20. Kumar, R., *Regenerative Brake: To Harness the Kinetic Energy of Braking*. Journal of Emerging Technologies and Innovative Research, 2015. **2**(1): p. 124-129.
21. Jiang, Y., et al., *Energy Harvesting for the Electrification of Railway Stations: Getting a charge from the regenerative braking of trains*. IEEE Electrification Magazine, 2014. **2**(3): p. 39-48.
22. Cody, J., et al., *Regenerative braking in an electric vehicle*. Zeszyty Problemowe – Maszyny Elektryczne, 2009. **81**: p. 113-117.
23. Ghaviha, N., et al., *Review of Application of Energy Storage Devices*

- in Railway Transportation. Energy Procedia, 2017. **105**: p. 4561-4568.
24. Kondo, K., *Recent Energy Saving Technologies on Railway Traction Systems*. Transactions on electrical and electronic engineering, 2010. **5**: p. 298-303.
25. Nishimura, K., T. Takasaki, and T. Sakai, *Introduction of large-sized nickel-metal hydride battery GIGACELL for industrial applications*. Journal of Alloys and Compounds 2013. **580**: p. S353-S358.
26. Gelman, V., *Energy Storage That May Be Too Good to Be True: Comparison Between Wayside Storage and Reversible Thyristor Controlled Rectifiers for Heavy Rail*. Vehicular Technology Magazine IEEE, 2013. **8**(4): p. 70-80.
27. Luo, X., et al., *Overview of current development in electrical energy storage technologies and the application potential in power system operation*. Applied Energy, 2015. **137**: p. 511-536.
28. Vazquez, S., et al., *Energy Storage Systems for Transport and Grid Applications*. IEEE TRANSACTIONS ON INDUSTRIAL ELECTRONICS, 2010. **57**(12): p. 3881-3895.
29. Rohit, A.K., K.P. Devi, and S. Rangnekara, *An overview of energy storage and its importance in Indian renewable energy sector Part I – Technologies and Comparison*. Journal of Energy Storage, 2017. **13**: p. 10-23.
30. Meinert, M., et al., *Energy storage technologies and hybrid architectures for specific diesel-driven rail duty cycles: Design and system integration aspects*. Applied Energy, 2015. **157**: p. 619-629.
31. Hannan, M.A., et al., *Review of energy storage systems for electric vehicle applications: Issues and challenges*. Renewable and Sustainable Energy Reviews, 2017. **69**: p. 771-789.
32. Lawson, B. *Battery Life (and Death)*. 2005 [cited 2017 20/10/2017]; Available from: <http://www.mpoweruk.com/life.htm>.
33. team, E.E.S.p., *Electrical energy storage: white paper. Technical report*, I.E.C. (IEC), Editor. 2011, Fraunhofer Institut für Solare Energiesysteme: Geneva, Switzerland.
34. Chen, H., et al., *Progress in electrical energy storage system: a critical review*. Progress in Natural Science 2009. **19** (3): p. 291-312.
35. (DOE), U.D.o.E. *Global energy storage database*. 2016 [cited 2017; Available from: <http://www.energystorageexchange.org/projects/69>].
36. Poullikkas, A., *A comparative overview of large-scale battery systems for electricity storage*. Renewable Sustainable Energy Reviews, 2013. **27**: p. 778-788.
37. WH, Z., et al., *Energy efficiency and capacity retention of Ni-MH batteries for storage applications*. Applied Energy, 2013. **106**(C): p. 307-313.
38. M.A.Fetcenko, et al., *Recent advances in NiMH battery technology*. Journal of Power Sources, 2007. **165**(2): p. 544-551.
39. Larminie, J. and J. Lowry, *Electric Vehicle Technology Explained*. 1st ed. 2003, New York: Wiley.
40. Meyers, R.A., *Encyclopedia of Sustainability Science and Technology*. 2012, New York.
41. King, C., G. Vecia, and I. Thompson, *Innovative Technologies for Light Rail and Tram: A European reference resource*, B.P.T.B.-N.a.P. Systems, Editor. 2015, University College London - Sintropher.
42. Young, K., et al., *Electric Vehicle Battery Technologies*, in *Electric Vehicle Integration into Modern Power Networks*, R. Garcia-Valle and J.A.P. Lopes, Editors. 2013.
43. Ogasa, M., *Application of Energy Storage Technologies for Electric Railway Vehicles—Examples with Hybrid Electric Railway Vehicles*. IEEE Transactions on electrical and electronic engineering, 2010. **5**: p. 304-311.

44. Lacôte, F., *Alstom – future trends in railway transportation*. Japan Railway & Transport Review 2005. **42**: p. 4-9.
45. Akiyama, S., K. Tsutsumi, and S. Matsuki, *The development of low floor battery-driven LRV “SWIMO”*. 2007, Kawasaki Heavy Industries Ltd.
46. Ogura, K., et al., *Test Results of a High Capacity Wayside Energy Storage System Using Ni-MH Batteries for DC Electric Railway at New York City Transit*, in *Green Technologies Conference*, IEEE, Editor. 2011. p. 1-6.
47. SIEMENS, *Sitras HES - Hybrid energy storage system for rail vehicles*, SIEMENS, Editor. 2010.
48. Swanson, J. and J. Smatlak, *State-of-the-Art in Light Rail Alternative Power Supplies*, in *APTA / TRB 2015 Light Rail Conference*, I.M.o. SNC-LAVALIN, Editor. 2015.
49. Rufer, A., *Energy Storage for Railway Systems, Energy Recovery and Vehicle Autonomy in Europe*, in *The 2010 International Power Electronics Conference*, IEEE, Editor. 2010, IEEE. p. 3124-3127.
50. Bresser, D., E. Paillard, and S. Passerini, *Lithium-ion batteries (LIBs) for medium- and large-scale energy storage: current cell materials and components*, in *Advances in Batteries for Medium and Large-Scale Energy Storage*, C. Menictas, M. Skyllas-Kazacos, and L.T. Mariana, Editors. 2014.
51. and T. Horiba, *Lithium-Ion Battery Systems - Invited paper*. Proceedings of the IEEE 2014. **102**(6): p. 1-12.
52. Sarre, G., P. Blanchard, and M. Brouse, *Aging of lithium-ion batteries*. Journal of Power Sources, 2004. **127**(1-2): p. 65-71.
53. González-Gil, A., R. Palacin, and P. Batty, *Sustainable urban rail systems: Strategies and technologies for optimal management of regenerative braking energy*. Energy Conversion and Management, 2013. **75**: p. 374-388.
54. Scrosati, B. and J. Hassoun, *Lithium batteries: current technologies and future trends*, in *Functional materials for sustainable energy applications*, J.A. Kilner, et al., Editors. 2012. p. 573-599.
55. Scrosati, B. and J. Garche, *Lithium Batteries: Status, prospects and future*. Journal of Power Sources, , 2010. **vol.195**(9): p. 2419-2430.
56. Warner, J., *Chapter 7- Lithium-Ion and Other Cell Chemistries*, in *John Warner Elsevier*, Editor. 2015.
57. Linden, D. and T.B. Reddy, *Lithium batteries*, in *Handbook of batteries*, D. Linden and T.B. Reddy, Editors. 2013, McGraw-Hill.
58. *Electrical Energy Storage-Executive summary*. IEC (International Electrotechnical Commission) White Paper, 2011. **Geneva, Switzerland, 2011**.
59. Newcomb, A. *Samsung Finally Explains the Galaxy Note 7 Exploding Battery Mess*. 2017 [cited 2017; Available from: <https://www.nbcnews.com/tech/tech-news/samsung-finally-explains-galaxy-note-7-exploding-battery-mess-n710581>].
60. Zhou, Z., et al., *A Review of Energy Storage Technologies for Marine Current Energy Systems*. Renewable and Sustainable Energy Reviews, 2013. **18**: p. 390-400.
61. Uebo, Y., et al., *Development of High Power Li-ion Cell "LIM25H" for Industrial applications*. GS Yuasa Technical Report, 2015. **12** (2): p. 12-17.
62. Mukai, D., et al., *Development of Large High-performance Lithium-ion Batteries for Power Storage and Industrial Use*. Mitsubishi Heavy Industries Technical Review, 2012. **49**(1): p. 6-11.
63. Corporation, G.Y. *GS Yuasa's Lithium-ion Batteries Adopted for "Twilight Express Mizukaze" ~Improving environmental performance and supporting train concept*. 2017 [cited 2017 25/10/2017]; Available from: <http://www.gs->

- yuasa.com/en/newsrelease/article.php?uicode=gs170320031609_345.
64. Nagaura, Y., et al., *Battery-powered Drive Systems: Latest Technologies and Outlook*, in *Hitachi Review*. 2017, Hitachi Ltd. p. 138-144.
 65. Shimada, M., et al., *Energy-saving Technology for Railway Traction Systems Using Onboard Storage Batteries*, H. Review, Editor. 2012, Hitachi Company Ltd. p. 312-318.
 66. Y.Kono, et al., *Catenary and Storage Battery Hybrid System for Electric Railcar Series EV-E301*, in *Power Electronics Conference* 2014.
 67. UK, B. *Success for Bombardier and its industry partners at the 2015 Railway Industry Innovation Awards*. 2015 [cited 2017 5/9/2017]; Available from: <http://uk.bombardier.com/en/media/newsList/details.BT-20150629-Success-for-Bombardier-and-its-industry-partners-at-the-2015-Railway-Industry-Innovation-Awards.gb.html>.
 68. Budiansky, N., et al., *Comparison of Selected Lithium-Ion Battery Chemistries*, A.o.h.w.v.c.w.-v.s. Exponent Testing Report, Editor. 2007, Exponent - Mechanical and Materials Practice.
 69. Railway Technology - News, v.a.c.f.t.g.R.i. *Independently Powered Electric Multiple-Unit (IPEMU)*, Essex, United Kingdom. 2015 [cited 2017; Available from: <http://www.railway-technology.com/projects/independently-powered-electric-multiple-unit-ipemu-essex/>.
 70. N.Takami, et al., *High power and long-life lithium-ion batteries using lithium titanium oxide anode for automotive and stationary power applications*. *Journal of Power Sources*, 2013. **244**: p. 469-475.
 71. Yamamoto, T., *Trends and Recent Studies on Hybrid Railway Vehicles*. Quarterly Report of Railway Technical Research Institute (RTRI), 2017. **58**(1): p. 1-5.
 72. Nikolaidis, P. and A. Poullikkas, *A comparative review of electrical energy storage systems for better sustainability*. *Journal of Power Technologies*, 2016. **Accepted Manuscripts**.
 73. Burke, A. and M. Miller, *The power capability of ultracapacitors and lithium batteries for electric and hybrid vehicle applications*. *Journal of Power Sources*, 2011. **196**: p. 514-522.
 74. Chukwuka, C. and K.A. Folly, *Batteries and super-capacitors*, in *Power Engineering Society Conference and Exposition in Africa (PowerAfrica)*, IEEE, Editor. 2012, IEEE: Johannesburg, South Africa.
 75. Commission, E., *RailEnergy – innovative integrated energy efficiency solutions for railway rolling stock, rail infrastructure and train operation*, in *final report deliverable*. 2009, European Commission: Brussels.
 76. Fröhlich, M., M. Kloor, and S. Pagiela, *Energy Storage System with UltraCaps on Board of Railway Vehicles*, in *2007 European Conference on Power Electronics and Applications*, IEEE, Editor. 2007, IEEE: Aalborg, Denmark. p. 1-10.
 77. SEKIJIMA, Y., et al., *Development of an Energy Storage System for DC Electric Rolling Stock by applying Electric Double Layer Capacitors*. *English Magazine Japanese Railway Engineering*, 2006. **46**(1).
 78. Meinert, M., et al., *Benefits of hybridisation of diesel driven rail vehicles: Energy management strategies and life-cycle costs appraisal*. *Applied Energy*, 2015. **157**: p. 897-904.
 79. Moskowitz, J.-P. and J.-L. Cohuau, *STEEM: ALSTOM and RATP experience of supercapacitors in tramway operation*, in *Vehicle Power and Propulsion Conference (VPPC)*, IEEE, Editor. 2010, IEEE: Lille, France.
 80. Östergård, R., *Flywheel Energy Storage—A Conceptual Study*. 2011, Uppsala Universitet: Uppsala.
 81. R.Sebastián and R.P. Alzola, *Flywheel energy storage systems: Review and simulation for an isolated wind power*

- system. *Renewable and Sustainable Energy Reviews*, 2012. **16**(9): p. 6803-6813.
82. Parfomak, P.W., *Energy Storage for Power Grids and Electric Transportation: A Technology Assessment in Congressional Research Services*. 2012: Washington, DC, USA.
83. Oliveira, J.G.D., *Power Control Systems in a Flywheel based All-Electric Driveline*. 2011, Uppsala Universitet: Uppsala, Sweden.
84. Zhang, X. and J. Yang. *An improved discharge control strategy with load current and rotor speed compensation for high-speed flywheel energy storage system*. in *The 17th International Conference on Electrical Machines and Systems (ICEMS)*. 2014. Hangzhou, China.
85. Pena-Alzola, R., et al. *Review of Flywheel based Energy Storage Systems*. in *International Conference on Power Engineering, Energy and Electrical Drives*. 2011. Malaga, Spain: IEEE.
86. Bolund, B., H. Bernhoff, and M. Leijon, *Flywheel energy and power storage systems*. *Renewable and Sustainable Energy Reviews*, 2007. **11**: p. 235-258.
87. Amiryar, M.E. and K.R. Pullen, *A Review of Flywheel Energy Storage System Technologies and Their Applications*. *Applied Sciences*, 2017. **7**(3).
88. Hadjipaschalis, I., A. Poullikkas, and V. Efthimiou, *Overview of current and future energy storage technologies for electric power applications*. *Renewable and Sustainable Energy Reviews*, 2009: p. 1513-1522.
89. Suzuki, Y., et al., *Novel applications of the flywheel energy storage system*. *Energy Conversion and Management*, 2005. **30**(11): p. 2128-2143.
90. Gee, A.M. and R.W. Dunn, *Analysis of Trackside Flywheel Energy Storage in Light Rail Systems*. *IEEE Transactions On Vehicular Technology*, 2015. **64**(9): p. 3858-3869.
91. Lee, H., et al., *Peak power reduction and energy efficiency improvement with the superconducting flywheel energy storage in electric railway system*. *Physica C: Superconductivity*, 2013. **494**: p. 246-249.
92. Rupp, A., et al., *Analysis of a flywheel energy storage system for light rail transit*. *Energy*, 2016. **107**: p. 625-638.
93. Spiriyagin, M., et al., *Application of flywheel energy storage for heavy haul locomotives*. *Applied Energy*, 2015. **157**: p. 607-618.
94. Ricardo, *Ricardo to showcase 'TorqStor' high efficiency flywheel energy storage at CONEXPO*, Ricardo, Editor. 2014.
95. Iwnicki, S., *Handbook of Railway Vehicle Dynamics*. 2006: Taylor & Francis Group.
96. Basu, S., et al., *Coupled electrochemical thermal modelling of a novel Lithium-ion battery pack thermal management system*. *Applied Energy*, 2016. **181**: p. 1-13.
97. Gao, L., S. Liu, and R.A. Dougal, *Dynamic Lithium-Ion Battery Model for System Simulation*. *IEEE TRANSACTIONS ON COMPONENTS AND PACKAGING TECHNOLOGIES*, 2002. **25**(3).
98. Tremblay, O., L.-A. Dessaint, and A.-I. Dekkiche, *A Generic Battery Model for the Dynamic Simulation of Hybrid Electric Vehicles*, in *Vehicle Power and Propulsion Conference*, IEEE, Editor. 2007: Arlington, TX, USA.

8. APPENDIX: Matlab™ program for dynamic simulation

```
clear all
close all
clc

WW = xlsread('todo4.xlsx',3);
time = WW(1:end,1);
distance = WW(1:end,2);
accel = WW(1:end,3);
speed = WW(1:end,4);
totbrakpow = WW(1:end,7);
% comple includes total power(traction + pneumatic and dynamic brake)
comple = WW(1:end,8);
% pow includes tractive and ED braking power
pow = WW(1:end,end-1);
slope = WW(1:end,end);
dtdt = 0.1;
etabatt = .90; % battery efficiency (for a complete charge/discharge cycle)
powaux = 191; % auxiliary power demand [kW]
%% PLOT duty cycle

figure(1)
[AX,H1,H2] = plotyy(time,speed,time,pow);
hold on
grid on
title('DUTY CYCLE','FontSize',8)
legend('speed [km/h]','power [kW]')
neworder = {
    'Start'
    'Stop. Reb.'
    'Dep. Reb.'
    'Stop PS'
    'Dep. PS'
    'Stop PN'
    'Dep. PN'
    'Stop PS (R)'
    'Dep. PS (R)'
    'Stop Reb.(R)'
    'Dep. Reb.(R)'
    'End'};
set(H1,'Linewidth',1.5);
set(H2,'Linewidth',1.5);
xticks([0.0 54.6 114.6 510.5 570.4 946.6 1006.6 1382.9 1442.9 1838.1 1898.1
time(end)])
set(gca,'Xticklabel',neworder(:,1),'FontSize',12);
xtickangle(35);

%% leggo i punti della curva di scarica dal datasheet
fileID = fopen('lc_curve_B_m.txt','r');
formatSpec = '%f';
% KK è formato da da una colonna che ha in px dispari la capacity e pari il
% voltaggio
[KK] = fscanf(fileID,formatSpec);
QQ = KK(1:2:end);
VV = KK(2:2:end);
QQ = [1-QQ];
VV = [VV];
```

```

%% caratteristiche modulo
Vnom = 27.6; % Volt
Mmodule = 15; %kg
Qrated = 45; %Ah @C/5
Qnom = QQ(1)*Qrated; % Ah

%% fitting di V = V(Q) presa dal datasheet in CHARGE

fileID = fopen('sab1.txt','r');
formatSpec = '%f';
[LL] = fscanf(fileID,formatSpec);
% QQc and VVc are the SOC and voltage fitted through the charge curve
QQc = LL(1:2:end);
VVc = LL(2:2:end);
VVc = [24.9;VVc];
QQc = [0.0;QQc];

%% Plotto le caratteristiche di CHARGE e DISCHARGE

figure(5)
plot([0:1:100],interp1(QQc,VVc,[.0:.01:1.0]))
hold on
grid on
plot([0:1:100],interp1(QQ,VV,[1:-.01:0.0]),'b')
legend('discharge','charge','location','S')
title('Charge and Discharge characteristics')
ylabel('Voltage [V]')
xlabel('Capacity [%]')

%% dynamic simulation with regenerative braking

np = 12; %rami in parallelo
ns = 38; % moduli in serie
Inom = 45; % Ampere corrente nominale

%% inizializzo le variabili

SOCinitial = .70;
Qc(1) = SOCinitial*Qnom; %[Ah] charged energy
SOC(1) = Qc(1)/Qnom*100;
Vbatt(1) = interp1(QQc,VVc,Qc(1)/Qnom); %[V] voltaggio iniziale modulo
Rege = zeros(length(time),1);
Vpack(1) = ns*Vbatt(1);% [V]
Ir(1) = 0;
Ipack(1) = 0;
Ebrak(1) = 0;
edis(1) = 0;
%% %%%%%%%%%% DYNAMIC SIMULATION START %%%%%%%%%%
for ii = 2:length(time)

    dt = (time(ii)-time(ii-1))/3600; % [h]

    %% 1) PURE TRACTION

    if (pow(ii-1)>0.0 && pow(ii)>=0.0)

        Ebrak(ii) = 0;
        Etract(ii) = abs(pow(ii)*dt);
        % Ir is the current required in each branch
        Ir(ii) = (powaux + pow(ii))*1000/(ns*np*interp1(QQ,VV,Qc(ii-1)/Qnom));
    end
end

```

```

% Qc is the SOC calculated through Coulomb method
Qc(ii) = Qc(ii-1) - abs(Ir(ii)*dt);
% Vbatt is the voltage of the single module
Vbatt(ii) = interp1(QQ,VV,Qc(ii-1)/Qnom);
% edis is the energy discharged by battery during dt
edis(ii) = Ir(ii)*dt*np*ns*Vbatt(ii)/1000;

%% 2) TRACTION --> BRAKING

elseif (pow(ii-1)>0.0 && pow(ii)<0.0)

    % Ebrak and Etract are braking and tractive energy in [kWh]
    Ebrak(ii) = abs(pow(ii)*dt);
    Etract(ii) = 0;

    if (Vbatt(ii-1) <= VVc(end) && Vbatt(ii-1) >= VVc(1) &&
abs(pow(ii)) > powaux)
        % 1) la Pbrake è maggiore della Paux --> RICARICO
        edis(ii) = 0;

        % interp1(QQc,VVc,Qc(ii-1)/Qnom) valuta la tensione sulla curva
        % di carica che avrebbe la batteria con la carica Q(i-1), cioè
        % all'inizio dell'istante i. Nota tale tensione, calcolo la
        % corrente che può accettare la batteria in RECHARGE.
        Ir(ii) = abs(pow(ii)+powaux)*1000/(ns*np*interp1(QQc,VVc,Qc(ii-
1)/Qnom));

        % posso ricaricare perchè Vmin_charge < Vbatt < Vmaxc_charge
        %limito corrente in carica

        if (Qc(ii-1)/Qnom <= 0.80)
            %posso usare 3C
            Irlim(ii) = min(abs(Ir(ii)),3*Inom);
            Qc(ii) = Qc(ii-1) + etabatt*abs(Irlim(ii))*dt;
        elseif ( Qc(ii-1)/Qnom > 0.80 && Qc(ii-1)/Qnom <= 0.90)
            %posso usare 1C
            Irlim(ii) = min(abs(Ir(ii)),Inom);
            Qc(ii) = Qc(ii-1) + etabatt*abs(Irlim(ii))*dt;
        elseif (Qc(ii-1)/Qnom > 0.90 && Qc(ii-1)/Qnom <= 1.0)
            Irlim(ii)= min(abs(Ir(ii)),Inom/5);
            Qc(ii) = Qc(ii-1) + etabatt*abs(Irlim(ii))*dt;
        end

        Vbatt(ii) = interp1(QQc,VVc,Qc(ii)/Qnom);

        % Rege indicates the effective energy accepted by battery
        Rege(ii) = abs(Irlim(ii)*dt)*np*Vbatt(ii)*ns/1000; % [kWh]
        Ir(ii) = (powaux + pow(ii))*1000/(ns*np*Vbatt(ii));

    elseif (Vbatt(ii-1) <= VVc(end) && Vbatt(ii-1) >= VVc(1) &&
abs(pow(ii)) < powaux)

        % 2) Pbrake < Paux --> SCARICO
        % quello che avviene è che da un certo punto in poi la EDbraque
        % power non è sufficiente per ricaricare le batterie quindi la
        % utilizzo per alimentare gli auxiliary. Dato che EDbraque power
        % può non bastare ad alimentare gli aux, allora scarico le
        % batterie per fornire la potenza mancante.

        % Durante la frenata passo quindi dalla carica alla scarica
        % dall'istante i-1 a i:

```

```

    Ir(ii) = (pow(ii)+powaux)*1000/(ns*np*interp1(QQ,VV,Qc(ii-
1)/Qnom));
    Qc(ii) = Qc(ii-1) - abs(Ir(ii))*dt;
    Vbatt(ii) = interp1(QQ,VV,Qc(ii)/Qnom);
    edis(ii) = Ir(ii)*dt*ns*np*Vbatt(ii)/1000; % [kWh]
    Ir(ii) = (powaux + pow(ii))*1000/(ns*np*Vbatt(ii));
else
    % WARNING!
    fprintf('caso non considerato nel tract2brake\n');
end

%% 3) PURE BRAKING

elseif (pow(ii-1) < 0.0 && pow(ii) < 0.0)

    Etract(ii) = 0.0;
    Ebrak(ii) = abs(pow(ii)*dt*1000);
    Ir(ii) = (powaux + pow(ii))*1000/(ns*np*interp1(QQc,VVc,Qc(ii-
1)/Qnom));

    % 1b) la Pbrake è maggiore della Paux --> RICARICO
    % 2b) la batteria ha Voltaggio compreso tra Vmin e Vmax della
    % curva di scarica.

    if (powaux < abs(pow(ii)) && Vbatt(ii-1) >= VVc(1) && Vbatt(ii-1)
<= VVc(end))
        edis(ii) = 0;
        Ir(ii) = (pow(ii)+powaux)*1000/(ns*np*interp1(QQc,VVc,Qc(ii-
1)/Qnom));
        % interp1(QQc,VVc,Qc(ii-1)/Qnom) valuta la tensione all'istante
        % i-1 sulla curva di carica
        % verifico il C-rate che la batteria riesce ad accettare in
base alla
        % carica contenuta alla fine dell'istante i-1, cioè all'inizio
        % dell'istante i.

        if (Qc(ii-1)/Qnom <= 0.80)
            %posso usare 3C
            Irlim(ii) = min(abs(Ir(ii)),3*Inom);
            Qc(ii) = Qc(ii-1) + etabatt*abs(Irlim(ii))*dt;

        elseif ( Qc(ii-1)/Qnom > 0.80 && Qc(ii-1)/Qnom <= 0.90)
            %posso usare 1C
            Irlim(ii) = min(abs(Ir(ii)),Inom);
            Qc(ii) = Qc(ii-1) + etabatt*abs(Irlim(ii))*dt;

        elseif (Qc(ii-1)/Qnom > 0.90 && Qc(ii-1)/Qnom <= 1.0)
            %posso usare 0.2C
            Irlim(ii)= min(abs(Ir(ii)),Inom/5);
            Qc(ii) = Qc(ii-1) + etabatt*abs(Irlim(ii))*dt;
        end

        Vbatt(ii) = interp1(QQc,VVc,Qc(ii)/Qnom);
        Rege(ii) = abs(Irlim(ii)*dt)*np*Vbatt(ii)*ns/1000; % [kWh]

    elseif (powaux > abs(pow(ii)) && Vbatt(ii-1)>= VVc(1) && Vbatt(ii-
1) <= VVc(end))
        flag = 0;
        % mi serve per capire in che situazione sono quando
        % passerò da braking a traction

```

```

% B) NON posso ricaricare perchè:
% 1) la |Pbrake| < Paux --> scarico le batterie
% per alimentare gli ausiliari--> tratto questa fase come
% DIScharge.

% all'istante i-1 ero sulla curva di carica; all'inizio
% dell'istante i passo sulla curva di scarica con la
% quantità di carica che avevo a 'i-1'--> valuto la tensione
% e calcolo la corrente che deve erogare la batteria
% per fornire la potenza pow(ii).
Ir(ii) = (powaux+pow(ii))*1000/(ns*np*interp1(QQ,VV,Qc(ii-
1)/Qnom));
Qc(ii) = Qc(ii-1) - abs(Ir(ii))*dt;
Vbatt(ii) = interp1(QQ,VV,Qc(ii)/Qnom);
edis(ii) = abs(Ir(ii))*ns*np*Vbatt(ii)*dt/1000;

elseif ( (Vbatt(ii-1) <= VVc(1) && Vbatt(ii-1) >= VVc(end) &&
powaux <= abs(pow(ii))))
% non posso ricaricare perchè sono già troppo carico, oppure
% sono troppo scarico per ricaricare @ I = cost;
Vbatt(ii) = Vbatt(ii-1);
Qc(ii) = Qc(ii-1);
edis(ii) = 0;
fprintf('dissipo su brake resistor in PURE BRAKING\n');
else
fprintf('CASO non considerato PURE BRAKING\n');
end

%% 4) BRAKING --> TRACTION

elseif (pow(ii-1)<0.0 && pow(ii)>0.0)

Ebrak(ii) = 0;
Etract(ii) = abs(pow(ii)*dt);

if flag == 1
% flag = 1significa che stavo ricaricando le batterie in
braking e che
% quindi devo spostarmi sulla curva di scarica con la quantità
% di carica che avevo all'istante i-1, calcolando la tensione
% e la corrente che potrebbe erogare la batteria.

Ir(ii) = (powaux + pow(ii))*1000/(ns*np*interp1(QQ,VV,Qc(ii-
1)/Qnom));
Qc(ii) = Qc(ii-1) - abs(Ir(ii))*dt;
Vbatt(ii) = interp1(QQ,VV,Qc(ii)/Qnom);
edis(ii) = Ir(ii)*dt*np*ns*Vbatt(ii)/1000;
else
% significa che flag = 0
% nella precedente fase di braking stavo scaricando le
batterie
% e quindi continuo sulla curva di scarica.
Ir(ii) = (powaux+pow(ii))*1000/(ns*np*interp1(QQ,VV,Qc(ii-
1)/Qnom));
Qc(ii) = Qc(ii-1) - abs(Ir(ii))*dt;
Vbatt(ii) = interp1(QQ,VV,Qc(ii)/Qnom);
edis(ii) = Ir(ii)*dt*np*ns*Vbatt(ii)/1000;
end

%% 5) COASTING --> BRAKING

```

```

elseif (pow(ii-1) == 0.0 && pow(ii) < 0.0)

    Ebrak(ii) = abs(pow(ii)*dt);
    Etract(ii) = 0;

    if (Vbatt(ii-1) <= VVc(end) && Vbatt(ii-1) <= VVc(1) &&
abs(pow(ii)) > powaux)

        % 1) la Pbrake è maggiore della Paux --> RICARICO
        % interp1(QQc,VVc,Qc(ii-1)/Qnom) valuta la tensione sulla curva
        % di carica che avrebbe la batteria con la carica Q(i-1), cioè
        % all'inizio dell'istante i. Nota tale tensione, calcolo la
        % corrente che può accettare la batteria in RECHARGE.

        Ir(ii) = (powaux+pow(ii))*1000/(ns*np*interp1(QQc,VVc,Qc(ii-
1)/Qnom));
        edis(ii) = 0;

        %limito corrente in carica
        if (Qc(ii-1)/Qnom <= 0.80)
            %posso usare 3C
            Irlim(ii) = min(abs(Ir(ii)),3*Inom);
            Qc(ii) = Qc(ii-1) + etabatt*abs(Irlim(ii))*dt;

        elseif ( Qc(ii-1)/Qnom > 0.80 && Qc(ii-1)/Qnom <= 0.90)
            %posso usare 1C
            Irlim(ii) = min(abs(Ir(ii)),Inom);
            Qc(ii) = Qc(ii-1) + etabatt*abs(Irlim(ii))*dt;

        elseif (Qc(ii-1)/Qnom > 0.90 && Qc(ii-1)/Qnom <= 1.0)
            %posso usare 0.2C
            Irlim(ii)= min(abs(Ir(ii)),Inom/5);
            Qc(ii) = Qc(ii-1) + etabatt*abs(Irlim(ii))*dt;
        end

        Vbatt(ii) = interp1(QQc,VVc,Qc(ii)/Qnom);
        Rege(ii) = abs(Irlim(ii)*dt)*np*Vbatt(ii)*ns/1000; % [kWh]
        edis(ii) = 0;

    elseif (powaux > abs(pow(ii)) && Vbatt(ii-1)> VVc(1) && Vbatt(ii-1)
< VVc(end))
        % la Pbrake < Paux --> la potenza mancante viene fornita dalle
        % batterie le quali seguono la curva di scarica anche se sto
        % frenando.

        Ir(ii) = (pow(ii)+powaux)*1000/(ns*np*interp1(QQ,VV,Qc(ii-
1)/Qnom));
        Qc(ii) = Qc(ii-1) - abs(Ir(ii))*dt;
        Vbatt(ii) = interp1(QQ,VV,Qc(ii)/Qnom);
        edis(ii) = Ir(ii)*dt*np*ns*Vbatt(ii)/1000;
    end

    %% 6) COASTING --> TRACTION

    elseif (pow(ii-1) == 0.0 && pow(ii) > 0.0)

        Ebrak(ii) = 0;
        Etract(ii) = abs(pow(ii)*dt);
        Ir(ii) = (powaux + pow(ii))*1000/(ns*np*interp1(QQ,VV,Qc(ii-
1)/Qnom));
        Qc(ii) = Qc(ii-1) + abs(Ir(ii))*dt;

```

```

        Vbatt(ii) = interp1(QQ,VV,Qc(ii)/Qnom);
        edis(ii) = Ir(ii)*dt*np*ns*Vbatt(ii)/1000;
        %% 7) BRAKING --> COASTING

    elseif (pow(ii-1) < 0.0 && pow(ii) == 0.0)

        Ebrak(ii) = 0;
        Etract(ii) = 0;
        Ir(ii) = (powaux + pow(ii))*1000/(ns*np*interp1(QQ,VV,Qc(ii-1)/Qnom));
        Qc(ii) = Qc(ii-1) - abs(Ir(ii))*dt;
        Vbatt(ii) = interp1(QQ,VV,Qc(ii)/Qnom);
        edis(ii) = Ir(ii)*dt*np*ns*Vbatt(ii)/1000;
        %% 8) TRACTION --> COASTING

    elseif(pow(ii-1) > 0.0 && pow(ii) == 0.0)

        Ebrak(ii) = 0.0;
        Etract(ii) = 0.0;
        Ir(ii) = (pow(ii)+powaux)*1000/(ns*np*interp1(QQ,VV,Qc(ii-1)/Qnom));
        Qc(ii) = Qc(ii-1) - abs(Ir(ii))*dt;
        Vbatt(ii) = interp1(QQ,VV,Qc(ii)/Qnom);

        %% 9) PURE COASTING: sto scaricando la batteria SOLO a causa degli ausiliari

    elseif (pow(ii-1) == 0.0 && pow(ii) == 0.0)

        Ebrak(ii) = 0;
        Etract(ii) = 0.0;
        Ir(ii) = (powaux+pow(ii))*1000/(ns*np*interp1(QQ,VV,Qc(ii-1)/Qnom));
        Qc(ii) = Qc(ii-1) - abs(Ir(ii))*dt;
        Vbatt(ii) = interp1(QQ,VV,Qc(ii)/Qnom);
        edis(ii) = Ir(ii)*dt*np*ns*Vbatt(ii)/1000;
    end

end

figure(6)
[AX,H1,H2]=plotyy(time(1:end),powaux+pow(1:end),time(1:end),ns*Vbatt(1:end));
% set(AX(2),'YLim',[18:.2:32.4]);
% set(AX(1),'YLim',[-5000 5000]);
hold on
grid on
title('traction & aux power [kW] and battery pack Voltage [V]')

figure(9)
plotyy(time(1:ii),Vbatt.*ns,time(1:ii),Ir.*np);
hold on
grid on
title('Pack Voltage and Current')
legend('V_p_a_c_k [V]','I_p_a_c_k [A]')

figure(13)
plotyy(time,Vbatt,time,powaux+pow);
hold on
grid on

```



```

title('Battery module voltage [V] - Power required (tract + aux) [KW]');
xlabel('time [s]');
legend('Voltage','Power');

Ereg = sum(Rege); % [kWh]
Ebrak1 = sum(Ebrak)/1000; % [kWh]
TractEne = sum(Etract); % [kWh]
Auxene = powaux*(time(end)-time(1))/3600; % [kWh]
fprintf('Configurazione pacco batterie:\n moduli serie %d\n rami parallelo
%d\n massa totale %d kg\n',ns,np,np*ns*Mmodule)
fprintf('total ED braking energy = %.2f kWh\n', Ebrak1);
fprintf('Auxiliary Energy demand = %.1f kWh\n',Auxene);
fprintf('Total Energy demand = %.1f kWh\n',TractEne + Auxene);
fprintf('Recovered energy / ED braking energy %.1f percent
\n',Ereg/Ebrak1*100);
fprintf('Recovered energy / tractive energy %.1f percent
\n',Ereg/TractEne*100);
fprintf('Recovered energy / total brake energy %.1f percent
\n',Ereg/Ebrak1*100);
fprintf('Max Voltage = %.1f [V]\n Minimum Voltage = %.1f
[V]\n',max(Vbatt)*ns,min(Vbatt)*ns)
fprintf('Max Current discharge = %.1f [A]\n Max Current charge = %.1f
[A]\n',max(Ir),abs(min(Ir)))
fprintf('Max C-rate in discharge = %.1f\n',max(Ir)/Inom);
fprintf('Average C-rate = %.1f\n',mean(Ir(find(Ir(1:end)>0))/Inom));
figure(17)
plotyy(time,Rege,time,powaux*pow);
legend('Regen Energy [kWh]','tract power + aux power [kW]')

figure(18)
plot(time,Rege.*1000)
hold on
grid on
xlabel('time')
ylabel('Recoverd energy [Wh]')

Cumulata(1) = 0;
Ede(1) = Etract(1);
for kk = 2:length(Rege)
    Cumulata(kk) = Cumulata(kk-1) + Rege(kk);
    Ede(kk) = Ede(kk-1)+Etract(kk)+ (powaux*(time(kk)-time(kk-1))/3600);
end
figure(19)
plot(time./60,Cumulata,time./60,Ede);
legend('Regenerative energy [kWh]','Energy Demand [kWh]')
hold on
grid on
line(time./60,pow)
xlabel('time [min]')

fprintf('Initial battery pack energy = %.1f
[kWh]\n',ns*np*Qc(1)*Vbatt(1)/1000);
fprintf('Final battery pack energy = %.1f
[kWh]\n',ns*np*Qc(end)*Vbatt(end)/1000);
fprintf('Battery pack used energy = %.1f [kWh]\n',sum(edis(1:end)));
fprintf('INITIAL SOC = %.1f percent\n',SOCinitial*100);
fprintf('FINAL SOC = %.1f percent\n',Qc(end)/Qnom*100);
fprintf('Regenerative energy = %.2f kWh\n ED Braking energy = %.2f kWh
\n',Ereg,Ebrak1);

figure(20)

```

```

subplot(3,1,1)
[ax1 h1 h2] = plotyy(time,Vbatt,time,Ir);
title('Voltage & Current')
ylabel(ax1(1), 'Voltage [V]')
ylabel(ax1(2), 'Current [A]')
hold on
grid on

subplot(3,1,2)
plot(time,powaux + pow)
title('Power [kW]')
hold on
grid on

subplot(3,1,3)
plot(time,Qc./Qnom.*100)
title('State of Charge')
ylabel('SOC[%]')
xlabel('time [s]')
hold on
grid on

%% calcolo tempo di ricarica
% in base a SOC(end) posso conoscere a che I ricaricare
jj=1;
SOClast = Qc(end)/Qnom;
L1 = .80;
L2 = .90;
L3 = 1.05;

if (SOClast <= L1 && SOCinitial < L1)
    % se finisco la tratta a SOC <= 80% e la SOC a cui voglio ricaricare
    % le batterie è <= 80% allora posso ricaricare @ 3C:
    time2charge = ((SOCinitial - SOClast)*Qnom)/(3*Inom)*60; % [min]
    fprintf('time to charge @ 3C = %.2f minutes \n',time2charge);

elseif (SOCinitial >= L1 && SOCinitial <= L2 && SOClast <= L2)

    time2charge = ((L1 - SOClast)*Qnom)/(3*Inom)*60 + (SOCinitial -
L1)*Qnom/(Inom)*60;
    fprintf('time to charge @ 3C = %.2f minutes \n time to charge @ 1C =
%.2f minutes \n total time to charge = %.2f minutes\n ',...
        (L1 - SOClast)*Qnom/(3*Inom)*60, (SOCinitial - L1)*Qnom/Inom*60,
time2charge);

elseif (SOCinitial > L2 && SOCinitial <= L3)
    time2charge = ((L1 - SOClast)*Qnom)/(3*Inom)*60 + (L2 -
L1)*Qnom/(Inom)*60 + (SOCinitial - L2)*Qnom/(Inom/5)*60;
    fprintf('time to charge @ 3C = %.2f minutes \n time to charge @ 1C =
%.2f minutes \n time to charge @ C/5 = %.2f minutes \n total time to charge
= %.2f minutes\n',...
        (L1 - SOClast)*Qnom/(3*Inom)*60, (L2 - L1)*Qnom/Inom*60,
(SOCinitial - L2)*Qnom/(Inom/5)*60, time2charge);
end

BRAKE(1) = 0;
for uu = 2:length(totbrakpow)
    deltat = time(uu)-time(uu-1);
    BRAKE(uu) = BRAKE(uu-1) + totbrakpow(uu)*deltat/3600;
end
fprintf('total brake energy = %.1f [kWh]\n',BRAKE(end));

```

```

figure(193)
x1 = time./60;
y1 = Qc./Qnom*100;
line(x1,y1,'Color','b','Linewidth',1.3)
u = axis();
ax1 = gca; % current axes
ax1.XColor = 'k';
ax1.YColor = 'b';
ax1_pos = ax1.Position; % position of first axes
ylabel('SOC [%]','Color','b','FontSize',15)
xlabel('time [min]','FontSize',13.5)
ax2 = axes('Position',ax1_pos,...
    'XAxisLocation','top',...
    'YAxisLocation','right',...
    'Color','none');
x2 = time./60;
y2 = pow+powaux;
line(x2,y2,'Parent',ax2,'Color','r','Linewidth',1.3)
ax2.YColor = 'r';
v=axis();
axis([v(1) u(2) v(3) v(4)]);
xticks([0.0 54.6./60 114.6./60 510.5./60 570.4./60 946.6./60 1006.6./60
1382.9./60 1442.9./60 1838.1./60 1898.1./60 time(end)./60])
set(gca,'Xticklabel',neworder(:,1));
xtickangle(-30);
hold on
grid on
ylabel('Power [kW]','Color','r','FontSize',15)

figure(194)
x1 = time./60;
y1 = speed;
line(x1,y1,'Color','b','Linewidth',1.3)
u = axis();
ax1 = gca; % current axes
ax1.XColor = 'k';
ax1.YColor = 'b';
ax1_pos = ax1.Position; % position of first axes
ylabel('Speed [km/h]','Color','b','FontSize',15)
xlabel('time [min]','FontSize',13.5)
ax2 = axes('Position',ax1_pos,...
    'XAxisLocation','top',...
    'YAxisLocation','right',...
    'Color','none');
x2 = time./60;
y2 = distance./1000;
line(x2,y2,'Parent',ax2,'Color','r','Linewidth',1.3)
ax2.YColor = 'r';
v=axis();
axis([v(1) u(2) v(3) v(4)]);
xticks([0.0 54.6./60 114.6./60 510.5./60 570.4./60 946.6./60 1006.6./60
1382.9./60 1442.9./60 1838.1./60 1898.1./60 time(end)./60])
set(gca,'Xticklabel',neworder(:,1));
xtickangle(-25);
hold on
grid on
ylabel('Distance [km]','Color','r','FontSize',15)

figure(195)
x1 = time./60;

```

```

y1 = ns*Vbatt;
line(x1,y1,'Color','b','Linewidth',1.3)
u = axis();
ax1 = gca; % current axes
ax1.XColor = 'k';
ax1.YColor = 'b';
ax1_pos = ax1.Position; % position of first axes
ylabel('Battery pack Voltage [V]','Color','b','FontSize',15)
xlabel('time [min]','FontSize',13.5)
ax2 = axes('Position',ax1_pos,...
    'XAxisLocation','top',...
    'YAxisLocation','right',...
    'Color','none');
x2 = time./60;
y2 = np*Ir;
line(x2,y2,'Parent',ax2,'Color','r','Linewidth',1.3)
ax2.YColor = 'r';
v=axis();
axis([v(1) u(2) v(3) v(4)]);
xticks([0.0 54.6./60 114.6./60 510.5./60 570.4./60 946.6./60 1006.6./60
1382.9./60 1442.9./60 1838.1./60 1898.1./60 time(end)./60])
set(gca,'Xticklabel',neworder(:,1));
xtickangle(-30);
hold on
grid on
ylabel('Total Current [A]','Color','r','FontSize',15)

figure(196)
x1 = time./60;
y1 = slope;
line(x1,y1,'Color','b','Linewidth',1.3)
u = axis();
ax1 = gca; % current axes
ax1.XColor = 'k';
ax1.YColor = 'b';
ax1_pos = ax1.Position; % position of first axes
ylabel('slope [%]','Color','b','FontSize',18)
xlabel('time [min]','FontSize',13.5)
ax2 = axes('Position',ax1_pos,...
    'XAxisLocation','top',...
    'YAxisLocation','right',...
    'Color','none');
x2 = time./60;
y2 = accel;
line(x2,y2,'Parent',ax2,'Color','r','Linewidth',1.3)
ax2.YColor = 'r';
v=axis();
axis([v(1) u(2) v(3) v(4)]);
xticks([0.0 54.6./60 114.6./60 510.5./60 570.4./60 946.6./60 1006.6./60
1382.9./60 1442.9./60 1838.1./60 1898.1./60 time(end)./60])
set(gca,'Xticklabel',neworder(:,1));
xtickangle(-25);
hold on
grid on
ylabel('Acceleration [m/s^2]','Color','r','FontSize',18)

figure(197)
x1 = time./60;
y1 = speed;
line(x1,y1,'Color','b','Linewidth',1.3)
u = axis();

```

```

ax1 = gca; % current axes
ax1.XColor = 'k';
ax1.YColor = 'b';
ax1_pos = ax1.Position; % position of first axes
ylabel('Speed [km/h]', 'Color', 'b', 'FontSize', 18)
xlabel('time [min]', 'FontSize', 13.5)
ax2 = axes('Position', ax1_pos, ...
    'XAxisLocation', 'top', ...
    'YAxisLocation', 'right', ...
    'Color', 'none');
x2 = time./60;
y2 = comple+powaux;
line(x2, y2, 'Parent', ax2, 'Color', 'r', 'Linewidth', 1.3)
ax2.YColor = 'r';
v=axis();
axis([v(1) u(2) v(3) v(4)]);
xticks([0.0 54.6./60 114.6./60 510.5./60 570.4./60 946.6./60 1006.6./60
1382.9./60 1442.9./60 1838.1./60 1898.1./60 time(end)./60])
set(gca, 'Xticklabel', neworder(:,1));
xtickangle(-25);
hold on
grid on
ylabel('Power [kW]', 'Color', 'r', 'FontSize', 18)

figure(198)
x1 = time./60;
y1 = Ir./Inom;
line(x1, y1, 'Color', 'b', 'Linewidth', 1.3)
u = axis();
ax1 = gca; % current axes
ax1.XColor = 'k';
ax1.YColor = 'b';
ax1_pos = ax1.Position; % position of first axes
ylabel('C-rate [-]', 'Color', 'b', 'FontSize', 18)
xlabel('time [min]', 'FontSize', 13.5)
ax2 = axes('Position', ax1_pos, ...
    'XAxisLocation', 'top', ...
    'YAxisLocation', 'right', ...
    'Color', 'none');
x2 = time./60;
y2 = Ir;
line(x2, y2, 'Parent', ax2, 'Color', 'r', 'Linewidth', 1.3)
ax2.YColor = 'r';
v=axis();
axis([v(1) u(2) v(3) v(4)]);
xticks([0.0 54.6./60 114.6./60 510.5./60 570.4./60 946.6./60 1006.6./60
1382.9./60 1442.9./60 1838.1./60 1898.1./60 time(end)./60])
set(gca, 'Xticklabel', neworder(:,1));
xtickangle(-25);
hold on
grid on
ylabel('Single module current [A]', 'Color', 'r', 'FontSize', 18)

```

List of figures

Figure 1 Million tCO ₂ by fuel combustion by sector from 1990 to 2013. Source: reference	7
Figure 2 Share of electrified railway tracks in selected countries and geographic areas. Source: [1]....	8
Figure 3 Recommendations for Diesel Rolling Stock (DMU). Source: [5]	10
Figure 4 Layout of the train arrangement.....	12
Figure 5 Roof-mounted equipment in car 2.....	13
Figure 6 Roof-mounted equipment in car 4.....	13
Figure 7 Power pack scheme.....	14
Figure 8 Power flow of the single car in acceleration phase.....	Errore. Il segnalibro non è definito.
Figure 9 Power flow of the single car in coasting operation.....	Errore. Il segnalibro non è definito.
Figure 10 Power flow of the single car in ED braking operation.....	Errore. Il segnalibro non è definito.
Figure 11 Amount of ED brake power and total brake power desired. Source:[13]	17
Figure 12 Simplified scheme of the electric-pneumatic braking system. Source: [15]	18
Figure 13 Dual operation of electric motor/generator. Source: [16].....	19
Figure 14 Principle of rheostatic braking. Source: [10]	19
Figure 15 Different power supply systems for urban rail vehicles. Source: [7]	27
Figure 16 Scheme of regenerative braking energy sent back to the grid. Source: [21].....	28
Figure 17 Identification of potential energy recovery sources	21
Figure 18 Heat recovery scheme for power production	22
Figure 19 Ideal scheme of the heat recovery strategy.....	26
Figure 20 Example of stationary energy storage system. Source: [25]	30
Figure 21 Comparison of specific energy and specific power for different ES technologies. Source:[27]	31
Figure 22 Specific Energy. Specific power and C-rate for different battery technologies. Source: [31]	31
Figure 23 List of EV and HEV using different battery technologies. Source:[42]	33
Figure 24 SWIMO by Kawasaki Heavy Industry Ltd (left) and ALSTOM Citadis (right) in catenary-free operation in Nice (France) and Sapporo respectively. Source:[7, 25]	34
Figure 25 SITRAS-HES by Siemens Mobility.....	34
Figure 26 GIGACELL module by Kawasaki Heavy Industry Ltd.	34
Figure 27 AVENIO vehicle in catenary-free operation, Doha (Qatar). Source: [48]	35
Figure 28 COMBINO operating in Portugal. Source: [49]	35
Figure 29 Schematic operating principle of a Li-ion battery. Source:	35
Figure 30 Specification of different Lithium-ion battery chemistries. Source: [56].....	36
Figure 31 Twilight Express Mizukaze. Courtesy of West JR Company	37
Figure 32 Specifications of high output density modules. Source: [64].....	38
Figure 33 Series HB-E300 train. Source: [65]	38
Figure 34 IPEMU class 379. Source: [67].	38
Figure 35 On-board battery pack for the Series EV-E301. Source: [66].....	38
Figure 36 24V-70Ah Altairnano module	39
Figure 37 Schematic diagram of a super-capacitor. Source:[27]	40
Figure 38 Roof-mounted MITRAC Energy Saver on LRV in Mannheim. Source:[76]	41
Figure 39 Series-313 equipped with EDLC. Source: [77]	41
Figure 40 Scheme of a modern flywheel. Source: [27]	42
Figure 41 Roof-mounted flywheel on the Citadis operating in Rotterdam. Source: [44]	43
Figure 42 Prototype of the wheel-mounted flywheel system developed by Ricardo. Source:[94]	43
Figure 43 Conceptual Scheme of the Hybridization Process.....	45
Figure 44 Track slope and acceleration profile	46
Figure 45 Speed and distance profile	46

Figure 46 ED braking characteristic. Source: [95]	47
Figure 47 Composition of gravitational force.....	47
Figure 48 Speed and power demand	48
Figure 49 Charge characteristics for different C-rate.....	49
Figure 50 Discharge characteristics for different C-rate	49
Figure 51 Algorithm adopted in the sizing process	51
Figure 52 Power demand comparison between baseline and retrofitted vehicle	52
Figure 53 Algorithm adopted for the simulation	54
Figure 54 Algorithms adopted in charging and discharging modes.....	55
Figure 55 Methodology adopted for evaluating voltage when vehicle moves from tractive to braking phase	55
Figure 56 Battery current limitations	56
Figure 57 SOC evolution in the given track	57
Figure 58 Voltage and current trend in the given track	58
Figure 59 Single module Voltage and C-rate evolution.....	58
Figure 60 SOC effect on regenerative energy	59
Figure 61 SOC evolution	60
Figure 62 Electrical parameters evolution	60

List of tables

Table 1 USA railway energy fuel mix evolution. Source: [1]	8
Table 2 Russia railway energy fuel mix. Source: [1]	8
Table 3 India railway energy fuel mix evolution. Source: [1]	9
Table 4 China railway energy fuel mix evolution. Source: [1]	9
Table 5 Car 2 and Car 4 technical details	12
Table 6 Vehicle's loads	13
Table 7 Diesel engine specifications. Source: Engine Datasheet	22
Table 8 Steam thermodynamic properties adopted in the calculus	23
Table 9 Results of the steam cycle calculation.....	24
Table 10 Thermodynamic properties of R245fa.....	25
Table 11 Exhaust gas combined with ORC results.....	25
Table 12 Technical requirements of the underfloor heating system.....	26
Table 13 Specifications of the GS Yuasa LIM25H-12. Source: [63].....	37
Table 14 Specifications of Altairnano LTO module	39
Table 15 List of hybrid battery-driven railway vehicles. Source: [71]	39
Table 16 Input data for battery pack sizing.....	48
Table 17 Toshiba battery module type 3-23	49
Table 18 Final battery pack configuration.....	51
Table 19 Vehicle operational modes.....	53
Table 20 Results of the dynamic simulation for different initial SOC values	59
Table 21 Results of simulation without regenerative braking	61
Table 22 Characteristics of the track Aosta-Turin	62
Table 23 Charging timetable	63